General Disclaimer

One or more of the Following Statements may affect this Document

- This document has been reproduced from the best copy furnished by the organizational source. It is being released in the interest of making available as much information as possible.

- This document may contain data, which exceeds the sheet parameters. It was furnished in this condition by the organizational source and is the best copy available.

- This document may contain tone-on-tone or color graphs, charts and/or pictures, which have been reproduced in black and white.

- This document is paginated as submitted by the original source.

- Portions of this document are not fully legible due to the historical nature of some of the material. However, it is the best reproduction available from the original submission.

Produced by the NASA Center for Aerospace Information (CASI)

OPTIMAL SYMMETRIC FLIGHT

WITH AN INTERMEDIATE VEHICLE

MODEL

P. K. A. MENON

H. J. KELLEY

E. M. CLIFF

SEPTEMBER 1983

AEROSPACE & OCEAN ENGINEERING DEPT.

VIRGINIA POLYTECHNIC INSTITUTE & STATE UNIVERSITY
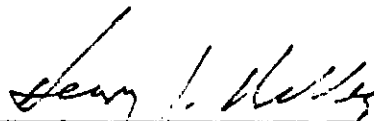BLACKSBURG, VIRGINIA

OPTIMAL SYMMETRIC FLIGHT WITH AN INTERMEDIATE VEHICLE MODEL

by

Padmanabhan K. A. Menon

Dissertation submitted to the Faculty of the

Virginia Polytechnic Institute and State University

in partial fulfillment of the requirements for the degree of

DOCTOR OF PHILOSOPHY

in

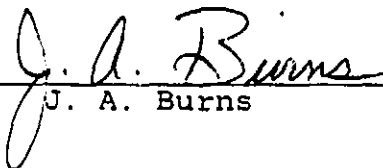Aerospace and Ocean Engineering

APPROVED:

H. J. Kelley, Chairman

E. M. Cliff

F. H. Lutze

J. A. Burns

L.R. Anderson

September, 1983
Blacksburg, Virginia

OPTIMAL SYMMETRIC FLIGHT WITH AN INTERMEDIATE VEHICLE MODEL

by

P. K. A. Menon

(ABSTRACT)

Optimal flight in the vertical plane with a vehicle model intermediate in complexity between the point-mass and energy models is studied. Flight-path angle takes on the rôle of a control variable. Range-open problems feature subarcs of vertical flight and singular subarcs as previously studied.

The class of altitude-speed-range-time optimization problems with fuel expenditure unspecified is investigated and some interesting phenomena uncovered. The maximum-lift-to-drag glide appears as part of the family, final-time-open, with appropriate initial and terminal transient maneuvers. A family of climb-range paths appears for thrust exceeding level-flight drag, some members exhibiting oscillations. Oscillatory paths generally fail the Jacobi test for durations exceeding a period and furnish a minimum only for short-duration problems.

Minimizing paths of long duration follow a certain corridor in the V-h chart. The features of the family

sharpen for the special case of thrust and drag independent of altitude, and considerable analytical attention is accorded to this for the insight it provides to the more general model.

The problem of "steepest climb" is found to be ill-posed with the vehicle model under consideration, straight-vertically-upward maneuver sequei.:es being furnished by a family of paths alternating between upward and downward vertical flight and including a limiting "chattering" member.

.

ACKNOWLEDGMENTS

LIST OF FIGURES

NOMENCLATURE

C_D................Drag Coefficient

C_{Do}................Zero-Lift Drag Coefficient

C_L................Lift Coefficient

D................Drag

E................Specific Energy, $h + \dfrac{V^2}{2g}$

g................Acceleration due to Gravity

h................Altitude

H................Variational Hamiltonian

K................Induced Drag Coefficient

L................Lift

M................Mach number

Q................Fuel Flow rate

s................Laplacian Operator

S................Aircraft Wing Surface area

T................Thrust

V................Airspeed

W................Weight

x................Downrange

y................Crossrange

GREEK SYMBOLS

α................Angle of Attack

γ................Flight-path Angle

η . . . . Throttle Coefficient

ϕ . . . . Bank Angle

χ . . . . Heading Angle

ρ . . . . Air density

λ_h . . . . Altitude Multiplier

λ_V . . . . Airspeed Multiplier

$\lambda_{\tilde{W}}$ . . . . Fuel Multiplier

λ_x . . . . Range Multiplier

TABLE OF CONTENTS

Chapter I

INTRODUCTION

There has been interest from the begining of optimal flight studies in approximations featuring simplified vehicle models (Refs 1 through 8). The motivation in these studies stems from the considerable difficulties encountered in optimizing atmospheric flight trajectories with a detailed system model. In general, straightforward application of the maximum principle to an "exact" model of an aircraft leads to a nonlinear two-point-boundary-value problem involving several unknown parameters, with attendant difficulties in obtaining solutions. Further, a combination of three control variables, viz., lift coefficient, bank angle, and throttle and the imposition of various constraints considerably adds to the complexity of the problem. Nevertheless, it is currently feasible to compute control histories, i.e., open-loop controls, for optimal control of sophisticated mathematical models of flight vehicles. The favored approach involves reformulating the problem as one of nonlinear programming by parameterizing the control history (Ref 9). Such direct methods are computationally less sensitive than the indirect methods of solution via the state-Euler system with split boundary conditions. With the availability of

improved numerical techniques such as multiple shooting (Refs 10, 11 and 12), indirect methods are again begining to appear attractive for solving aircraft trajectory optimization problems (Ref 13).

While numerical optimization techniques are of considerable value, they are expensive to use and with the current state-of-the-art in computing technology (Ref 14), virtually impossible to implement on-board an aircraft. Moreover, the results obtained are restricted to a particular set of boundary conditions and when these are altered, the numerical exercise must be carried out all over again. It may be added that these techniques are ill-suited for use in preliminary design stages where it is desirable to have the capability to assess the effect of design changes rapidly and economically.

Experience from flight tests as well as comparisons between various solutions of the optimal-control problem often reveals that the improvement in performance is minimal when the exact optimal trajectory is compared with a suboptimal one obtained from simpler analysis (Ref 15). Specifically, for the purposes of flight-path optimization for transport aircraft that do not generally indulge in violent maneuvers, reduced-order models have been found adequate (Ref 16). The simplified analysis has the added

advantage that the resulting solution is close to optimal and can sometimes be corrected for the effects of neglected dynamics. The use of simplified approximations is not free of difficulties, however. For instance, in Ref 17., optimal control resulting from the introduction of various approximations into the equations of motion was compared with the optimal control based on an "exact" set of motion equations and it was found that, in some cases, the resulting controls violated the assumptions made. It is prudent, therefore, to exercise caution in the use of these approximations and in the interpretation of results.

Extensive work has been done using the lowest-order model for aircraft flight, viz., the energy model (Refs 1 to 3 and 18 through 22). In this approximation, the aircraft-performance problem is presented in terms of the sum of kinetic and potential energies. The control variable is either the altitude or airspeed and the state variables are the specific energy (kinetic plus potential per unit weight), fuel consumed and down-range. A major assumption employed with the energy model is that the aerodynamic drag can be approximated by its level-flight value. Several aircraft trajectory-optimization problems have been handled using this model, for example; minimum-time climb, minimum-fuel climb, minimum-time turns in a plane, and cruise

trajectories have been reported (Refs 15 through 27). The relationship between the optimal paths emerging from the energy model have been compared with optimal trajectories according to more complex models to a certain extent (Refs 28 through 32).

The energy model began as an ad hoc approximation (Refs 1,2,3) and found a theoretical basis in the singular-perturbation theory of ordinary differential equations (Refs 33 through 38). The concept of singular perturbation technique in problems of flight mechanics was introduced by Kelley (Refs 36, 37 and 38) and applied in different formulations by Calise (Ref 39), Ardema (Ref 32) and others (Refs 40 through 45). It has been demonstrated that singular-perturbation methods are useful for extending energy-state modeling approachs to more general problem formulations. These methods constitute a reduced-order-analysis approach wherein the system dynamics are separated into slow and fast modes. This permits the solution of higher-order problems to be approximated in terms of the solutions of a series of low-order problems. The singular-perturbation procedure has been applied to several problems of flight mechanics and has resulted in guidance laws that have a nonlinear-feedback form (Refs 46 through 57). These schemes may be useful for on-board mechanization. If the

present trends continue, this approach appears to hold considerable promise.Recently (Ref 58), a new set of state variables which offer attractive replacements for altitude and airspeed in singular-perturbation procedures has been suggested with a view to enhancing the fidelity of the zeroth-order solution as far as possible. Even if the results from reduced-order modeling are not directly used for on-board implementation, the boundary-layer structure and hierarchical ideas from singular perturbations sometimes suggest the synthesis of near-optimal guidance schemes (Refs 59 and 60).

Using the assumption that aerodynamic drag can be approximated by its level-flight value, a model intermediate in complexity between point-mass and energy models can be obtained for aircraft in symmetric flight. In this model, the flight-path angle is relegated to the status of a control variable and the state variables are altitude, airspeed, fuel consumed and down-range. An apparent advantage of the intermediate vehicle model over the energy model is that it can generate possibly realistic path angles along optimal trajectories. There is obviously trouble ahead with this modeling should the time derivative of path angle turn out to be large in optimized maneuvering or, worse yet, should the path angle exhibit jump behavior.

Although there is some documented research work using this model (Refs 61 through 65), it has been less popular than the energy model. Notably, Kelley (Ref 61) used this model to analyze a class of time-fuel-range problems. In Ref 62, a version of this model has been used to examine fuel-optimal paths for transport aircraft. Speyer (Ref 66) investigated the solution for aircraft cruise given in Ref 63 using higher-order necessary conditions and concluded that, in general, steady-state cruise is nonoptimal. He further suggested that the optimal-cruise trajectory may be oscillatory, and this provided the impetus for research efforts reported in Refs 67 through 69. Since oscillatory trajectories surfaced in Ref 61 also, in connection with the range-optimal climb problem, it was conjectured that these might be somehow related. The motivation for the present work arose out of these issues. It is of interest to note that in Ref 63, a variant of the intermediate vehicle model was used to analyze the aircraft-cruise problem. The key difference between the model of Refs 61, 65, and Ref 63 is that the Sinγ and Cosγ terms arising in the system have been replaced by their small-angle approximations.

With this background, it is the objective of this study to investigate optimal time-fuel-range trajectories in symmetric flight for aircraft using the intermediate vehicle

model. It is stressed at the outset that the investigation is oriented in a research spirit of exposing any quirks in the model rather than towards any specific application. The analysis is based in part upon an exploration of Euler solutions for the path-angle-as-control model carried out in Ref 61. It happens that under a constant-density-atmosphere assumption, the Euler equation for this model can be solved in closed form, permitting extensive analytical investigation of the solution family. Specifically, optimal-range climb and glide problems, and the climb-dash intercept problem similar to that in Ref 13 are studied in detail. Through second-order necessary conditions it will be shown that the minimum-range-to-climb problem (the "steepest climb" of Ref 5) has no proper minimum or even a lower bound. This problem is found to be ill-posed with the vehicle model under consideration, with straight-vertically-upward maneuver sequences being furnished by a family of paths alternating between upward and downward vertical flight and including a limiting chattering member. Investigation of the maximum-range-glide problem using higher-order necessary conditions is also discussed. For the climb-dash intercept problem, the choice of Lagrange multiplier ratios and the selection of an optimal trajectory from the Euler-solution family employing the conjugate-point

test is given in some detail. An interesting result (Ref 70), on the relation between a class of singular optimal-control problems and the identically non-regular problems in the Calculus of Variations, obtained while analyzing the higher-order necessary conditions for minimum time climb and fixed-throttle minimum-fuel climb trajectories is presented in an appendix. Numerical investigations, including a numerical conjugate point test, carried out to verify the conclusions from simplified analysis using typical high-performance aircraft (F-4) data are also discussed in detail.

The Euler equation for the time-fuel-range optimal-control problem using the intermediate vehicle model appears in a nonlinear-feedback form and a cursory analysis reveals a scheme for possible on-board implementation; however, aerodynamic-drag modeling is questionable.

1.1   EQUATIONS OF MOTION FOR AIRCRAFT FLIGHT

The point-mass dynamical model of aircraft flight in three dimensions incorporating the assumptions of thrust-along-path, zero side-force and flight over flat earth is given by

$$\dot{V} = g[\{(T-D)/W\} - Sin\gamma] \tag{1.1}$$

$$\dot{h} = V \, Sin\gamma \tag{1.2}$$

$$\dot{\gamma} = (g/V) \, [\{L \, Cos\phi/W\} - Cos\gamma] \tag{1.3}$$

$$\dot{\chi} = g \; L \; Sin\phi/(W \; V \; Cos\gamma) \tag{1.4}$$

$$\dot{x} = V \; Cos\gamma \; Cos\chi \tag{1.5}$$

$$\dot{y} = V \; Cos\gamma \; Sin\chi \tag{1.6}$$

$$\dot{\tilde{W}} = Q \tag{1.7}$$

Additional assumptions embodied in these equations are that the throttle is fixed, the variation in weight due to fuel expenditure is ignored and winds aloft are zero. The control variables in this model are the bank angle ϕ and the lift coefficient C_L or the angle of attack α . The drag is modeled as a parabolic function of the lift coefficient:

$$C_D = C_{Do} + K \; C_L^2 \tag{1.8}$$

The zero-lift-drag coefficient C_{Do} and the induced-drag coefficient K are functions of Mach number

$$C_D = C_{Do} \; (M) \quad and \quad K = K(M)$$

The thrust is a function of Mach number and altitude.

$$T = T(M,h)$$

1.2   SYMMETRIC FLIGHT

In the present work attention will be focussed on aircraft maneuvers in the vertical plane. Consequently, the bank angle ϕ and the flight path heading angle χ can be set to zero, resulting in

$$\dot{V} = g[\{(T-D)/W\} - \sin\gamma] \qquad (1.9)$$

$$\dot{h} = V \sin\gamma \qquad (1.10)$$

$$\dot{\gamma} = (g/V) [\{L/W\} - \cos\gamma] \qquad (1.11)$$

$$\dot{x} = V \cos\gamma \qquad (1.12)$$

$$\dot{\tilde{W}} = Q \qquad (1.13)$$

Note that the introduction of symmetric-flight assumptions has decreased the number of state variables by two. The only control variable in this model is the lift coefficient C_L or the angle of attack α.

1.3   INTERMEDIATE VEHICLE MODEL

In the spirit of model order-reduction, the sweeping assumption that aerodynamic drag can be approximated by its level-flight value is next invoked. This allows the treatment of drag as a function of airspeed and altitude only. As a consequence, the flight-path angle γ is relegated

to the status of a control variable and the equation (1.11) can be deleted from the system. The lift coefficient, C_L, or the angle-of-attack α , previously a control variable, is correspondingly assumed to be such as to satisfy equation (1.11). An additional order-reduction would lead to the energy-state model with altitude or airspeed as the control variable. A discussion on the validity of the approximation made with regards to the aerodynamic drag is given in Ref 71. Thus the intermediate vehicle model for aircraft flight is given by:

$$\dot{V} = g[\{(T-D)/W\} - \sin\gamma] \qquad (1.14)$$

$$\dot{h} = V \sin\gamma \qquad (1.15)$$

$$\dot{x} = V \cos\gamma \qquad (1.16)$$

$$\dot{\tilde{W}} = Q \qquad (1.17)$$

The drag coefficient C_D is now in the form

$$C_D = C_{Do} + K \; 4 \; W^2/(\rho \; V^2 \; S)^2 \qquad .$$

Note that the $\sin\gamma$ and $\cos\gamma$ terms occurring in the system equations have been left unmodified although consistency demands their replacement by small-angle approximations in accordance with the assumption made regarding lift. This is done to avoid imposing an artificial bound on path-angle as

will be required otherwise to obtain sensible results along certain optimized paths (Ref 17). It should be noted that the approximation carried out here cannot properly be classed as a singular perturbations procedure as in Ref 38. It must, therefore, be accepted at the outset that those solutions which violate the assumption that $\dot{\gamma}$ is small along substantial portions of the optimized trajectory should be interpreted with caution. In the model given above, the throttle has been assumed fixed. It will be seen in subsequent portions of this work that the throttle control can be reinstated without excessive difficulty. However, this tends to complicate the analysis somewhat and is treated in the present work only for completeness.

1.4 OPTIMAL-CONTROL PROBLEM

To state the optimal-control problem concisely, it is desired to find the control history $\gamma(t)$ such that the system described by (1.14) through (1.17) be transferred from initial state $(V_o, h_o, x_o, \widetilde{W}_o, t_o)$ to the final state $(V_f, h_f, x_f, \widetilde{W}_f, t_f)$, not all of whose components are specified, such that a functional $P(V_f, h_f, x_f, \widetilde{W}_f, t_f)$ takes on a minimum value.

From a practical viewpoint, the time-range optimal-control problems are of main interest since minimum-fuel

problems with fixed throttle rarely occur in applications.
Therefore, major attention is focussed on the analysis of
full-throttle, minimum-range climb (Steepest climb of
Ref.5), power-off maximum-range glide and the climb-dash
intercept problems. Out of these three, the climb-dash
intercept problem requires some explanation. This trajectory
occurs in aircraft pursuit-evasion problems (Ref 13, 38) as
a transient leading to the dash point or the high speed
point on the level flight envelope. In general, the time
spent during the climb is much smaller than the time spent
in the dash. This maneuver normally ends with a terminal
transient as mentioned in Ref. 13. The treatment in this
work, however, will not include any discussion of this
terminal transient.

Chapter II

OPTIMAL CONTROL WITH INTERMEDIATE VEHICLE MODEL

Introduction of the assumption that the aerodynamic drag can be approximated by its level-flight value in the equations of motion for symmetric flight leads to a model intermediate in complexity between point-mass and energy models. The chief advantage gained in employing this approximation is the reduction in model order offering analytical and numerical simplicity. The control variable in this model is the flight path angle γ and the state variables are the airspeed, altitude, down-range and fuel consumed. Presumably, the solutions emerging from this modeling may have validity at least along central portions of the optimized path. It should be noted, however, that the intermediate vehicle model permits jumps in the path-angle and, hence, the assumption of small $\dot{\gamma}$ is violated along the optimized trajectory. Consequently, care should be exercised in the interpretation of the results.

The optimal-control problem under consideration is the minimization of a function of the state-variables and time final values, subject to the differential constraints given by the equations (1.14) through (1.17), with satisfaction of any boundary conditions that may be imposed. To this end, the variational Hamiltonian function is formed as

14

$$H = \lambda_V \, g \, [\{(T-D)/W\} - Sin\gamma] + \lambda_h \, V \, Sin\gamma$$

$$+ \lambda_x \, V \, Cos\gamma + \lambda_{\widetilde{W}} \, Q \qquad (2.1)$$

The Euler-Lagrange equations are

$$\dot{\lambda}_V = -\lambda_V \frac{g}{W} \frac{\partial}{\partial V}(T-D) - \lambda_h \, Sin\gamma$$

$$- \lambda_x \, Cos\gamma - \lambda_{\widetilde{W}} \frac{\partial Q}{\partial V} \qquad (2.2)$$

$$\dot{\lambda}_h = -\lambda_V \frac{g}{W} \frac{\partial}{\partial h}(T-D) - \lambda_{\widetilde{W}} \frac{\partial Q}{\partial h} \qquad (2.3)$$

$$\dot{\lambda}_x = 0 \qquad (2.4)$$

$$\dot{\lambda}_{\widetilde{W}} = 0 \qquad (2.5)$$

The optimality condition $\frac{\partial H}{\partial \gamma} = 0$, is given by

$$-\lambda_V \, g \, Cos\gamma + \lambda_h \, V \, Cos\gamma - \lambda_x \, V \, Sin\gamma = 0 \qquad (2.6)$$

In these equations, $Sin\gamma$ and $Cos\gamma$ terms have been retained unmodified, although it is evident that consistency demands their replacement by small-angle approximations in accordance with the assumption made concerning the aerodynamic drag. This has important bearing on the question of imposed boundary conditions, as will be seen subsequently. The analysis presented in this section closely follows that of Ref 61.

Equations (1.14) through (1.17) and the equations (2.2) through (2.6) together with specified boundary conditions and appropriate transversality conditions form the two-point-boundary-value problem, which needs to be solved to obtain the optimal control $\gamma(t)$. If desired, a numerical solution can be obtained for this system. Be that as it may, the approach adopted here is in a different direction. It can be noted from the Euler-Lagrange equations (2.2) through (2.6) that the only costates that are variable in the Hamiltonian are those associated with the airspeed and altitude, viz., λ_V and λ_h . If these can be eliminated using algebraic manipulations, then a first integral of the motion, i.e., the variational Hamiltonian, can be obtained in a closed form.

In the following, the time-derivatives of the optimality condition (equation 2.6) will be used to eliminate the costates λ_V and λ_h in favor of the control variable γ and its derivatives. Note that this procedure is somewhat formal since the derivatives of the path angle may not exist at certain points on the optimized trajectory. Using equation (2.6)

$$\lambda_V = \frac{V}{g} (\lambda_h - \lambda_x \, \mathrm{Tan}\gamma) \qquad (2.7)$$

Differentiating the above expression once with respect to time,

$$\dot{\lambda}_V = \frac{\dot{V}}{g}(\lambda_h - \lambda_x \tan\gamma) + \frac{V}{g}(\dot{\lambda}_h - \lambda_x \dot{\gamma} \sec^2\gamma) \tag{2.8}$$

Now, substituting for λ_V in equation (2.3) from equation (2.7)

$$\dot{\lambda}_h = -\frac{V}{W}(\lambda_h - \lambda_x \tan\gamma)\frac{\partial}{\partial h}(T-D) - \lambda_{\widetilde{W}}\frac{\partial Q}{\partial h} \tag{2.9}$$

Similarly, the equation (2.2) becomes,

$$\dot{\lambda}_V = -\frac{V}{W}(\lambda_h - \lambda_x \tan\gamma)\frac{\partial}{\partial V}(T-D) - \lambda_h \sin\gamma$$
$$- \lambda_x \cos\gamma - \lambda_{\widetilde{W}}\frac{\partial Q}{\partial V} \tag{2.10}$$

Substituting next for λ_V from equation (2.8) in the equation (2.10), one obtains a second expression for λ_h as

$$\dot{\lambda}_h = -\lambda_h \frac{g}{W}\left[\frac{(T-D)}{V} + \frac{\partial}{\partial V}(T-D)\right]$$
$$- \lambda_x \left[\frac{g}{V\cos\gamma} - \dot{\gamma}\sec^2\gamma - \frac{g}{W}\tan\gamma\left\{\frac{(T-D)}{V}\right.\right.$$
$$\left.\left. + \frac{\partial}{\partial V}(T-D)\right\}\right] - \lambda_{\widetilde{W}}\frac{g}{V}\frac{\partial Q}{\partial V} \tag{2.11}$$

Equations (2.9) and (2 11) can now be used to eliminate $\dot{\lambda}_h$, resulting in the following expression relating λ_h, λ_x, and $\lambda_{\widetilde{W}}$.

$$\frac{\lambda_h}{W} \left[\frac{\partial}{\partial h}[V(T-D)] - \frac{g}{V}\frac{\partial}{\partial V}[V(T-D)] \right]$$

$$- \frac{\lambda_x}{W} \left[Tan\gamma \left\{ \frac{\partial}{\partial h}[V(T-D)] - \frac{g}{V}\frac{\partial}{\partial V}[V(T-D)] \right\} \right.$$

$$\left. + \frac{g}{V\ Cos\gamma} - \dot{\gamma}\ Sec^2\gamma \right] + \lambda_{\widetilde{W}} \left[\frac{\partial Q}{\partial h} - \frac{g}{V}\frac{\partial Q}{\partial V} \right] = 0$$

(2.12)

The expressions (2.7) and (2.12) for λ_V and λ_h is next substituted in the variational Hamiltonian (2.1) with the following expression resulting

$$Cos\gamma\ H \left\{ \left(\frac{\partial}{\partial h} - \frac{g}{V}\frac{\partial}{\partial V} \right) [V(T-D)] \right\}$$

$$- Cos\gamma\ \lambda_{\widetilde{W}}\ Q^2 \left\{ \left(\frac{\partial}{\partial h} - \frac{g}{V}\frac{\partial}{\partial V} \right) [V(T-D)/Q] \right\}$$

$$-\lambda_x \left\{ V^2 \left(\frac{\partial}{\partial h} - \frac{g}{V}\frac{\partial}{\partial V} \right)[T-D] - \frac{(T-D)V}{Cos\gamma}\ \dot{\gamma} \right\} = 0$$

(2.13)

It may be noted that

$$\left(\frac{\partial}{\partial h} - \frac{g}{V}\frac{\partial}{\partial V} \right) [\ \ ] = \frac{\partial}{\partial h} [\ \ ] \bigg|_{E\ =\ Constant}$$

where $E = h + \frac{V^2}{2g}$, the specific energy.

The first integral of motion (2.13) is now independent of the multipliers λ_V and λ_h. If the required data is available, this expression together with the differential equations (1.14) through (1.17) can be numerically

integrated to obtain optimal trajectories; provided the initial value of path-angle is known. Such solutions are given elsewhere in this work. Rather than attempting to generate numerical solutions immediately, it is desirable at this point to examine specific cases to gain better insight into the nature of trajectories emerging from the expression (2.13).

For completeness, the inclusion of throttle control in the above formulation is next considered. One of the ways to do this is to introduce a multiplicative parameter, η, on thrust, T, and fuel-consumption rate, Q, in the state-Euler system, with

$$0 \leqslant \eta \leqslant 1 \qquad ,$$

The thrust and fuel-consumption rates appearing in these equations are then their maximum values at each altitude and airspeed. In such a situation, the Minimum Principle (Ref 24) requires that the throttle setting be chosen at each instant such that

$$\eta = 0, \text{ if } \left[\lambda_V \frac{g}{W} T + \lambda_{\widetilde{W}} Q \right] > 0$$

$$\eta = 1, \text{ if } \left[\lambda_V \frac{g}{W} T + \lambda_{\widetilde{W}} Q \right] < 0$$

The multiplier λ_V required in the switching function can be determined from equations (2.7) and (2.12). Note that a singular arc arises whenever

$$\lambda_V \, \frac{g}{W} \, T + \lambda_{\widehat{W}} \, Q \; \equiv \; 0$$

over a nonzero interval of time. In this case, the control, η, is determined by equating successive time derivatives of the switching function to zero. It is also known that the Generalized Legendre-Clebsch necessary condition, sometimes known as the Kelley-Contensou test (Ref 72), should hold along the minimizing singular arcs. This will not be pursued any further in the present work and, in the treatment that follows, the throttle will be assumed fixed at its maximum value.

2.1 PROPERTIES OF THE SOLUTION

In order to investigate the implications of expression (2.13), three distinct cases will be considered in the following. These are minimum-time-to-climb, minimum-fuel-to-climb and range-optimal climb and glide trajectories. To illustrate the approach, consider, for example, that the final values of range and time are open. Then the transversality conditions $\lambda_x = 0$, $H = 0$ apply and the optimization problem is a trade-off between the final values of fuel-consumed, altitude and airspeed, the maximum or minimum value of one of these variables or some function of these variables being sought without regard to the final values of range and time.

2.1.1   Minimum-Time-To-Climb Trajectory

If time to climb is to be minimized, then the Hamiltonian H has a value of -1 (Ref 23,61), $\lambda_x = 0$, $\lambda_{\widetilde{W}} = 0$ and the expression (2.13) reduces to

$$\cos\gamma \left\{ \left(\frac{\partial}{\partial h} - \frac{g}{V} \frac{\partial}{\partial V} \right) [V(T-D)] \right\} = 0 \qquad (2.14)$$

which may also be written as

$$\cos\gamma \; \frac{\partial}{\partial h} [V(T-D)] \bigg|_{E = \text{Constant}} = 0 \qquad (2.15)$$

The equation (2.14) can be satisfied either by $\cos\gamma = 0$, vertical flight, or by the vanishing of the expression in brackets. This expression is the derivative of the so-called "excess power" in the flight performance literature with respect to altitude with the specific-energy held constant. The minimum-time-to-climb trajectory may be conceived as a path in the altitude-airspeed chart which passes over each specific-energy curve at a local maximum of specific excess power along that curve. This trajectory carries the name "energy climb" (Ref 1) due to its close association with the specific-energy concept. It is appropriate to point out that the vertical-flight result would not have been obtained if the $\sin\gamma$ and $\cos\gamma$ terms in the system had been replaced by small-angle approximations.

Thus the solution to this, or any, altitude-airspeed-time optimal problem is made up of vertical climbs, vertical dives and energy climbs pieced together in proper sequence; a result noted by several researchers (Refs 1 through 6 and 15, 18, 19 and 61).

2.1.2 Minimum-Fuel-To-Climb Trajectory

To generate a minimum-fuel climb path, with final values of time and range open, the natural boundary condition $\lambda_x = 0$ and H = 0 can be used in equation (2.13), with the following result

$$\text{Cos}\gamma \left\{ \left(\frac{\partial}{\partial h} - \frac{g}{V} \frac{\partial}{\partial V} \right) [V(T-D)/Q] \right\} = 0 \qquad (2.16)$$

Just as in the energy-climb case, the expression (2.16) can be satisfied either by $\text{Cos}\gamma = 0$, vertical flight, or by vanishing of the bracketed expression. This quantity is the derivative of the excess power per unit fuel-flow with respect to altitude, with specific energy held constant. Hence, the solution of minimum-fuel-to-climb is made up of vertical climbs, vertical dives and a path in the altitude-airspeed chart which passes over each specific energy curve at a local maximum of the excess power per unit fuel-flow along that curve. This trajectory is sometimes referred to as an "economy climb".

2.1.3   Range-Optimal Climb and Glide Paths

If the range is to be minimized or maximized with final time and fuel unspecified, then $\lambda_x = \pm 1$ and $H = \lambda_W = 0$, and a first-order differential equation emerges from expression (2.13) for path inclination as follows

$$V^2 \left(\frac{\partial}{\partial h} - \frac{g}{V} \frac{\partial}{\partial V} \right)[T-D] - \frac{(T-D)V\,\dot{\gamma}}{\cos\gamma} = 0$$

(2.17)

Note that the $\dot{\gamma}$ term would not have appeared in the above if small-angle approximation had been used in the equations of motion. This has a significant impact on the nature of optimal trajectories for this problem, as will be seen later in this chapter. The system consisting of equations (1.14) through (1.17) and (2.17) generates a trajectory family for the range-optimal problem. The possibility of obtaining analytical solution to this system for the case of thrust and drag as arbitrary functions of altitude and airspeed is remote. As a result, the interpretation of expression (2.17) is not as straightforward as it was in the minimum-time-to-climb and minimum-fuel-to-climb cases.

However, introducing the assumption of constant-density atmosphere with thrust and drag dependent on airspeed only, it is feasible to obtain an analytical solution to this

system (Ref 61). This assumption has been employed in the past for the analysis of some optimal aircraft trajectories, see Refs 73 and 74, for example. Results obtained from this analysis may perhaps be characteristic of more general solutions as well.

The equation (2.17) can be rewritten as

$$\frac{\dot{\gamma}}{Cos\gamma} = \frac{V}{(T-D)} \left\{ \left(\frac{\partial}{\partial h} - \frac{g}{V} \frac{\partial}{\partial V} \right) [T-D] \right\}$$

(2.18)

Since time is not of particular interest in the problem, it may be eliminated in favor of airspeed as an independent variable. In the following, several transformations of the independent variable are carried out without attention to monotonicity requirements, the thought being to fit solution segments obtained into families in due course. The temptation of range as independent variable will be avoided, however, in anticipation of purely-vertical-motion segments. In the interest of brevity, designate the acceleration variable $\mu = (T-D)/W$,

$$\frac{1}{Cos\gamma} \frac{d\gamma}{dV} (\mu - Sin\gamma) = \frac{V}{g\mu} \left(\frac{\partial}{\partial h} - \frac{g}{V} \frac{\partial}{\partial V} \right) \mu$$

(2.19)

With altitude dependence of thrust and drag supressed, the path angle γ is determined as the solution of the first-order differential equation

$$\frac{1}{\mathrm{Cos}\gamma}\frac{d\gamma}{dV}\,(\mathrm{Sin}\gamma - \mu)\;=\;\frac{1}{\mu}\frac{d\mu}{dV} \tag{2.20}$$

Further simplification is obtained by another change of independent variable, this time from airspeed V to μ

$$\frac{1}{\mathrm{Cos}\gamma}\frac{d\gamma}{d\mu}\,(\mathrm{Sin}\gamma - \mu)\;=\;\frac{1}{\mu} \tag{2.21}$$

If the rôles of independent and dependent variables are now regarded as reversed, this equation takes the form

$$\frac{d\mu}{d\gamma}\,+\,\frac{1}{\mathrm{Cos}\gamma}\,\mu^2\,-\,\mu\,\frac{\mathrm{Sin}\gamma}{\mathrm{Cos}\gamma}\;=\;0 \tag{2.22}$$

which is a form of the Bernoulli differential equation

$$\frac{d\mu}{d\gamma}\,+\,f_1(\gamma)\,\mu^2\,+\,f_2(\gamma)\,\mu^{\beta}\;=\;0 \tag{2.23}$$

with $\beta = 1$. According to Kamke, (Ref 75), this equation has the solution

$$\frac{1}{\mu}\,=\;E(\gamma)\int\frac{f_1(\gamma)}{E(\gamma)}\;\;d\gamma \tag{2.24}$$

where

$$E(\gamma)\;\;=\;\;e^{\int f_2(\gamma)\,d\gamma} \tag{2.25}$$

with the identification of f_1 and f_2 as

$$f_1(\gamma)\;\;=\;\frac{1}{\mathrm{Cos}\gamma} \tag{2.26}$$

$$f_2(\gamma) = - \int \frac{\sin\gamma}{\cos\gamma} \, d\gamma \tag{2.27}$$

The solution (2.24) becomes as follows

$$E(\gamma) = e^{\ln \cos\gamma} = \cos\gamma \tag{2.28}$$

$$\frac{1}{\mu} = \cos\gamma \left[\int \frac{d\gamma}{\cos^2\gamma} + C \right]$$

Or

$$\frac{1}{\mu} = \sin\gamma + C \cos\gamma \tag{2.29}$$

Before expressing this relationship in the form $\gamma = \gamma(\mu)$, one may relate the integration constant C' to equilibrium values of μ and γ corresponding to unaccelerated flight. Such values may be designated with a superscribed bar :

$$\bar{\mu} = \sin\bar{\gamma} \tag{2.30}$$

$$C = \cot\bar{\gamma} \tag{2.31}$$

The solution can then be expressed as :

$$\sin\bar{\gamma} \sin\gamma + \cos\bar{\gamma} \cos\gamma = \frac{\bar{\mu}}{\mu} \tag{2.32}$$

or as

$$\gamma = \bar{\gamma} + \cos^{-1} \left[\frac{\bar{\mu}}{\mu} \right] \tag{2.33}$$

Here $\bar{\mu}$ is the value of μ in unaccelerated flight and

$$\bar{\gamma} = \sin^{-1}\bar{\mu} \qquad\qquad (2.34)$$

In Fig. 1, the solution (2.33) for the range-optimal problem is illustrated for various values of μ. Note that the range of the flight-path angle γ has been restricted to $\pm180^{\circ}$ in this plot.

The solution family in Fig. 1 is not related sufficiently closely to the state variables in the system to be very illuminating. This may be remedied in part by reinstating airspeed as the independent variable. To this end, consider first the case of unpowered flight with a quadratic distribution of power variable vs airspeed as shown in the upper part of Fig. 2. The solution family generated by substituting the assumed quadratic in equation (2.33) for various values of parameter $\bar{\mu}$ is sketched in the lower portion of the figure. The point identified by a circle corresponds to steady flight at minimum-drag airspeed or L/D_{max} glide. The arrows on the solution family indicate the direction of increasing time, determined from the differential equation for airspeed, viz.,

$$\dot{V} = g[\mu - \sin\gamma] \qquad\qquad (2.35)$$

The family of transients leading to and from the L/D_{max} point can also be seen in this figure. Other paths to the right and left of this plot appear to be connected with transient dive and zoom solutions which do not involve prolonged operation at or near the minimum-drag airspeed. Thus, according to the present modeling, the solution to maximum-range glide is comprised of the following. A transient path leading from the initial condition to the L/D_{max} flight condition, flight at the minimum-drag speed, and another transient terminating at the final boundary conditions; all this provided that the terminal conditions are attainable in gliding flight. If the initial condition does not lie on a transient path leading to the L/D_{max} point, a jump in the path angle γ is indicated, which places the vehicle on the appropriate trajectory. Similarly, if the terminal boundary condition is off a transient path leading away from the minimum-drag airspeed, another jump in path angle is required. Therefore, with intermediate vehicle modeling, the maximum-range glide path, in general, will contain points at which the path-angle jumps. Consequently, the assumptions made with regards to the magnitude of the derivative of the path angle will be violated along the optimized path unless the specified boundary conditions happen to be on a transient path and sufficiently close to the equilibrium flight condition.

When a positive margin of thrust over drag exists, a family of oscillatory solutions corresponding to minimum-range climb can be generated, again by assuming a quadratic relation between the acceleration variable and airspeed, as depicted in Fig.3. The innermost circled point in this chart corresponds to flight along $(T-D)_{max}$. A family of oscillatory solutions about this point appears with an outermost limiting member along which the path angle switches between $\pm 90^{\circ}$. Interpretation of these trajectories, in the light of results given in Ref 5 for the "steepest climb" problem, is not straightforward. However, an examination of second-order necessary conditions to be presented in the next chapter will reveal that the "steepest climb" problem does not possess a minimum or even a lower bound, when a positive margin of thrust over drag exists.

With the experience gained from the analysis of various special cases, the next obvious step is to tackle the more general time-fuel-range problem. If one chooses $\lambda_x = -1$, $\lambda_{\widetilde{W}} = 0$, and a fixed value of H (to be determined), the expression (2.13) is the Euler equation for the problem of maximizing range with a fixed final time. Similarly, if $\lambda_x = -1$, $H = 0$ and $\lambda_{\widetilde{W}}$ is fixed, the Euler equation for maximum-range trajectory with fixed final value of fuel is obtained. It may be noted that the range-maximization problem without

time or fuel constraints does not have a proper maximum or an upper bound. It is clear that fixed-throttle range-fuel optimum problems are of little interest in practical situations. Hence, in the next section, attention will be focussed on the problem of maximizing the range with a specified final time.

2.2   TIME-RANGE OPTIMAL PATHS

With $\lambda_x = -1$, $\lambda_{\tilde{W}} = 0$, and a fixed value of H, expression (2.13) is the Euler equation for the time-range problem. In its original form, this equation is not amenable to detailed analysis due to its nonlinear nature and the appearance of arbitrary thrust and drag functions. However, it happens that, if one employs the constant-density-atmosphere assumption, analytical solution to the general expression (2.13) can be obtained using the variation-of-parameters technique (Refs 76 and 77) on the solution for the range problem. Required transversality conditions can then be imposed to study specific cases.

Under the constant-density-atmosphere assumption, equation (2.13) can be written as

$$\dot{\gamma} = -g\left\{\frac{\text{Cos}\gamma}{\mu}\frac{d\mu}{dV} - \text{Cos}^2\gamma\,(H/\lambda_x)\,(1/V^2\mu)\,\frac{d}{dV}(V\mu)\right.$$

$$\left. + \text{Cos}^2\gamma\,(\lambda_{\tilde{W}}/\lambda_x)\,(Q^2/V^2\mu)\,\frac{d}{dV}[V\mu/Q]\right\}$$

$$(2.36)$$

The independent variable is now changed from time to airspeed, resulting in

$$\frac{d\gamma}{dV}(\operatorname{Sin}\gamma - \mu) = \frac{\operatorname{Cos}\gamma}{\mu}\frac{d\mu}{dV}$$

$$- \operatorname{Cos}^2\gamma \ (H/\lambda_x) \ (1/V^2\mu) \ \frac{d}{dV}(V\mu)$$

$$+ \operatorname{Cos}^2\gamma \ (\lambda_{\widetilde{W}}/\lambda_x) \ (Q^2/V^2\mu) \ \frac{d}{dV}[V\mu/Q]$$

$$(2.37)$$

Rearranging,

$$\frac{d\gamma}{dV}(\operatorname{Sin}\gamma - \mu) - \frac{\operatorname{Cos}\gamma}{\mu}\frac{d\mu}{dV} = -\operatorname{Cos}^2\gamma\left[(H/\lambda_x)\ (1/V^2\mu)\ \frac{d}{dV}(V\mu)\right.$$

$$\left. - (\lambda_{\widetilde{W}}/\lambda_x)\ (Q^2/V^2\mu)\ \frac{d}{dV}[V\mu/Q]\right]$$

$$(2.38)$$

The analytical solution for the first-order differential equation (2.38) with the right members set to zero is the expression (2.29). The equation (2.29) may now be differentiated with respect to airspeed,

$$-\frac{1}{\mu^2}\frac{d\mu}{dV} = (\operatorname{Cos}\gamma - C\operatorname{Sin}\gamma)\frac{d\gamma}{dV} + \frac{dC}{dV}\operatorname{Cos}\gamma$$

$$(2.39)$$

Note that C is no longer a constant, but a function of the independent variable V. Substituting for μ in equation (2.39) from (2.29),

$$\frac{1}{\mu}\frac{d\mu}{dV} = - \frac{\left[(Cos\gamma - C\,Sin\gamma)\frac{d\gamma}{dV} + \frac{dC}{dV}Cos\gamma\right]}{(Sin\gamma + C\,Cos\gamma)}$$

$$(2.40)$$

Employing the expression (2.40) in (2.38) and carrying out algebraic manipulations, one obtains a first order differential equation for C as

$$\frac{Cos^2\gamma}{Sin\gamma + C\,Cos\gamma}\frac{dC}{dV} = - Cos^2\gamma\,(H/\lambda_x)\,(1/V^2\mu)\frac{d}{dV}(V\mu)$$

$$+ Cos^2\gamma\,(\lambda_{\widetilde{W}}/\lambda_x)\,(Q^2/V^2\mu)\frac{d}{dV}[V\mu/Q]$$

$$(2.41)$$

Simplifying (2.41) using equation (2.29)

$$\frac{dC}{dV} = -(H/\lambda_x)\left\{(1/V^2\mu) + (1/V\mu^2)\frac{d\mu}{dV}\right\}$$

$$+ (\lambda_{\widetilde{W}}/\lambda_x)\left\{(Q/V^2\mu) + (Q/V\mu^2)\frac{d\mu}{dV} - (1/V\mu)\frac{dQ}{dV}\right\}$$

$$(2.42)$$

The quantities within the brackets can be identified as

$$- \frac{d}{dV}[1/V\mu] = (1/V^2\mu) + (1/V\mu^2)\frac{d\mu}{dV} \qquad (2.43)$$

and

$$- \frac{d}{dV} [Q/V\mu] = - (1/V\mu) \frac{dQ}{dV} + (Q/V\mu^2) \frac{d\mu}{dV} + (Q/V^2\mu)$$

(2.44)

from which

$$\frac{dC}{dV} = (H/\lambda_x) \frac{d}{dV} [1/V\mu] - (\lambda_{\widetilde{W}}/\lambda_x) \frac{d}{dV} [Q/V\mu] \qquad (2.45)$$

Equation (2.45) is readily integrated to yield

$$C = \frac{H}{\lambda_x} \frac{1}{V\mu} - \frac{\lambda_{\widetilde{W}}}{\lambda_x} \frac{Q}{V\mu} + C_1 \qquad (2.46)$$

Where C_1 is an arbitrary constant.

Hence, the solution for time-range-fuel optimal control problem with altitude dependence of thrust and drag suppressed is

$$\frac{1}{\mu} = \sin\gamma + \left[\frac{H}{\lambda_x} \frac{1}{V\mu} - \frac{\lambda_{\widetilde{W}}}{\lambda_x} \frac{Q}{V\mu} + C_1 \right] \cos\gamma$$

(2.47)

To express the above result in the form $\gamma = \gamma(\mu)$, the integration constant C_1 needs to be related to equilibrium values of μ and γ corresponding to unaccelerated flight. Unlike the situation in the range optimal problem, the interpretation of the solution (2.47) is not

straightforward, partly due to the involvement of time-range and fuel-range multiplier ratios in this expression.

As discussed earlier, fixed-throttle minimum-fuel trajectories are of limited interest in practical situations. Hence, in the following, primary attention will be focussed on the time-range optimal-control problem. This permits the deletion of a term in (2.47) resulting in

$$\frac{1}{\mu} = Sin\gamma + \left[\frac{H}{\lambda_x} \frac{1}{V\mu} + C_1 \right] Cos\gamma \qquad (2.48)$$

To investigate the range of permissible H/λ_x values, the equilibrium flight conditions obtained from equations (2.13) and (2.35) are next examined. Setting $\dot{V}$ and $\dot{\gamma}$ equal to zero in these expressions results in

$$Sin\overline{\gamma} = \overline{\mu} \qquad (2.49)$$

$$\frac{H}{\lambda_x} = V^2 \frac{d\mu}{dV} / \left[Cos\overline{\gamma} \frac{d}{dV}(V\mu) \right] \qquad (2.50)$$

Combining equations (2.49) and (2.50), an equation for the multiplier ratio H/λ_x corresponding to equilibrium flight conditions, in terms of airspeed and the acceleration variable emerges as

$$\frac{H}{\lambda_x} = V^2 \frac{d\mu}{dV} / \left[\sqrt{1-\overline{\mu}^2} \frac{d}{dV}(V\mu) \right] \qquad (2.51)$$

The equation (2.51) may be evaluated in the range of airspeeds of interest to obtain permissible values of the

multiplier ratio H/λ_x. In Fig. 4 a typical parabolic distribution of the acceleration variable μ vs airspeed is illustrated. Employing this distribution in equation (2.51), one can identify the permissible values of H/λ_x. A plot resulting from this calculation is shown in Fig. 5. In this figure, three distinct regimes may be identified. H/λ_x values to the left of $(T-D)_{max}$ point (marked A in Fig. 5) are positive, while those between the $(T-D)_{max}$ point and the $V(T-D)_{max}$ point (marked B) have a negative sign. All H/λ_x values to the right of the airspeed for $V(T-D)_{max}$ are positive. Any of these values may be used to evaluate the arbitrary constant C_1 as follows. As in (2.30),

$$\bar{\mu} = Sin\bar{\gamma} \tag{2.52}$$

$$\bar{V} = V \Big| \tag{2.53}$$

$$\text{Equilibrium value of } \frac{H}{\lambda_x}$$

$$Cot\bar{\gamma} = \frac{H}{\lambda_x} \frac{1}{\bar{V}\bar{\mu}} + C_1 \tag{2.54}$$

Or

$$C_1 = Cot\bar{\gamma} - \frac{H}{\lambda_x} \frac{1}{\bar{V}\bar{\mu}} \tag{2.55}$$

Using (2.55) in (2.48),

$$\frac{1}{\mu} = Sin\gamma + \left[\frac{H}{\lambda_x} \left\{ \frac{1}{V\mu} - \frac{1}{\bar{V}\bar{\mu}} \right\} + Cot\bar{\gamma} \right] Cos\gamma \tag{2.56}$$

Now, put

$$\Delta = \frac{H}{\lambda_x} \left\{ \frac{1}{V\mu} - \frac{1}{\overline{V\mu}} \right\} + \cot\bar{\gamma}$$

and using a well known trignometric identity,

$$\gamma = \tan^{-1}\left[\frac{1}{\Delta}\right] + \cos^{-1}\left[\frac{1}{\mu\sqrt{\Delta^2+1}}\right] \tag{2.57}$$

Expression (2.57) is the solution of the Euler equation for the time-range optimal control problem with altitude dependence of μ suppressed. In Fig. 6, the solution (2.57) evaluated using a representative H/λ_x value from the first equilibrium regime is shown. From this figure it may be observed that solution family is oscillatory about the equilibrium point. A similar family of solutions is obtained if the multiplier ratio H/λ_x from the second equilibrium regime is used, as illustrated in Fig. 7. Using H/λ_x values from the third equilibrium regime, i.e., values to the right of $V(T-D)_{max}$ in Fig. 5, results in the solution family given in Fig. 8. In this figure a pair of transients leading to and away from the equilibrium point may be observed. Other transient paths appear to be connected with those flight conditions which do not involve prolonged operation at or near the equilibrium point. It is of interest at this juncture to point out the similarity of Figs. 6 and 7 to Fig. 3. The solutions in Fig. 8 bear some resemblance to the plot of Fig. 2. It will be seen

subsequently that the oscillatory paths of Fig. 6 and 7
generally fail the conjugate-point test for durations
exceeding one period and furnish a minimum only for short-
duration problems. According to Fig. 8, then, "long"
optimal time-range trajectories are made up of a transient
path leading to the equilibrium conditions, flight at the
equilibrium condition and a transient path leading to the
terminal boundary conditions. If the boundary conditions are
off the transient paths, jumps in path-angle take place.
Hence, it is clear that the assumption made with regard to
the magnitude of $\dot{\gamma}$ will be violated on segments of the
optimal time-range trajectory unless the boundary conditions
happens to be on a transient path and sufficiently close to
the equilibrium flight condition.

2.3 CONCLUSIONS

In this chapter a study of the time-range-fuel optimal
control problem for aircraft using the intermediate vehicle
model was presented. Employing the constant-density-
atmosphere assumption, the range optimum climb and glide,
and the time-range optimum problems were studied. One notes
that the range problem has oscillatory solutions when a
positive margin of thrust over drag exists. With zero
thrust, the solution obtained is the flattest glide with a

family of transients leading to and from the L/D_{max} point. For the time-range problem, values of the multiplier ratio H/λ_x to the left (low-speed side) of the $V(T-D)_{max}$ point produce oscillatory solutions. With H/λ_x values chosen to the right of airspeed corresponding to $V(T-D)_{max}$, a solution family consisting of a set of transients leading to and from the equilibrium point, defined by the particular choice of the the multiplier ratio, is obtained. Optimality of these Euler solutions are investigated in the next chapter using second-order necessary conditions. To verify the conclusions arrived at in this chapter, numerical computations are carried out using the data for the F-4 aircraft in Chapter IV.

Chapter III

SECOND - ORDER NECESSARY CONDITIONS

It is known that the sufficient conditions for a functional $J(x)$ to have a "weak" minimum for $x = x^*$ are that the first variation $\delta J(x)$ vanishes for $x = x^*$ and that the second variation $\delta^2 J(x)$ be strongly positive for $x = x^*$ (Ref 78). Investigation of the conditions for vanishing of the first variation leads to the Euler-Lagrange equations and transversality conditions. The positivity requirement of second variation of the functional $J(x)$ leads to the Legendre-Clebsch and Jacobi necessary conditions. If both the strengthened Legendre-Clebsch condition and strengthened Jacobi test are satisfied by an extremal, it can be shown that the second variation of the performance index $J(x)$ is positive for sufficiently small variations (Refs 78 through 86). Thus, the functional $J(x)$ has a weak relative minimum if the extremal satisfies 1) the transversality conditions 2) the strengthened Legendre-Clebsch necessary condition and, 3) the strengthened Jacobi condition. In addition, if the extremal satisfies the Weierstrass condition, it affords a strong relative minimum for $J(x)$. In optimal-control problems, when the control vector is not subject to inequality constraints, it can be shown that the Pontryagin

maximum principle is equivalent to the Weierstrass condition (Refs 24,79,86 and 87). Hence, in these problems if the extremal satisfies the transversality conditions and the strengthened Legendre-Clebsch necessary condition together with the strengthened Jacobi condition, it provides a strong relative minimum for the performance index $J(x)$. For a relative maximum the preceding sufficiency test applies if the inequality associated with the strengthened Legendre-Clebsch test is reversed.

In the following, families of Euler solutions obtained in Chapter II for range-optimal climb and glide, and time-range optimal problems are examined using the Legendre-Clebsch and Jacobi necessary conditions. It will be seen that the constant-density-atmosphere assumption enables the analytical treatment of the Jacobi test for these problems.

3.1   LEGENDRE-CLEBSCH NECESSARY CONDITIONS

From Euler-Lagrange equation (2.6), with the fuel multiplier $\lambda_{\widetilde{W}}$ set to zero,

$$\frac{\partial H}{\partial \gamma} = - \lambda_V \, g \, \cos\gamma + \lambda_h \, V \, \cos\gamma - \lambda_x \, V \, \sin\gamma \tag{3.1}$$

and

$$\frac{\partial^2 H}{\partial \gamma^2} = (\lambda_V \, g - \lambda_h \, V) \, \sin\gamma - \lambda_x \, V \, \cos\gamma \tag{3.2}$$

Setting the left member of equation (3.1) to zero as required for a stationary minimum of the Hamiltonian leads to

$$\text{Tan}\gamma = (\lambda_h V - \lambda_V g)/\lambda_x V$$

Or

$$\text{Tan}\gamma = (\lambda_V g - \lambda_h V)/(- \lambda_x V) \qquad (3.3)$$

From (3.3), then

$$\cdot \text{Sin}\gamma = \frac{(\lambda_h V - \lambda_V g)\; \sigma}{\sqrt{(\lambda_h V - \lambda_V g)^2 + \lambda^2_x V^2}} \qquad (3.4)$$

and

$$\text{Cos}\gamma = \frac{\lambda_x V \sigma}{\sqrt{(\lambda_h V - \lambda_V g)^2 + \lambda^2_x V^2}} \qquad (3.5)$$

where $\sigma = \pm 1$. Employing (3.4) and (3.5) in (3.2), the sign of σ can be determined.

Next, the transversality conditions for the range problem, viz., $\lambda_x = 1$ for range minimization and $\lambda_x = -1$ for range maximization is used in (3.2), with the following result.

$$\lambda_x = 1, \quad \frac{\partial^2 H}{\partial \gamma^2} > 0 \text{ if } \gamma \text{ lies in the}$$

second or third quadrant   (3.6)

$\lambda_x = -1$, $\frac{\partial^2 H}{\partial \gamma^2} < 0$ if γ lies in the

first or fourth quadrant   (3.7)

From (3.6) it is clear that, with no restrictions on path angle γ, the minimum-range-climb trajectory is that which maximizes the range in the negative direction, a result which is perhaps obvious. The implication is that with no constraint on the final value of time or fuel, the "steepest climb" problem does not possess a minimum or even a lower bound.

Attention is drawn to the solution to this problem given by Miele (Ref 5) using the Green's theorem device. According to Ref 5, the optimal trajectory for the "steepest climb" problem consists of a central path flown along the $(T-D)_{max}$ locus in the airspeed-altitude chart with vertical climb/dive transitions at the ends to meet the boundary conditions if they are off the $(T-D)_{max}$ path. There is an important difference in vehicle modeling from that of the present work which should be noted as a key to resolving disparities between the character of optimal paths emerging: The analysis of Ref 5 in essence replaces $Cos\gamma$ in equation (1.16) with unity so that the problem solved is maximum altitude in a given distance (arc length) rather than in a given range.

Consider, next, the imposition of limits on path-angle γ, say $-90^{\circ} \leqslant \gamma \leqslant 90^{\circ}$. In this case, one observes that by alternating between vertical-climb and vertical-dive paths, the range-to-climb can be made identically zero. This is a consequence of the intermediate vehicle modeling in which there is no limit to the steepness of climb. Examination of energy rate

$$\dot{E} = V(T-D)/W$$

shows that it is positive as long as there exists a positive margin of thrust over drag. Since energy can be traded-in for altitude or airspeed, any combination of these can be reached in zero range using a composite vertical climb/dive trajectory. Additionally, there is no preferred location within the flight envelope for switching from vertical climb to vertical dive and vice versa. It is concievable, therefore, that in the limiting case, the minimum-range-climb path will tend to a "chattering arc" with infinite number of switchings between the climb and dive flight segments.

Chattering arcs can also arise in the minimum-time climb and minimum-fuel climb problems. Consider, for example, a parabolic distribution of specific excess power vs airspeed as shown in Fig. 9. In Chapter II it was shown,

for the minimum-time climb problem, that the Euler equation (2.14) can be satisfied either by vertical flight, $\cos\gamma = 0$, or by flight at the airspeed corresponding to the local maximum of specific excess power ($\widetilde{V}$ in Fig. 9) at each energy level. Choosing a pair of airspeeds V^* and V^{**} about $\widetilde{V}$, a trajectory consisting only of vertical climb/dive flight segments switching between V^* and V^{**} can be constructed. The choice of these airspeeds is arbitrary, as long as the specific excess power $V(T-D)/W > 0$, since this will ensure a net gain in energy. If V^* and V^{**} are chosen just to the left and just to the right of $\widetilde{V}$, minimum-time performance is approached. In the limit as they approach $\widetilde{V}$, a chattering solution is defined along with a lower bound on the time index. For general end conditions, straight-up and/or straight-down transients precede and follow the chattering subarc in a composite solution.

On the other hand, the Legendre-Clebsch necessary condition is met in the strengthened form along the maximum-range-glide and time-range optimal trajectories for the values of path angle γ in the first and fourth quadrants.

It may be noted at this point that in the cases of time or fuel-minimization problems with range open, the Legendre-Clebsch necessary condition is met only in weak form along central arcs and hence, these trajectories fall in the class

of singular extremals. In general, demonstrating sufficient conditions for singular extremals to be minimizing is a nontrivial task, though extensive results exist (Refs 72,88, and 89). However, a theorem originally due to Mancill (Ref 90), and widely applied (Refs 4 through 7 and 91) in problems of flight mechanics, enables one to establish the sufficient condition for a strong relative minimum, along central arcs, for minimum-time-climb and minimum-fuel-climb problems as

(i) Minimum-time-to-climb

$$\frac{\partial}{\partial h}[V(T-D)]\Big|_{E = \text{Constant}} = 0 \qquad (3.8)$$

$$\frac{\partial^2}{\partial h^2}[V(T-D)]\Big|_{E = \text{Constant}} < 0 \qquad (3.9)$$

(ii) Minimum-fuel-climb

$$\frac{\partial}{\partial h}[V(T-D)/Q]\Big|_{E = \text{Constant}} = 0 \qquad (3.10)$$

$$\frac{\partial^2}{\partial h^2}[V(T-D)/Q]\Big|_{E = \text{Constant}} < 0 \qquad (3.11)$$

In Ref 72, the inequality (3.9) was obtained using the Generalized Legendre-Clebsch necessary condition in conjunction with energy modeling. A question that arises naturally here is the relation between Mancill's work and

the Generalized Legendre-Clebsch necessary condition. In an appendix, this is discussed in detail. Suffice it to state here that, for problems containing two non-ignorable state variables and one control, under a smoothness hypothesis, this theorem yields a sufficient condition for a strong relative minimum.

3.2   JACOBI'S NECESSARY CONDITION

In the earlier section, it was shown that the Legendre-Clebsch necessary condition is met with a margin for maximum-range glide and the time-range optimal problems. Consequently, the Euler solutions for these problems are optimal for initial and terminal boundary conditions sufficiently close together. For extremals of finite length, however, the task of ensuring that the second variation is non-negative for admissible neighboring paths leads to the accessory-minimum problem in the Calculus of Variations. This in essence boils down to a search for a system of admissible variations, not identically zero, which offer the most severe competition in the sense of minimizing the second variation. If a system of nonzero variations can be found which makes the second variation zero, then it is clear that a neighboring path is competitive and that the test extremal furnishes at best an improper minimum and at

worst a merely stationary value (Ref 92). The first value of the independent variable $x = x^+ > x_o$ for which such a non trivial system can be found defines a conjugate point. One approach to the accessory-minimum problem in optimal-control theory consists of expanding the augmented criterion (the variational Hamiltonian) to second order and all constraints to first order to obtain a matrix-Riccati equation (Refs 23 and 87). Existence of a bounded symmetric-matrix solution to this Riccati equation, then, determines the existence of a conjugate point. An alternate procedure for the conjugate-point test was suggested in Ref 92, involving the examination of the rank of a matrix of variations of the states with respect to the initial values of the costates. This procedure will be adopted in the present work. It needs to be stressed that both these approachs lead to the same conclusions and choice between them is entirely a matter of convenience.

According to the analysis of Ref 92, for the Mayer problem, the rank of the matrix of variations of states and the multiplier corresponding to the state being minimized with respect to the initial values of the costates, evaluated along the test extremal, viz.

the rank of

$$\begin{bmatrix} \dfrac{\partial x_2}{\partial \lambda_{1_0}} & \dfrac{\partial x_2}{\partial \lambda_{2_0}} \cdots \cdots \cdots \cdots & \dfrac{\partial x_2}{\partial \lambda_{n_0}} \\ \vdots & \vdots & \vdots \\ \vdots \cdots \cdots & \vdots \cdots \cdots \cdots \cdots \cdots \cdots & \vdots \\ \vdots & \vdots & \vdots \\ \dfrac{\partial x_n}{\partial \lambda_{1_0}} & \dfrac{\partial x_n}{\partial \lambda_{2_0}} \cdots \cdots \cdots \cdots & \dfrac{\partial x_n}{\partial \lambda_{n_0}} \\ \dfrac{\partial \lambda_1}{\partial \lambda_{1_0}} & \dfrac{\partial \lambda_1}{\partial \lambda_{2_0}} \cdots \cdots \cdots \cdots & \dfrac{\partial \lambda_1}{\partial \lambda_{n_0}} \end{bmatrix} \qquad (3.12)$$

provides the criterion for the existence of a conjugate point. If the rank of the matrix (3.12) drops at any point along the test extremal, it is indicative of the existence of a conjugate point.

It is evident that numerical procedures may be set up to evaluate the elements of the Jacobi-test matrix, see Ref 93 for example. Details of one such scheme will be discussed in the next chapter. The intention is to test the Euler solutions obtained for maximum-range glide and time-range optimal problems with altitude dependence of thrust and drag supressed, for conjugate points. In view of the particularly simple form of the conjugate-point test for these problems, it seems reasonable to attempt to obtain analytical approximations for the partial derivatives required in the Jacobi test matrix.

3.2.1   Conjugate-Point Test for Maximum-Range Glide

The maximum-range glide problem may be thought of as the maximization of the final altitude with zero thrust, for a specified range with time and fuel open. Since it is convenient to work with range as the independent variable, the equations of motion (1.14) through (1.16) are rewritten as

$$V' = \frac{g(T-D)}{W\,V\,\cos\gamma} - \frac{g}{V}\,\tan\gamma \tag{3.13}$$

$$h' = \tan\gamma \tag{3.14}$$

where

$$' \equiv \frac{d}{dx}$$

Note that equation (1.17) corresponding to fuel consumption has been deleted in the above set. The Euler equation for the range problem is

$$\gamma' = \frac{1}{(T-D)}\left\{\left(\frac{\partial}{\partial h} - \frac{g}{V}\frac{\partial}{\partial V}\right)[T-D]\right\} \tag{3.15}$$

The initial value of the path angle γ_o may be considered to be playing the role of λ_{V_0}, and since λ_h is constant, the Jacobi-test matrix (3.12) becomes

$$\begin{bmatrix} \dfrac{\partial V}{\partial \lambda_{h_0}} & \dfrac{\partial V}{\partial \gamma_0} \\[2ex] \dfrac{\partial \lambda_h}{\partial \lambda_{h_0}} & \dfrac{\partial \lambda_h}{\partial \gamma_0} \end{bmatrix} = \begin{bmatrix} \dfrac{\partial V}{\partial \lambda_{h_0}} & \dfrac{\partial V}{\partial \gamma_0} \\[2ex] 1 & 0 \end{bmatrix} \tag{3.16}$$

It is clear that the rank of the test matrix (3.16) is determined by the term $\frac{\partial V}{\partial \gamma}_0$. Therefore, if the sign of this quantity changes along the Euler solution, it is indicative of the existence of a conjugate point.

Considering, next, the case of constant-density-atmosphere, the altitude becomes an ignorable state variable and the equations (3.13) through (3.15) becomes

$$V' = \frac{g(T-D)}{W\ V\ \cos\gamma} - \frac{g}{V}\ \tan\gamma \qquad (3.17)$$

$$\gamma' = -\frac{1}{(T-D)}\ \frac{g}{V}\ \frac{\partial}{\partial V}(T-D) \qquad (3.18)$$

To obtain analytical approximation to the term $\frac{\partial V}{\partial \gamma}_0$, the equations (3.17) and (3.18) are linearized about an equilibrium point defined by

$$\bar{\gamma} = \sin^{-1}\left[\frac{T-D}{W}\right] \qquad (3.19)$$

and, V obtained from

$$\frac{\partial}{\partial V}(T-D) = 0 \qquad (3.20)$$

resulting in

$$\delta V' = -A_1\ \delta V - A_2\ \delta\gamma \qquad (3.21)$$

$$\delta\gamma' = A_3\ \delta V \qquad (3.22)$$

where

$$A_1 = \frac{g}{W\ \cos\gamma}\ \frac{T-D}{V^2} - g\ \frac{\tan\gamma}{V^2} \qquad (3.23)$$

$$A_2 = - \left[\frac{g(T-D) \, Sin\gamma}{W \, V \, Cos^2\gamma} - \frac{g}{V} \, Sec^2\gamma \right]$$

$$(3.24)$$

$$A_3 = - \frac{g}{V(T-D)} \frac{\partial^2}{\partial V^2}(T-D) \qquad (3.25)$$

upon further simplification, equations (3.23) through (3.25) become

$$A_1 = 0 \qquad\qquad (3.26)$$

$$A_2 = \frac{g}{V} \qquad\qquad (3.27)$$

$$A_3 = - \frac{g}{V(T-D)} \frac{\partial^2}{\partial V^2}(T-D) \qquad (3.28)$$

Using Laplace transforms, equations (3.21) and (3.22) can be written as

$$\delta V(s) = - \frac{A_2}{s} \, \delta\gamma(s) \qquad\qquad (3.29)$$

$$\delta\gamma(s) = \frac{A_3}{s} \, \delta V(s) + \frac{\delta\gamma_0}{s} \qquad (3.30)$$

Note that $\delta V_0 = 0$. Combining (3.29) and (3.30),

$$\delta V(s) = - \frac{A_2}{s} \left[\frac{A_3 \, \delta V(s) + \delta\gamma_0}{s} \right] \qquad (3.31)$$

Or

$$\frac{\delta V(s)}{\delta\gamma_0} = - \frac{A_2}{s^2 + A_2 A_3} \qquad\qquad (3.32)$$

The roots of the denominator polynomial in expression (3.32) are either real or complex conjugates depending on the sign of the term $A_2 A_3$. These two cases are considered separately in the following.

(i) $A_2 A_3 < 0$, the roots are $\pm \sqrt{-A_2 A_3}$, real and symmetric about the imaginary axis in the complex plane. In this case, inverse Laplace transform of (3.32) yields

$$\frac{\delta V}{\delta \gamma}_o = - A_2 \frac{\text{Sinh } (\theta x)}{\theta} \tag{3.33}$$

where $\theta = \sqrt{-A_2 A_3}$.

It is clear that the expression (3.33) is zero only at $x = 0$. Consequently, if $A_2 A_3 < 0$, the rank of the test matrix (3.16) remains constant along the Euler solution and conjugate points will not occur.

(ii) $A_2 A_3 > 0$, the roots are $\pm i \sqrt{A_2 A_3}$. Inverse transformation of (3.32) then results in

$$\frac{\delta V}{\delta \gamma}_o = - A_2 \frac{\text{Sin } (\Psi x)}{\Psi} \tag{3.34}$$

where $\Psi = \sqrt{A_2 A_3}$.

In this case, the expression (3.34) changes sign at

$$x = \frac{n \pi}{\Psi} \tag{3.35}$$

and conjugate points will occur for sufficiently large range x.

From the above, the condition for non-occurrence of conjugate points is

$$A_2 A_3 < 0 \qquad\qquad (3.36)$$

or

$$- (g/V)^2 \ \frac{1}{(T-D)} \ \frac{\partial^2}{\partial V^2} (T-D) < 0 \qquad\qquad (3.37)$$

For the glide problem, $T = 0$, and the expression (3.37) yields the following result :

$$\text{if} \ \ \frac{\partial^2 D}{\partial V^2} > 0, \ \text{conjugate points will not occur.} \qquad (3.38)$$

The inequality (3.38) specifies a drag vs airspeed distribution which will be satisfied in all but very unusual aircraft configurations. This expression requires the aircraft to operate at the airspeed corresponding to minimum drag to maximize the range in gliding flight, and is consistent with engineering intuition. Note that the result (3.38) can be obtained by using a version of the energy model in conjunction with Mancill's theorem (Ref 90).

Hence, the Euler solution for maximum-range glide under constant-density-atmosphere assumption satisfies the strengthened Jacobi necessary condition. Since these

trajectories also satisfy the strengthened Legendre-Clebsch necessary condition, the Euler solution affords a relative maximum for this problem.

A similar exercise is next carried out for the time-range problem.

3.2.2 Conjugate-Point Test for the Time-Range Problem

The optimal-control problem in this case is the maximization of the final altitude for a specified range with fixed final time. The equations of motion (3.13) and (3.14) will be used in the following analysis also. With the interpretation of H as the time multiplier, the Jacobi test matrix for this problem becomes

$$
\begin{bmatrix}
\frac{\partial V}{\partial \lambda_{h_0}} & \frac{\partial V}{\partial H_0} & \frac{\partial V}{\partial \gamma_0} \\[2ex]
\frac{\partial t}{\partial \lambda_{h_0}} & \frac{\partial t}{\partial H_0} & \frac{\partial t}{\partial \gamma_0} \\[2ex]
\frac{\partial \lambda_h}{\partial \lambda_{h_0}} & \frac{\partial \lambda_h}{\partial H_0} & \frac{\partial \lambda_h}{\partial \gamma_0}
\end{bmatrix}
$$

Or

$$
\begin{bmatrix}
\frac{\partial V}{\partial \lambda_{h_0}} & \frac{\partial V}{\partial H_0} & \frac{\partial V}{\partial \gamma_0} \\[2ex]
\frac{\partial t}{\partial \lambda_{h_0}} & \frac{\partial t}{\partial H_0} & \frac{\partial t}{\partial \gamma_0} \\[2ex]
1 & 0 & 0
\end{bmatrix}
\tag{3.39}
$$

Hence, the sign of

$$\frac{\partial V}{\partial H_o} \frac{\partial t}{\partial \gamma_o} - \frac{\partial V}{\partial \gamma_o} \frac{\partial t}{\partial H_o} \qquad (3.40)$$

evaluated along the Euler solution determines the rank of the test matrix (3.39). If the expression (3.40) changes its sign along the Euler solution for the time-range problem, it is indicative of the existence of a conjugate point.

Note that time appears in this problem as a state-like variable with

$$t' = \frac{1}{V \cos\gamma} \qquad (3.41)$$

As before, a prime on the variables denote differentiation with respect to the range variable x. The analysis given in the following will employ the constant-density-atmosphere assumption, permitting the deletion of expression (3.14) from the system. In this case, the Euler equation is

$$\gamma' = \frac{\cos\gamma}{V^3(T-D)} \ g \ (H/\lambda_x) \ \frac{\partial}{\partial V}[V(T-D)]$$

$$- \frac{g}{V(T-D)} \ \frac{\partial}{\partial V}(T-D) \qquad (3.42)$$

The equations (3.13), (3.41) and (3.42) are next linearized about an equilibrium point at a particular altitude,

$$\delta V' = a_o \ \delta V - a_1 \ \delta\gamma \qquad (3.43)$$

$$\delta t' = - a_2 \ \delta V + a_3 \ \delta\gamma \qquad (3.44)$$

$$\delta\gamma' = a_4 \ \delta V - a_5 \ \delta\gamma + a_6 \ \delta H_o \qquad (3.45)$$

where

$$a_o = \frac{g}{W \, V \, Cos\gamma} \frac{\partial}{\partial V}(T-D) \tag{3.46}$$

$$a_1 = \frac{g}{V} \tag{3.47}$$

$$a_2 = \frac{1}{V^2 \, Cos\gamma} \tag{3.48}$$

$$a_3 = \frac{Sin\gamma}{V \, Cos^2\gamma} \tag{3.49}$$

$$a_4 = -\frac{Cos\gamma}{V^4} g \, (H/\lambda_x)$$

$$+ \frac{\partial}{\partial V}(T-D) \frac{g}{V^2(T-D)}\left[1 - \frac{Cos\gamma}{V} \, (H/\lambda_x)\right]$$

$$+ \frac{g}{V(T-D)^2}\left\{\frac{\partial}{\partial V}(T-D)\right\}^2 \left[1 - \frac{Cos\gamma}{V}(H/\lambda_x)\right]$$

$$+ \frac{g}{V(T-D)} \frac{\partial^2}{\partial V^2}(T-D)\left[\frac{Cos\gamma}{V} \, (H/\lambda_x) - 1\right]$$

$$\tag{3.50}$$

$$a_5 = a_o \tag{3.51}$$

$$a_6 = \frac{Cos\gamma}{V^3(T-D)} \quad \frac{g}{\lambda_x}\left\{V \frac{\partial}{\partial V}(T-D) + (T-D)\right\} \tag{3.52}$$

Equations (3.43), (3.44) and (3.45) constitute a linear, constant-coefficient system which can be put in the following form using Laplace transforms (initial conditions on δV and δt are zero)

$$\frac{\delta V(s)}{\delta\gamma_o} = \frac{-a_1}{s^2 + (a_1 a_4 - a_o a_5)} \tag{3.53}$$

$$\frac{\delta V(s)}{\delta H_o} = \frac{-a_1 a_6}{s[s^2 + (a_1 a_4 - a_o a_5)]} \tag{3.54}$$

$$\frac{\delta t(s)}{\delta \gamma_o} = -\frac{[(a_o a_3 - a_1 a_2) - a_3 s]}{s[s^2 + (a_1 a_4 - a_o a_5)]} \tag{3.55}$$

$$\frac{\delta t(s)}{\delta H_o} = -\frac{[(a_o a_3 - a_1 a_2) - a_3 s]}{s^2[s^2 + (a_1 a_4 - a_o a_5)]} \tag{3.56}$$

putting $\omega_n^2 = (a_1 a_4 - a_o a_5)$ \qquad\qquad (3.57)

and

$$T = \frac{-a_3}{(a_o a_3 - a_1 a_2)} . \tag{3.58}$$

and cancelling out common constants in the numerator, the equations (3.53) through (3.56) can be brought to the form

$$\frac{\delta V(s)}{\delta \gamma_o} = \frac{\omega_n^2}{s^2 + \omega_n^2} \tag{3.59}$$

$$\frac{\delta V(s)}{\delta H_o} = \frac{\omega_n^2}{s(s^2 + \omega_n^2)} \tag{3.60}$$

$$\frac{\delta t(s)}{\delta \gamma_o} = \frac{(1 + Ts)\,\omega_n^2}{s(s^2 + \omega_n^2)} \tag{3.61}$$

$$\frac{\delta t(s)}{\delta H_o} = \frac{(1 + Ts) \, \omega_n^2}{s^2(s^2 + \omega_n^2)}$$

(3.62)

Equations (3.61) and (3.62) may be further simplified using the expressions (3.59) and (3.60).

$$\frac{\delta t(s)}{\delta \gamma_o} = \frac{\delta V(s)}{\delta H_o} + T \frac{\delta V(s)}{\delta \gamma_o}$$ (3.63)

$$\frac{\delta t(s)}{\delta H_o} = \frac{\omega_n^2}{s^2(s^2 + \omega_n^2)} + T \frac{\delta V(s)}{\delta H_o}$$

(3.64)

Equations (3.63) and (3.64) imply

$$\frac{\delta t(x)}{\delta \gamma_o} = \frac{\delta V(x)}{\delta H_o} + T \frac{\delta V(x)}{\delta \gamma_o}$$ (3.65)

$$\frac{\delta t(x)}{\delta H_o} = L^{-1}\left\{ \frac{\omega_n^2}{(s^2 + \omega_n^2)s^2} \right\} + T \frac{\delta V(x)}{\delta H_o}$$

(3.66)

using (3.65) and (3.66) in (3.40)

$$- \frac{\delta V}{\delta \gamma_o} \frac{\partial t}{\delta H_o} + \frac{\partial V}{\partial H_o} \frac{\partial t}{\partial \gamma_o} =$$

$$-\frac{\delta V(x)}{\delta \gamma_o} L^{-1}\left\{ \frac{\omega_n^2}{s^2(s^2 + \omega_n^2)} \right\} + \left\{ \frac{\delta V(x)}{\delta H_o} \right\}^2$$

(3.67)

And consequently, one needs to obtain the inverse transform of only three transfer functions, namely

$$\frac{\delta V(s)}{\delta \gamma_O} \quad , \quad \frac{\delta V(s)}{\delta H_O} \quad , \quad \frac{\omega_n^2}{s^2(s^2 + \omega_n^2)}$$

Two distinct cases can be seen to arise here.

(i) $\omega_n^2 > 0$, the roots of the denominator polynomial is a complex conjugate pair and the inverse Laplace transformation yields

$$\frac{\partial V}{\partial H_O} \frac{\partial t}{\partial \gamma_O} - \frac{\partial V}{\partial \gamma_O} \frac{\partial t}{\partial H_O} =$$

$$2 - \omega_n \, x \, Sin(\omega_n x) - 2 \, Cos(\omega_n x) \qquad (3.68)$$

The expression (3.68), after being zero at $x = 0$, will subsequently become zero at

$$x = \frac{2\pi}{\omega_n} \qquad (3.69)$$

Hence, in this case the rank of the Jacobi test matrix (3.39) will drop at the range defined by expression (3.69) implying the existence of a conjugate point

(ii) $\omega_n^2 < 0$, the roots of the denominator polynomial are real, distinct and symmetric about the imaginary axis in the complex plane. In this case

$$\frac{\partial V}{\partial H_O} \frac{\partial t}{\partial \gamma_O} - \frac{\partial V}{\partial \gamma_O} \frac{\partial t}{\partial H_O} =$$

$$2 + x \, \Omega \, \text{Sinh}(\Omega x) - 2 \, \text{Cosh}(\Omega x) \qquad\qquad (3.70)$$

where $\Omega = \sqrt{- \, \omega_n^2}$

The expression (3.70) is zero only at $x = 0$. Consequently, the rank of the test matrix (3.39) will not change along the Euler solution and conjugate points will not occur.

The expression (3.57) for ω_n^2 is next evaluated with the multiplier ratio H/λ_x chosen from each of the three equilibrium points discussed in section 2.2. Unlike the maximum-range glide situation, the expression (3.57) is too involved to be amenable to analytical treatment. This forces one to evaluate ω_n^2 numerically. It is found that ω_n^2 is less than zero only in the third equilibrium regime, i.e., H/λ_x values to the right of the $V(T-D)_{max}$ point. Hence, the oscillatory solutions shown in Figs 6 and 7 fail the conjugate point test for durations exceeding one period and furnish a minimum only for short-duration problems. On the other hand, Euler solutions generated with the time-range multiplier ratio H/λ_x chosen to the right of the airspeed for $V(T-D)_{max}$ satisfy the strengthened Legendre-Clebsch and Jacobi necessary conditions, and hence are optimal trajectories for the time-range problem.

3.3   CONCLUSIONS

The Legendre-Clebsch and the Jacobi necessary conditions for the range optimal climb and glide, and the time-range optimal problems were examined in this chapter. It is found that the minimum-range climb or the "steepest climb" problem without any constraint on path angle possess no proper minimum or even a lower bound. If an artificial limit on path angle, say $-90^\circ \leqslant \gamma \leqslant 90^\circ$, is imposed, the minimum-range trajectory consists of vertical up-down flight segments and any altitude-airspeed pair can be reached in zero range if there exists a positive margin of thrust over drag. On the other hand, the maximum-range glide path satisfies the strengthened Legendre-Clebsch and Jacobi necessary condition if a proper minimum-drag point exists.

The Euler solutions for time-range problem meets the Legendre-Clebsch necessary condition with a margin. However, the strengthened Jacobi necessary condition is satisfied for "long" paths only by non-oscillatory solutions generated with the time-range multiplier ratio H/λ_x chosen to the right of airspeed corresponding to $V(T-D)_{max}$ in Fig. 5.

The analysis presented so far employed the constant-density-atmosphere assumption. In the next chapter, a numerical study of Euler equation using typical high performance aircraft (F-4) data is given. The discussions

there will also include a numerical conjugate-point test for
the time-range optimal-control problem.

Chapter IV

NUMERICAL SOLUTIONS

With the insight gained for the range and time-range optimal problems with altitude dependence of thrust and drag supressed, a numerical study of the more general case in which the aerodynamic coefficients are functions of Mach number and the thrust is Mach-altitude dependent, is next undertaken. The data for a version of the F-4 aircraft with afterburner operative is used in this study. The thrust data is presented in Table. 1, and the zero-lift drag coefficient C_{Do} and the induced drag coefficient are given as functions of Mach number in Tables 2 and 3 respectively. A cubic-spline representation (Ref 104) is used to interpolate the aerodynamic coefficients. The drag coefficient is computed as

$$C_D = C_{Do} + K \, C_L^2$$

where $C_L = 2 \, W/(\rho \, V^2 \, S)$

The drag is then obtained as the usual product of drag coefficient, dynamic pressure and the aircraft wing area. A cubic-spline lattice (Ref 104) is used to interpolate the value of thrust at a given altitude and Mach number. Atmospheric density and speed of sound as functions of

altitude are interpolated from standard atmosphere tables using cubic splines. The system differential equations (1.14) through (1.17) and the Euler equation (2.13) are integrated using a fifth-order Runge-Kutta-Verner method with variable step size.

The level-flight envelope for the aircraft under consideration is shown in Fig. 10 along with the "energy climb" path, generated by determining the maximum of specific excess power at each energy level. A discontinuity in the energy climb schedule due to transonic drag rise may be noted (Ref 44).

4.1 RANGE-OPTIMAL TRAJECTORIES

Range-optimal trajectories are generated by setting the fuel multiplier λ_W and the variational Hamiltonian H to zero in the general Euler equation (2.13). If the initial data is given, the numerical solution for the system (1.14) through (1.17) and (2.13) can be generated. The full-thrust case is considered first.

Typical time histories of altitude, airspeed and path-angle for the case in which a positive margin of thrust over drag exists, is shown in Figs 11, 12 and 13 respectively. As observed in Chapter II, the solutions are oscillatory, with the amplitude of oscillation depending on the particular

choice of initial conditions. For instance, if the initial value of altitude and airspeed are such that the partial derivative of (T-D) with respect to altitude, with specific energy held constant, vanishes, the oscillation has zero amplitude. As the initial conditions move away from the path

$$\frac{\partial}{\partial h}(T\text{-}D)\bigg|_{E = Constant} = 0,$$ the amplitude of oscillation in

the Euler solution increases. If one were to superimpose the numerical solution on the locus of $(T\text{-}D)_{max}$ points in the airspeed-altitude plane, the oscillations would be found to take place about this locus. It will be seen later in this chapter that the oscillatory paths do not satisfy the Jacobi test for durations exceeding half a period and hence, are not optimal.

The situation with thrust set to zero is interesting, however. In this case, the Euler solutions are non-oscillatory and highly sensitive in nature. A maximum-range glide path is shown in the airspeed-altitude chart in Fig. 14. This path is generated by adjusting the initial value of flight-path angle γ_o and integrating the system equations until the resulting trajectory passes through the desired terminal conditions. In the present case, the adjustment in γ_o had to be carried out to 10-or 12-decimal-place accuracy on an IBM-370/158 computer with quadruple precision. The temporal evolution of altitude, airspeed and flight-path

angle corresponding to this path are given in Figs. 15, 16 and 17 respectively. These trajectories will be seen to satisfy the Jacobi necessary condition and are optimal for maximum-range glide. Note that jumps in path angle must be permitted at the initial and final points unless the specified boundary condition on γ happens to be the same as that emerging from computations.

4.2   TIME-RANGE OPTIMAL PATHS

The numerical investigation of time-range optimal paths is considerably more complex than for the range-optimal problem, mainly due to the involvment of the time-range multiplier ratio H/λ_x. Of the various time-range optimal paths, a trajectory of particular interest in practical applications is the climb-dash intercept path (Ref 13). This trajectory occurs in aircraft pursuit problems as a transient leading to the dash point or high speed point on the level-flight envelope, arising whenever the evader is at a sufficiently large distance from the interceptor. In this section, numerical computations carried out to generate the optimal climb-dash intercept trajectory will be discussed in detail. Note that the fuel multiplier $\lambda_{\widetilde{W}} = 0$.

To obtain the value of the time-range multiplier ratio corresponding to the climb-dash path, an equilibrium

analysis along the lines of section 2.2 is first undertaken. Setting the time derivatives in equations (1.14) through (1.17) and (2.13) to zero, the time-range multiplier ratio H/λ_x can be computed, with the specific energy $E = h + \frac{V^2}{2g}$ held constant. A sample plot resulting from these computations is shown in Fig. 18, with specific energy frozen at a typical value of 60,000 feet. Three regimes identified in section 2.2 can also be seen in this figure. The multiplier ratios, H/λ_x, to the left of the point marked A (the $(T-D)_{max}$ point) in this figure are all positive. Depending on the nature of thrust and drag, there may exist points at which H/λ_x is zero. H/λ_x values between point A and the point marked B (the $V(T-D)_{max}$ point) are negative. The time-range multiplier ratio H/λ_x is positive to the right of $V(T-D)_{max}$ point. Numerical solutions with H/λ_x values chosen to the left of $V(T-D)_{max}$ point at various energy levels indicated that they are oscillatory, similar in nature to the trajectories obtained in the full-thrust minimum-range climb problem. It will be seen subsequently that these oscillatory paths fail the Jacobi test for durations exceeding a period and furnish a minimum only for short-duration problems.

The time-range optimal solutions generated with multiplier ratio H/λ_x chosen to the right of $V(T-D)_{max}$ point

at each energy level, are nonoscillatory and highly
sensitive in nature. These paths satisfy the Jacobi
necessary condition and are time-range optimal. To obtain
the value of the multiplier ratio corresponding to the
climb-dash path, a plot of the locus of equilibrium points
with a particular value of H/λ_x, is made. The value of the
multiplier ratio is adjusted next so that the locus of
equilibrium points terminates at the dash point on the
level-flight envelope. This value of H/λ_x is used to
generate optimal climb-dash trajectories. The equilibrium
climb-dash path along with the "energy climb" schedule is
shown in Fig. 19. The flight envelope is superimposed on
this figure for clarity of presentation. As one decreases
the value of the range multiplier λ_x it is clear that the
equilibrium climb-dash path will approach the energy climb
schedule. In the limit $\lambda_x = 0$, i.e., final value of range is
no longer of interest, the two paths merge, a result
consistent with engineering intuition.

With the time-range multiplier chosen from the
aforesaid analysis, all that remains to obtain the optimal
trajectory is to determine the initial value of the control
variable γ_o for a given set of initial conditions on
altitude and airspeed. An Euler solution for initial values
of altitude and airspeed close to the equilibrium climb-dash

locus is shown in Fig. 20. The level flight envelope, energy climb schedule and the equilibrium climb-dash locus are also shown in this figure. It can be seen that the Euler solution stays close to the equilibrium locus. To determine this trajectory, an iteration was undertaken on the initial value of the control variable γ. With quadruple precision on the IBM-370/158, γ_o had to be determined to 13 significant digits. To illustrate the sensitivity of the Euler solution to the initial value of the path angle γ, the last digit of γ_o is perturbed in the positive and negative sense with trajectories 1 and 2 shown in Fig. 20 resulting. A few more Euler solutions with initial conditions far removed from the equilibrium locus are shown in Fig. 21. The temporal evolution of altitude, airspeed and path angle corresponding to the trajectory "a" in Fig. 21 is given in Figs. 22, 23 and 24 respectively.

An interesting feature of the Euler solutions for the Climb-dash intercept problem is that they funnel rapidly into a certain corridor in the airspeed-altitude chart, in the vicinity of the equilibrium locus corresponding to unaccelerated flight. This feature of the solution family may be exploited to simplify the computation of optimal trajectories.

4.3   NUMERICAL CONJUGATE-POINT TEST

To carry out the conjugate-point test for the range-optimal and time-range optimal paths discussed in the earlier sections, the matrices (3.16) and (3.39) need to be evaluated along the Euler solutions.   The numerical evaluation of the elements of these Jacobi test matrices evidently require computer codes considerably more complex than those required for the calculation of Euler soltions. As an alternative to the numerical solution of equations of variations, Cicala (Refs 92 and 93) suggested a scheme in which the partial derivatives with respect to the λ_{1_o} are calculated approximately in terms of difference quotients. Thus, small increments in the initial λ_i are employed in the evaluation of neighboring solutions of the system (1.14) through (1.17) and (2.13). A computer code was assembled based on Cicala's suggestion (Ref 93) to evaluate the partial derivatives required in matrices (3.16) and (3.39). This code generates three trajectories corresponding to each multiplier, the first being the nominal and next two, the neighboring trajectories obtained by perturbing the initial value of the multiplier in the positive and negative sense. The required partial derivatives are then computed using a central differencing scheme (Ref 105).

One of the main difficulties encountered in this approximation is the errors arising from higher-order effects. Such errors can be controlled to a certain extent by checking the linearity of the $x_i(t)$ differences versus the magnitude of the corresponding increment in the initial λ value. This check has been incorporated in the computer program.

The oscillatory minimum-range climb path is tested for conjugate points first. It is then found that the term $\partial V/\partial \gamma_0$ in the matrix (3.16) changes sign every half cycle of oscillation indicating the appearance of a conjugate-point. Hence these paths are non-minimizing. The maximum-range glide paths, however, satisfy the conjugate-point test. This result is consistent with that obtained in section 3.2.1 for the restricted case of constant-density-atmosphere.

For the time-range problem, the conjugate point test is carried out for various values of H/λ_x picked from the three equilibrium regimes at a particular energy level. It is then found that the oscillatory solutions obtained with H/λ_x values from the first two equilibrium regimes indicate the existence of a conjugate-point after a cycle of oscillation. The non-oscillatory trajectories corresponding to H/λ_x values on the right of $V(T-D)_{max}$ at a particular energy level, on the other hand, satisfy the no-conjugate-point

condition. Hence, the climb-dash trajectories presented in Fig. 21 are optimal.

4.4   CONCLUSION

Numerical solution of the Euler equation for range-optimal and time-range-optimal problems was presented in this chapter. A method for choosing the time-range multiplier ratio H/λ_x for the climb-dash mission was discussed in detail. A numerical conjugate-point test based on a scheme suggested by Cicala (Ref 93) was also presented.

It is found that the maximum-range glide paths and non-oscillatory time-range solutions satisfy the Jacobi necessary condition and are optimal. Oscillatory time-range trajectories fail the Jacobi test for durations exceeding one cycle of oscillation.

Numerical solutions of the Euler equation and numerical conjugate-point test has essentially reinforced the conclusions arrived at in Chapters II and III, wherein the constant-density-atmosphere asssumption was used in the analysis.

Chapter V

CONCLUSIONS

In this work, optimal flight in the vertical plane with a vehicle model intermediate in complexity between point-mass and energy models was studied. Flight-path angle takes on the role of control variable, and range-open problems feature subarcs of vertical flight and singular subarcs as previously reported.

Minimum-range climb problem (the steepest climb of Ref 5) has been found to have no minimum, not even a lower bound. In Ref 5, the steepest-climb problem was studied using the Green's theorem device of reference 4 and 90. There is an important difference in the vehicle modeling from that of the present work which should be noted as a key to resolving disparities between the character of optimal paths emerging. The analysis of Ref 4 and 5 in essense replace $\cos\gamma$ in equation (1.16) with unity so that the problem solved is maximum altitude in a given distance (i.e. arc length) rather than in a given range. This is a necessity with the linear-integral approach which can accomodate only problems of dimension two and a very special form of state equations. A detailed discussion of the linear-integral approach and its relation to singular

optimal control is given in an appendix. The solution to the distance-climb problem consists of a central path flown along a $(T-D)_{max}$ locus in the airspeed-altitude plane with vertical climb and dive transitions at the ends to meet specified boundary conditions. Imposition of a constraint on the path angle, $-90^{\circ} \leqslant \gamma \leqslant 90^{\circ}$, showed that the "solution" to the steepest climb can be constructed from vertical climb and dive flight segments alone, and that any altitude-airspeed pair can be reached in zero range. The possibility of this composite climb/dive path tending to a "chattering arc" was touched upon. Maximum-range glide paths emerging from the intermediate vehicle modeling were found to satisfy the strengthened Legendre-Clebsch and Jacobi necessary conditions. The use of constant-density-atmosphere assumption enabled detailed analysis of the Euler solutions and the Jacobi test for this problem.

Since fixed-throttle minimum-fuel trajectories are not of interest in practical situations, main attention has been focussed on the time-range optimal control problem. For the special case in which thrust and drag depend only on airspeed, a plot of the ratio of time and range mutipliers H/λ_{x} for equilibrium corresponding to unaccelerated flight, revealed the existence of three regimes. Positive values of H/λ_{x} on the low-speed side of $V(T-D)_{max}$ and all negative

values of H/λ_x were shown to yield oscillatory solutions. Although these meet the Legendre-Clèbsch necessary conditions, they fail the conjugate-point test. Euler solutions with H/λ_x chosen to the right of the $V(T-D)_{max}$ point satisfy both the Legendre-Clebsch and Jacobi necessary conditions and are nonoscillatory in character.

Numerical solution of the Euler equation and a numerical conjugate-point test for the F-4 aircraft data reinforced the conclusions arrived at in the analytical exercise.

From a practical viewpoint, the time-range trajectories which terminate at the "dash-point" on the level-flight envelope are of particular interest. The mutiplier ratio H/λ_x corresponding to this point is determined using the locus of equilibrium points at each energy level corresponding to unaccelerated flight. With this value of H/λ_x, Euler solution for any altitude-airspeed pair is obtained by iterating on the initial value of γ, the control variable. Euler equations were obtained for various initial conditions. One observes that these tend to funnel rapidly into a certain corridor in the airspeed-altitude chart, in the vicinity of the equilibrium locus corresponding to unaccelerated flight. This feature of the solution family can be exploited in practical situations to simplify the computation of optimal trajectories.

5.1   <u>FUTURE</u> <u>WORK</u>

An important task to be undertaken is the comparison of the results obtained from the intermediate vehicle modeling with those generated by solving the complete two-point-boundary-value problem for aircraft. This will enable quantitative evaluation of the intermediate vehicle model and its usefulness in applications.

Another interesting investigation would be the study of time-fuel-range problem with throttle control included.

REFERENCES

1. Kaiser, F.,'Der Steigflug mit Strahlflugzeugen - Teil I, Bahngeschwindigkiet für Besten Steigens', Versuchsbericht 262 - 02 - L44', Messerschmitt A.G., Augsburg, April 1944 (Translated as Ministry of supply RTP/TIB translation GDC/15/148T)

2. Lush, K.J., 'A Review of the Problem of Choosing a Climb Technique with Proposals for a New Climb Technique for High Performance Aircraft', Aeronautical Research Council Report Memo, No. 2557, 1951.

3. Rutowski, E.S., 'Energy approach to the general aircraft performance problem', Journal of the Aeronautical Sciences, Vol. 21, March 1954, pp 187-195.

4. Miele, A., 'Problemi di Minimo Tempo Nel Volo Non-Stazionario degli Aeroplani', Atti della Accademia delle Scienze di Torino, Vol. 85, 1950-1951.

5. Miele, A., 'General Solutions of Optimum problems in Nonstationary Flight', NACA TM 1388, Oct. 1955.

6. Miele, A., 'Optimum Flight Paths of Turbojet Aircraft', NACA TM-1389, Sept. 1955.

7. Miele, A., 'On Nonsteady Climb of Turbojet Aircraft', Journal of the Aeronautical Sciences, Vol. 21, 1959, pp 781-783.

8. Miele, A., and Capellari, J.O., 'Approximate Solutions to Optimum Flight Trajectories for a Turbojet-Powered Aircraft, NASA TN D-152, Sept. 1959.

9. Johnson, I.L., 'Optimization of Solid-Rocket Assisted Space Shuttle Ascent Trajectory', Journal of Space Craft and Rockets, Vol. 12, Dec. 1975, pp 765-769

10. Bulirsch, R., 'Die Mehrzielmethode zur numerischen Losung von Nichtlinearen Randwertproblemen und Aufgaben der Optimalen Steuerung', Vortrag im Lehrgang Flugbahnoptimierung der Carl-Cranz Gesellschaft. V. October, 1971.

11. Keller, H.B., 'Numerical Methods for Two-Point boundary value Problems', Blaisdell, London, 1968.

12. Keller, H.B., 'Numerical Solution of Two Point Boundary Value Problems', CBMS-NSF Regional Conference series in Applied Mathematics, Vol. 24, SIAM, Philadelphia, PA, 1976.

13. Weston, A.R., 'On-board Near-Optimal Climb-Dash Energy Management', Ph.D. Dissertation, Virginia Polytechnic Institute and State University, Blacksburg, VA., December 1982.

14. Stengel, R.F., and Miller, G.E., 'Flight tests of a Microprocessor Control System', Journal of Guidance and Control, Vol.3, Nov-Dec 1980, pp 494-500

15. Vinh, N.X., 'Optimal Trajectories in Atmospheric Flight', Elsevier, New York, 1981.

16. Gordon, C.N., 'Flight Software for Optimal Trajectories in Transport Aircraft', AIAA Guidance and Control Conference, Gatlinburg, TN., Aug. 15-17, 1983.

17. Leitmann, G., 'On Optimum Control of Lifting Vehicles', Proceedings of the Fourth U.S National Congress on Applied Mechanics, Vol.1, 1962, pp 243-249

18. Kelley, H.J., 'Reduced Order Modeling in Aircraft Mission Analysis', AIAA Journal, Vol.9, Feb. 1971, pp 349-350.

19. Bryson, A.E., Desai, M.N., and Hoffman, K., 'Energy-State Approximation in Performance Optimization of Supersonic Aircraft', Journal of Aircraft, Vol.6, Nov-Dec. 1969, pp 481-488.

20. Kelley, H.J., and Lefton, L., 'Supersonic Aircraft Energy Turns', Automatica, Vol.8, Sept 1972, pp 575-580.

21. Parsons, M.G., Bryson, A.E., and Hoffman, W.C., 'Long Range Energy State Maneuvers for Minimum Time to a Specified Terminal Conditions', 11th Aerospace Sciences meeting, Jan. 1973, AIAA paper No.73-229; also JOTA, Vol.17, Dec. 1975, pp 447-463.

22. Hedrick, J.K., and Bryson, A.E., 'Three-Dimensional Minimum-Time Turns for a Supersonic Aircraft', Journal of Aircraft, Vol.9, Feb. 1972, pp 115-121.

23. Lin, C.F., 'Optimum Maneuvers of Supersonic Aircraft', Ph.D. Dissertation, University of Michigan, Ann Arbor, Michigan, 1980.

24. Bryson, A.E., and Ho, Y.C., 'Applied Optimal Control', Blaisdell, Waltham, Mass., 1969.

25. Zagalsky, N.B., Irons, R.P., and Schultz, R.L., 'Energy-State Approximation and Minimum-Fuel Fixed-Range Trajectories', Journal of Aircraft, Vol.8, June 1971, pp 488-490.

26. Houlihan, S.C., Cliff,E.M., and Kelley, H.J., 'A Study of Chattering Cruise', Journal of Aircraft, Vol.19, Feb. 1982, pp 119-124.

27. Gilbert, E.G., and Parsons, M.G., 'Periodic Control and the Optimality of Aircraft Cruise', Journal of Aircraft, Vol.13, Oct. 1976, pp 828-830.

28. Heermann, H., and Kretsinger, P., 'The Minimum-Time Problem', Journal of Astronautical Sciences, Vol.II, Winter 1964, pp 83-107.

29. Kelley, H.J., Falco, M., and Ball, D.J., 'Air Vehicle Trajectory Optimization', SIAM Symposium on Multivariable System Theory, Cambridge, Mass., Nov. 1-3, 1962.

30. Falco, M., and Kelley, H.J., 'Aircraft Symmetric Flight Optimization', in Control and Dynamic Systems, Vol.10, C.T.Leondes (Ed.), Academic Press, New York 1973, pp 89-129.

31. Shinar, J., Merari, A., Blank, D., and Medinah, E.M., 'Analysis of Optimal Turning Maneuvers in the Vertical Plane', Journal of Guidance and Control, Vol.13, Jan-Feb 1980, pp 69-77.

32. Ardema, M.D., 'Solution of the Minimum-Time-To-Climb Problem by Matched Asymptotic Expansions', AIAA Journal, Vol. 14, July 1976, pp 843-850.

33. Wasow, W., 'Asymptotic expansions for Ordinary Differential Equations', John Wiley and Sons, New York, 1975.

34. Tihonov, A.N., 'Systems of Differential Equations Containing Small Parameters in the Derivatives', Mathematichiskii Sbornik, Vol.31, 1952.

35. Bender, C.M., and Orzag, S.A., 'Advanced Mathematical Methods for Scientists and Engineers', McGraw-Hill Publishing Co., New York, 1978.

36. Kelley, H.J., 'Flight-Path Optimization with Multiple Time Scales', Journal of Aircraft, Vol.8, April 1971, pp 238-240.

37. Kelley, H.J., and Edelbaum, T.N., 'Energy Climbs, Energy Turns and Asymptotic Expansions', Journal of Aircraft, Vol.7, Jan-Feb 1970, pp 93-95.

38. Kelley, H.J., 'Aircraft Maneuver Optimization by Reduced Order Approximation', in Control and Dynamic Systems, Vol.10, C.T.Leondes (Ed.), Academic Press, New York, 1973, pp 131-178.

39. Calise, A.J., 'Singular-Perturbation Methods for Variational Problems in Aircraft Flight', IEEE Transactions on Automatic Control, Vol. AC-21, June 1976, pp 345-353.

40. Breakwell, J.V., 'Optimal Flight-Path-Angle Transitions in Minimum-Time Airplane Climbs', Journal of Aircraft, Vol.14, Aug. 1977, pp 782-786.

41. Ardema, M.D., 'Linearization of the Boundary-Layer Equations of the Minimum Time-to-Climb Problem', Journal of Guidance and Control, Vol.2, Sept-Oct. 1979, pp 434-436.

42. Breakwell, J.V., 'More about Flight-Path-Angle Transitions in Optimal Airplane Climbs', Journal of Guidance and Control, Vol.1, May-June 1978, pp 205-208.

43. Mehra, R.K., Washburn, R.B., Sajan, S., and Carrol, J.V., 'A Study of the Application of Singular Perturbation Theory', NASA CR-3167, 1979.

44. Weston, A.R., Cliff, E.M., and Kelley, H.J., 'Altitude Transitions in Energy Climbs', Automatica, Vol.19, March 1983, pp 199-202.

45. Gracey, C., and Price, D.B., 'Altitude/Path Angle Transitions in Fuel-Optimal Problems for Transport Aircraft', American Control Conference, San Francisco, CA., June 22-24, 1983.

46. Kelley, H.J., 'An Optimal Guidance Approximation Theory', IEEE Transactions on Automatic Control, Vol. AC-9, Oct. 1964, pp 375-380.

47. Kelley, H.J., 'Guidance Theory and Extremal Fields', IRE Transactions on Automatic Control, Vol. AC-7, Oct. 1962, pp 75-82.

48. Breakwell, J.V., Speyer, J.L., and Bryson, A.E., 'Optimization and Control of Nonlinear Systems using the Second Variation', SIAM Journal of Control, Vol.1, 1963, pp 193-223.

49. Dayton, A.D.(Editor), 'Is Real-Time, On-Line Optimal Control Feasible?', Report No. AFOSR 70-1379TR, June 1970.

50. Calise, A.J., and Moerder, D.D., 'Singular-Perturbation Techniques for Real-Time Aircraft Trajectory Optimization and Controls', NASA CR-3597, Aug. 1982.

51. Sridhar, B., and Gupta, N.K., 'Missile Guidance Laws based on Singular Perturbations Methodology', Journal of Guidance and Control, Vol.3, March-April 1980, pp 158-165.

52. Calise, A.J., 'Extended Energy Management for Variational Problems in Aircraft Flight', AIAA Journal, Vol.15, March 1977, pp 314-321.

53. Calise, A.J., 'Singular Perturbation Analysis of Optimal Thrust Control with Proportional Navigation Guidance', Journal of Guidance and Control, Vol.14, July-Aug. 1980, pp 312-318.

54. Calise, A.J., 'Singular Perturbation Techniques for On-Line Optimal Flight-Path Control', Journal of Guidance and Control, Vol.4, July-Aug. 1981, pp 398-405.

55. Chakravarty, A.J.M., and Vagners, J., 'Application of Singular Perturbations Theory to On-Board Aircraft Optimization', AIAA Aerospace Sciences Meeting, St. Louis, Missouri, Jan. 1981.

56. Chakravarty, A.J.M., and Vagners, J., 'Development of 4-D Time-Controlled Guidance Laws using Singular Perturbations Methodology', American Control Conference, Arlington, VA., June 14-16, 1982, Session WP4, p 1107.

57. Chakravarty, A.J.M., and Vagners, J., '4-D Aircraft Flight Path Management in Real Time', American Control Conference, Sanfrancisco, CA., June 22-24, 1983, Session TP7, p 794

58. Kelley, H.J., Cliff, E.M, and Weston, A.R., 'Energy State Revisited', AIAA Atmospheric Flight Mechanics Conference, Gatlinburg, TN., Aug. 15-17, 1983, paper No. AIAA-83-2138.

59. Kelley, H.J., and Well, K., 'An Approach to Intercept On-Board Calculations', American Control Conference Proceedings, San Francisco, CA., June 22-24, 1983, Session TP7, p 799.

60. Weston, A.R., Cliff, E.M, and Kelley, H.J., 'On-Board Near-Optimal Climb-Dash Energy Management', American Control Conference, San Francisco, CA., June 22-24, 1983, Session TA7, pp 534-539.

61. Kelley, H.J., 'An Investigation by Variational Methods of Flight Paths for Optimum Performance', Sc.D Dissertation, New York University, New York, May 1958.

62. Collins, B.P., 'Energy Modeling for Aviation Fuel Efficiency', International Air Transportation Conference, Atlantic City, N.J., May 1981, Paper No. AIAA-81-0789-CP.

63. Schultz, R.L., and Zagalsky, N.R., 'Aircraft Performance Optimization', Journal of Aircraft, Vol.9, Feb. 1972, pp 108-114.

64. Speyer, J.L., 'On Fuel Optimality of Cruise', Journal of Aircraft, Vol.10, Dec.1973, pp 763-765.

65. Menon, P.K.A., Kelley, H.J., and Cliff, E.M., 'Optimal Symmetric Flight with an Intermediate Vehical Model', AIAA Guidance and Control Conference, Gatlinburg, TN., Aug. 15-17, 1983, paper No. AIAA-83-2238-CP.

66. Speyer, J.L., 'Nonoptimality of Steady-State Cruise for Aircraft', AIAA Journal, Vol.14, Nov.1976, pp 1604-1610.

67. Gilbert, E.G., and Lyons, D.T., 'Improved Aircraft Cruise by Periodic Control: The Computation of Optimal Specific Range Trajectories', Proceedings of the Conference on Information Science and Systems, Princeton University, Princeton, NJ., March 1980.

68. Breakwell, J.V., and Shoaee, H., 'Minimum Fuel Flight Paths for a Given Range', Astrodynamics Conference, Danvers, Mass., Aug. 11-13, 1980, AIAA/AAS paper 80-1160.

69. Proceedings of the workshop on 'Cyclic Cruise Flight', NASA Langley Research Center, Hampton, VA., June 28-29, 1982.

70. Menon, P.K.A., Kelley, H.J., and Cliff, E.M., 'Singular Optimal Control and the Identically Non-Regular Problem in the Calculus of Variations', paper in preparation.

71. Miele, A., 'Flight Mechanics', Addison-Wesley, Reading, MA., 1962.

72. Kelley, H.J., Kopp, R.E., and Moyer, G.H., 'Singular Extremals', in Topics in Optimization, Ed. G. Leitmann, Chapter 3, Academic Press, New York, 1967.

73. Uehara, S., 'Theoretical Investigation of Minimum-Time-Loop Maneuvers for Jet Aircraft', Ph.D Dissertation, California Institute of Technology, Pasadena, California, 1974.

74. Uehara, S., Stewart, H.J.,and Wood, L.J., 'Minimum-Time-Loop Maneuvers of Jet Aircraft', Journal of Aircraft, Vol.15, Aug. 1978, pp 449-455.

75. Kamke, E., 'Differentialgleichungen, Losungmethoden und Losungen, Band 1, Gewohnliche Differentialgleichungen, Third edition, Chelsea Publishing Co., New York, N. Y., 1948.

76. Boyce, W.E., and DiPrima, R.C., 'Elementary Differential Equations and Boundary Value Problems', John Wiley and Sons, New York, N.Y., 1977.

77. Rainville, E.D., and Bedient, P.E., 'Elementary Differential Equations', Macmillan Publishing Co., New York, N.Y., 1974.

78. Gelfand, I.M., and Fomin, S.V., 'Calculus of Variations', Prentice Hall Inc., Englewood Cliffs, N.J., 1963.

79. Hestenes, M.R., 'Calculus of Variations and Optimal Control Theory', Robert E. Krieger Publishing Co., New York, 1980.

80. Bolza, O., 'Lectures on the Calculus of Variations', G. E. Stechert and Co., New York, 1931.

81. Bliss, G.A., 'Calculus of Variations', The Open Court Publishing Co., La Salle, IL., 1925.

82. Bliss, G.A., 'Lectures on the Calculus of Variations', University of Chicago Press, Chicago, 1946.

83. Pierre, D.A., 'Optimization Theory with Applications', John Wiley and Sons, New York, 1969.

84. Caratheodory, C., 'Calculus of Variations and Partial Differential Equations of the First Order - Part II Calculus of Variations', Holden - Day Inc., San Francisco, 1967.

85. Larew, G.A., 'Necessary Conditions in the Problem of Mayer in the Calculus of Variations', Transactions of the American Mathematical Society, Vol. XX, 1919, pp 1-22.

86. Leitmann, G., 'The Calculus of Variations and Optimal Control', Plenum Press, New York, 1981.

87. Lawden, D.F., 'Analytical Methods of Optimization', Scottish Academic Press, London, 1975.

88. Bell, D.J., and Jacobson, D.H., 'Singular Optimal Control Problems', Academic Press, New York, 1975.

89. Moyer, G.H., 'Sufficient Conditions for a Strong Minimum in Singular Control Problems', SIAM Journal of Control, Vol. 11, 1973, pp 620-636.

90. Mancill, J.D., 'Identically Non-Regular Problems in the Calculus of Variations', Mathematica Y Fisica Teorica, Universidad Nacional del Tucuman, Republica Argentina, Vol. 7, No. 2, June 1950.

91. Miele, A., 'Extremization of Linear Integrals by Green's Theorem', in Optimization Techniques, Ed. G. Leitmann, Chapter 3, Academic Press, New York, 1962.

92. Kelley, H.J., and Moyer, G.H., 'Jacobi's Necessary Condition', in Topics in Optimization Theory, Grumman Research Department Report RE-159, June 1962.

93. Cicala, P., 'An Engineering Approach to the Calculus of Variations', Levrotto-Bella, Torino, Italy, 1957.

94. Isaacs, R.P., 'Differential Games', Robert E. Krieger Publishing Co., New York, 1975.

95. Haynes, G.W., 'On the Optimality of a Totally Singular Vector Control : An Extention of the Green's Theorem Approach to Higher Dimension', SIAM Journal of Control, Vol. 4, 1966, pp 662-677.

96. Goh, B.S., 'The Second Variation for the Singular Bolza Problem', SIAM Journal of Control, Vol. 4, 1966, pp 309-325.

97. Courant, R., 'Calculus of Variations and Supplementary notes Notes and Exercises', Mimeographed class notes, New York University, 1945-46.

98. Petrov, I.P., 'Variational Methods in Optimum Control Theory', Academic Press, New York, 1968.

99. Kelley, H.J., 'A Transformation Approach to Singular Subarcs in Optimal Trajectory and Control Problems', SIAM Journal of Control, Vol.2, 1965, pp 234-240.

100. McShane, E.J., 'The Calculus of Variations from the beginning through Optimal Control Theory', in Optimal Control and Differential Equations, Eds: A.B.Schwarzkopf, W.G.Kelley, and S.B.Eliason, Academic Press, New York, 1978.

101. Mancill, J.D., 'Unilateral Variations with Variable Endpoints', American Journal of Mathematics, Vol. LXIX, 1947, pp 121-138.

102. Young, L.C., 'Lectures on the Calculus of Variations and Optimal Control Theory', W.B.Saunders Co., Philadelphia, 1969.

103. Krotov, V.F., 'The Principal Problem of the Calculus of Variations for the Simplest Functional on a Set of Dis-continuous Functions', Soviet Mathematics Doklady, Vol. 2, 1961, pp 231-234.

104. Mummolo, F., and Lefton, L., 'Cubic Splines and Cubic-Spline Lattices for Digital Computation', Analytical Mechanics Associates, Inc. Report No. 72-88, July 1972. Revision dated December 1974.

105. Carnahan, B., Luther, H.A., and Wilkes, J.O., 'Applied Numerical Methods', John Wiley and Sons, New York, 1969.

C - 2

Appendix A

SINGULAR OPTIMAL CONTROL AND THE IDENTICALLY NON-REGULAR PROBLEM IN THE CALCULUS OF VARIATIONS

A.1   INTRODUCTION

In optimal-control problems featuring scalar control appearing linearly in the system differential equations, singular subarcs can sometimes arise. Along singular subarcs which are minimizing, the Generalized Legendre-Clebsch necessary condition should hold (Refs 72 and 88). A class of such optimal-control problems can be recast as identically non-regular problems in the classical Calculus of Variations if the dimension is low. Specifically, this transformation appears feasible if there are at most two non-ignorable state variables and one control variable. In general, the procedure involves a change in the independent variable under appropriate smoothness and monotonicity assumptions (Ref 94). (The phrase "classical Calculus of Variations" employed here refers to unconstrained problems, i.e., not to Lagrange-Mayer-Bolza problems.)

For this class of problems, Mancill (Ref 90) has obtained conditions for a minimizing singular arc. In Ref 90, Mancill made use of Green's theorem on line integrals to establish conditions for a strong relative minimum. Miele

(Refs 4 through 7 and 91) used the Green's theorem approach for problems with control bounds, extended the technique to handle isoperimetric constraints and carried out applications to several flight problems. Haynes (Ref 95) discussed an extension of the Green's theorem approach to higher dimensions using exterior Calculus, for the optimal control of systems with n state variables and n-1 controls appearing linearly in the state equations. The question of existence of totally singular vector control is discussed in considerable detail in this work. Goh (Ref 96) examined the singular Bolza problem and noted the connection between Miele's work and the identically non-regular problem in the Calculus of variations.

This appendix deals with an evaluation of Mancill's work and its relation to the Generalized Legendre-Clebsch necessary condition. A critique on the nature of transversality conditions for this class of problems is presented. Three illustrative examples are also given.

A.2   IDENTICALLY NON-REGULAR PROBLEM
The identically non-regular problem with fixed endpoints in the Calculus of Variations (Refs 80 and 90) is the minimization of an integral of the form

$$J = \int_{t_1}^{t_2} [P(t,x) + Q(t,x)\dot{x}]dt \tag{A.1}$$

with

$$x(t_1) = x_1 \quad \text{and} \quad x(t_2) = x_2 \tag{A.2}$$

Note that

$$[P(t,x) + Q(t,x)\dot{x}]_{\ddot{x}\ddot{x}} = 0 \tag{A.3}$$

It is known that the Euler's equation for this problem is either an identity or a finite equation (Refs 80,86,90 and 97). If it is an identity, the integral is independent of the path joining two fixed points and no proper minimum exists. On the other hand, if it is a finite equation, the Euler's equation is satisfied only along certain paths which in general do not pass through the specified end points.

These functionals are sometimes called "degenerate" because the Euler equation for such functionals is not a differential equation, but a finite equation without any derivatives of the unknown function (Ref 98).

Two theorems by Mancill (Ref 90), yield the necessary and sufficient conditions for a strong local minimum in these problems. These are presented in the following.

THEOREM 1. If E_{12} is of class D' and minimizes the integral J in the class of admissible curves joining 1 and 2, where $P(t,x)$ and $Q(t,x)$ are of class C^{2n} in R, then

$$\partial^{2n-1}P/\partial x^{2n-1} = \partial^{2n-1}Q/\partial t\partial x^{2n-2},$$

$$\partial^{2n}P/\partial x^{2n} \geqslant \partial^{2n}Q/\partial t\partial x^{2n-1}, \qquad \text{(I)}$$

if $\partial^{k}P/\partial x^{k} = \partial^{k}Q/\partial t\partial x^{k-1}$, $k = 1,2,3,\ldots\ldots 2n-2$, along arcs interior to R, including all isolated points in common with the boundary of R;

$$\partial^{r}P/\partial x^{r} \geqslant \partial^{r}Q/\partial t\partial x^{r-1} \qquad \text{(I}_B\text{)}$$

if $\partial^{k}P/\partial x^{k} = \partial^{k}Q/\partial t\partial x^{k-1}$, $k = 1,2,3\ldots r-1$, along arcs E_B in common with the boundary of R.

Let (I') and (I$_B'$) represent conditions (I) and (I$_B$) respectively with the inequalities $\geqslant$ replaced by the strict inequality $>$. This is a familiar notation in the classical Calculus of Variations and it will be employed in this work.

The first part of (I) with $n = 1$, is the Euler's necessary condition for this problem. The inequality in (I) with $n = 1$, is derived from the second variation. For $n > 1$ the conditions (I) are obtained from higher variations.

THEOREM 2. If $P(t,x)$ and $Q(t,x)$ are of class C^{2n} in R and the conditions (I') and (I$_B'$) are satisfied along an

admissible curve E_{12} joining 1 and 2, then E_{12} furnishes a strong proper relative minimum for the integral J in the class of admissible curves joining 1 and 2.

It is implied in Theorem 2 that the Euler equation is not an identity. This Theorem is proved using Green's theorem on line integrals. Mancill has given two additional theorems on the necessary and sufficient conditions for the identically non-regular problem with variable end points. However, the interpretation of these in the light of modern optimal-control theory points to the violation of the smoothness assumption essential to the results in Mancill's work. A detailed discussion of this is presented in section A.4.

At this point, it is perhaps interesting to compare the results obtained by Mancill with those of Miele (Refs 4 through 7 and 91). The first part of condition (I) in Theorem 1 with n = 1 is termed the "fundamental function" $\omega(t,x)$ in Miele's work. The inequality in (I) appears as a specification on the direction of traverse along the extremal. Similarly, the condition (I_B) of Mancill also appears in Miele's work as a specification on the direction of traverse along the boundary of the admissible region, applicable whenever the arcs interior to the admissible region are non-optimal.

A.3   THE PROBLEM IN AN OPTIMAL-CONTROL FORMAT

With a short development it will be shown that with $n = 1$, the inequality in (I) is the Generalized Legendre-Clebsch necessary condition for $q = 1$.

Consider the optimal control problem

$$
\text{Min} \int_{t_o}^{t_f} [P(t,x) + Q(t,x)u]dt \tag{A.4}
$$

subject to the differential constraint $\dot{x} = u$.

It is apparent that this problem is equivalent to the identically non-regular problem in the Calculus of Variations. Note that the control u is unbounded.

To proceed via the "modern" approach one defines the variational Hamiltonian

$$
H(\lambda,x,t,u) = P(t,x) + Q(t,x)u + \lambda u \tag{A.5}
$$

and forms the adjoint equation

$$
\dot{\lambda} = - P_x - Q_x u \tag{A.6}
$$

From the expression (A.5) for H, one has that along a singular subarc

$$
H_u = Q(t,x(t)) + \lambda(t) \tag{A.7}
$$

Differentiating this with respect to time, substituting $\dot{x} = u$ and using (A.6) for $\dot{\lambda}$, one finds

$$\frac{d}{dt}[H_u] = Q_t(t,x) - P_x(t,x) \tag{A.8}$$

Differentiating with respect to time again, while using $\dot{x} = u$, leads to

$$\frac{d^2}{dt^2}[H_u] = Q_{tt} - P_{xt} + (Q_{tx} - P_{xx})u \tag{A.9}$$

Hence the Generalized Legendre-Clebsch necessary condition for first order singular arc is

$$\frac{\partial}{\partial u}\left\{\frac{d^2}{dt^2}[H_u]\right\} = Q_{tx} - P_{xx} \leqslant 0 \tag{A.10}$$

that is

$$P_{xx} \geqslant Q_{tx} \tag{A.11}$$

The inequality (A.11) is the same as that in condition (I) of Mancill.

One notes that the inequality (I) of Mancill for $n > 1$ is not equivalent to the Generalized Legendre-Clebsch necessary condition with $q > 1$ but is something more general.

A.4   TRANSFORMATION TO CANONICAL FORM

To investigate the situations in which specified boundary conditions are off the path defined by the conditions (I), and the variable endpoint problem, a transformation approach discussed in Ref 99 is next employed. The identically non-regular problem is first brought into the Mayer format :

$$\dot{y} = P(t,x) + Q(t,x)u \qquad (A.12)$$

$$\dot{x} = u \qquad (A.13)$$

with t_1, t_2, $x(\tau_1) = x_1$, $x(t_2) = x_2$ specified. A minimum of $y(t_2)$ is sought with $y(t_1) = 0$.

Next a transformation of state variables will be performed so that the state system has a special form. The new state variables are z and x and the system is to have the control variable u appearing in only one of the state equations, the one for x.

The system is

$$\dot{z} = P(t,x) + \frac{\partial R}{\partial t}(t,x) \qquad (A.14)$$

$$\dot{x} = u \qquad (A.15)$$

and the choice of z leading to it is

$$z = y + R(t,x) \qquad (A.16)$$

where

$$R(t,x) = - \int^{x} z(t,\xi)d\xi \qquad\qquad (A.17)$$

(Refs 72 and 99). The end conditions are t_1, t_2, $x(t_1) = x_1$, $x(t_2) = x_2$ specified as before. The initial value of z is $z(t_1) = R(t_1, x_1)$ and a minimum of $z(t_2)$ is sought.

Since there are no bounds on the control u, it can behave impulsively and $x(t)$ can jump. If the equation (A.15) is discarded and a solution sought in the class of functions $x(t)$ piecewise continuous, x becomes control-like (Refs 72,99). At points $t_1 < t < t_2$, x minimizes the right member of equation (A.14).

$$x = \text{Arg min}_{x} \left[P(t,x) + \frac{\partial R}{\partial t}(t,x) \right] \qquad\qquad (A.18)$$

possibly exhibiting jump discontinuities in the interior of the interval depending on the nature of the time dependence of equation (A.14). The variable x will generally jump at the initial and final times to satisfy the end conditions unless the value emerging from expression (A.18) happens fortuitously to satisfy them.

The situation with endpoint freedom is interesting. Consider for example, t_1 and t_2 fixed as before, but $x(t_2)$ unspecified. To minimize $y(t_2)$, x should jump at the final time t_2 to the value

$$x(t_2) = \text{Arg max}_{x} R(t_2, x) \qquad\qquad (A.19)$$

This seems to be the nearest thing to a transversality condition that one can have with x control-like.

A.5   ILLUSTRATIVE EXAMPLES

To gain a better appreciation of Mancill's work, three examples are given in the following.

(1) Two elementary examples :

(a)   Min $\displaystyle\int_{t_o}^{t_f} x^2 \, dt$, subject to $\dot{x} = u$

$x(t_o) = x_o$ and $x(t_f) = x_f$ specified.

   Since there are no bounds on the control, the differential constraint is inactive. Hence, the problem in classical Calculus of Variations format is

$$\text{Min} \int_{t_o}^{t_f} x^2 \, dt \tag{A.20}$$

With the identification of

$$P(t,x) \equiv x^2 \tag{A.21}$$

$$Q(t,x) \equiv 0 \qquad\qquad (A.22)$$

The necessary conditions of Mancill (Ref 90) become,

$$2x = 0 \qquad\qquad (A.23)$$

and

$$2 \geqslant 0 \qquad\qquad (A.24)$$

The sufficient condition

$$2 > 0 \qquad\qquad (A.25)$$

is met in the strengthened form along the arc $x = 0$ and hence, the trajectory $x = 0$ affords a strong relative minimum. The result (A.25) was obtained in Ref 72 via the Generalized Legendre-Clebsch necessary condition.

If the initial and final conditions are off the $x = 0$ path, jumps in x are required at the end points. Such motions have no effect on the performance index.

The next example is chosen to illustrate the necessary conditions of Mancill for $n > 1$.

(b)   Min $\displaystyle\int_{t_o}^{t_f} x^4\, dt$, subject to $\dot{x} = u$

The conditions $x(t_o) = x_o$ and $x(t_f) = x_f$ specified. Since there are no bounds on the control variable, the problem in the Calculus of Variations format is

$$\text{Min} \int_{t_o}^{t_f} x^4\, dt \qquad\qquad (A.26)$$

The necessary conditions for a minimum are

$$4x^3 = 0 \qquad\qquad (A.27)$$

Hence $x = 0$ is the extremal. Further,

$$12x^2 = 0 \qquad\qquad (A.28)$$

$$24x = 0 \qquad\qquad (A.29)$$

$$24 \geq 0 \qquad\qquad (A.30)$$

Note that the sufficient condition, (A.30) with strengthened inequality, is met for $n = 4$.

Just as in the previous example, jumps in x must be permitted at the endpoints if the specified conditions are off the $x = 0$ path.

(2) Minimum-time aircraft climb

Following Miele (Ref 4 through 7), a model of aircraft in symmetric flight under the assumptions of constant weight and small path-angle is

$$\dot{V} = g[\{(T-D)/W\} - \text{Sin}\gamma]$$ (A.31)

$$\dot{h} = V \text{ Sin}\gamma$$ (A.32)

Differential equations for range rate and fuel-flow rate have been dropped from the system, since they are ignorable in this problem. The optimal-control problem is the minimization of time required to fly from an initial (V,h) pair to a final (V,h) pair, viz.

$$\text{Min} \int_{(V_i,h_i)}^{(V_f,h_f)} dt$$ (A.33)

Changing the independent variable from time to altitude,

$$V' = \frac{dV}{dh} = \frac{g(T-D)}{W \ V \ \text{Sin}\gamma} - \frac{g}{V}$$ (A.34)

$$\text{Min} \int_{(V_i,h_i)}^{(V_f,h_f)} \frac{dh}{V \ \text{Sin}\gamma}$$ (A.35)

Substituting next for $\sin\gamma$ in (A.35) from (A.34), the problem in the classical Calculus-of-Variations format is

$$\text{Min} \int_{(V_i,h_i)}^{(V_f,h_i)} \frac{W}{V(T-D)} + \frac{W\,V'}{g(T-D)} \; dh \qquad (A.36)$$

In this development, the monotonicity of the altitude variable has been tacitly assumed. If desired, $\sin\gamma$ may be constrained by defining an admissible region in the V-h space as suggested in Ref 5; however, this falls outside the Mancill model. Employing conditions (I) in Theorem 1, the necessary conditions for a minimum for arcs interior to the admissible region, are

$$\frac{\partial}{\partial V} \left\{ \frac{W}{g(T-D)} \right\} = \frac{\partial}{\partial h} \left\{ \frac{W}{V(T-D)} \right\} \qquad (A.37)$$

$$\frac{\partial^2}{\partial V^2} \left\{ \frac{W}{g(T-D)} \right\} \geq \frac{\partial^2}{\partial h \partial V} \left\{ \frac{W}{V(T-D)} \right\} \qquad (A.38)$$

The expressions (A.37) and (A.38) may be put in the following form

$$\frac{\partial}{\partial h} \left[V(T-D) \right] \bigg|_{E = \text{Constant}} = 0 \qquad (A.39)$$

$$\frac{\partial^2}{\partial h^2} \left[V(T-D) \right] \bigg|_{E = \text{Constant}} \leq 0 \qquad (A.40)$$

The sufficient condition for a strong relative minimum, then, is

$$\frac{\partial^2}{\partial h^2}\left[V(T-D)\right]\Bigg|_{E = Constant} < 0 \tag{A.41}$$

This result was obtained in Ref 72 using the Generalized Legendre-Clebsch necessary condition. The expression (A.39) corresponds to stationary points of excess power $V(T-D)$ along contours of constant energy $h + \frac{V^2}{2g}$. Inequality (A.41) implies that the stationary points of excess power along constant energy contours must be maxima, a result in accord with engineering intuition.

If the endpoints are off the path defined by (A.39) jumps in airspeed and altitude must be permitted to meet the boundary condition. With bounds on control, on the other hand, operation at one of the control limits is indicated.

The minimum-fuel climb problem may be handled in an analogous manner.

A.6   SMOOTHNESS DIFFICULTIES AND THEIR IMPACT

In Mancill's paper (Ref 90), and in classical Calculus of Variations treatments generally, the function $x(t)$, which appears along with its derivative, $x(t)$, as an argument of the integrand, is assumed to possess a first derivative which is at least piecewise continuous. The various theorems

of Ref 90 do not apply to discontinuous solutions of the type examined in the preceding section. In the classical setting one would say that no minimum exists in the class of admissible functions, but only a lower bound. For this reason, the classical Calculus of Variations is sometimes dubbed the "naive" theory (Refs 86,100). Indeed the classical treatments (Refs 80,86 and 97) focus entirely on the degenerate case in which the integral is independent of the path.

One is faced with the choice between extending the theory to admissible $x(t)$ piecewise continuous, or the introduction of bounds on control $u(t)$. Neither of these were done in Ref 90,and hence, this work is of limited applicability due to the explicit smoothness hypothesis. Another unwelcome complication in Mancill's work is the incorporation of state-inequality constraints, a relic of his earlier work on this special type of problem (Ref 101), which do not alleviate the smoothness difficulties.

Treatment of variational problems with $x(t)$ piecewise-continuous only has been given by Young (Ref 102) and Krotov (Ref 98 and 103). Bounded-control problems approached by Green's theorem have been studied by Miele (Refs 4 through 7 and 91). In Ref 91, the control bounds are imposed by defining an admissible region in the state-space.

A.7   CONCLUDING REMARKS

Mancill's two Theorems given in the present work are of interest and seem to have been ahead of their time. For the narrow class of problems considered by Mancill, the inequality (I) with n = 1 is equivalent to the generalized Legendre-Clebsch condition. Perhaps equally important was Mancill's introduction of the Green's Theorem device for the study of problems of small dimension.

Table. 1 . Thrust Data for F-4 Aircraft

MACH NUMBER

ALTITUDE	0.0	0.20	0.40	0.60	0.80	1.00	1.20	1.40	1.60	1.80	2.00	2.20	2.40	2.60
0.0	32.20	32.20	33.40	34.80	39.20	42.00	41.40	40.20	39.60	39.60	39.60	39.60	39.60	39.60
10.00	23.40	23.40	25.00	27.40	31.20	36.00	42.20	44.00	43.00	42.00	42.00	42.00	42.00	42.00
20.00	16.40	16.40	17.20	19.60	23.20	27.60	32.60	38.00	42.40	44.80	43.00	43.00	43.00	43.00
30.00	11.00	11.00	11.60	13.20	16.00	19.60	24.00	28.60	33.20	37.20	38.60	37.80	36.00	36.00
40.00	6.60	6.60	7.20	8.20	10.00	12.60	15.80	19.40	23.00	26.40	28.40	28.60	26.00	20.40
50.00	4.20	4.20	4.40	5.00	5.80	7.60	9.40	11.60	14.00	16.20	17.60	17.80	16.40	12.80
60.00	2.60	2.60	2.80	3.00	3.60	4.60	5.60	7.00	8.40	9.80	10.60	10.80	10.20	7.60
70.00	2.00	2.00	2.00	2.20	2.40	2.80	3.40	4.00	4.80	5.60	6.20	6.40	6.00	4.60

ALTITUDE * 1000 FT, THRUST * 1000 LBS

Table. 2 . Zero-Lift Drag Coefficient Data for F-4 Aircraft

MACH NO.	C_{Do}
0.0	0.0205
0.2000	0.0205
0.6500	0.0205
0.7500	0.0205
0.8000	0.0205
0.8500	0.0206
0.9000	0.0210
0.9500	0.0242
1.0000	0.0324
1.0500	0.0359
1.1000	0.0374
1.2000	0.0384
1.4000	0.0385
1.6000	0.0386
1.8000	0.0387
2.0000	0.0397
2.2000	0.0403
2.4000	0.0403
2.6000	0.0403

WEIGHT = 35000.0 LBS   WING AREA = 530 FT

Table. 3 . Induced Drag Coefficient Data for F-4 Aircraft

MACH NO.	K
0.0	0.1980
0.2000	0.1980
0.6500	0.1980
0.7500	0.2010
0.8000	0.2050
0.8500	0.2110
0.9000	0.2180
0.9500	0.2280
1.0000	0.2390
1.0500	0.2520
1.1000	0.2650
1.2000	0.2970
1.4000	0.3680
1.6000	0.4530
1.8000	0.5440
2.0000	0.6400
2.2000	0.7200
2.4000	0.7440
2.6000	0.7440
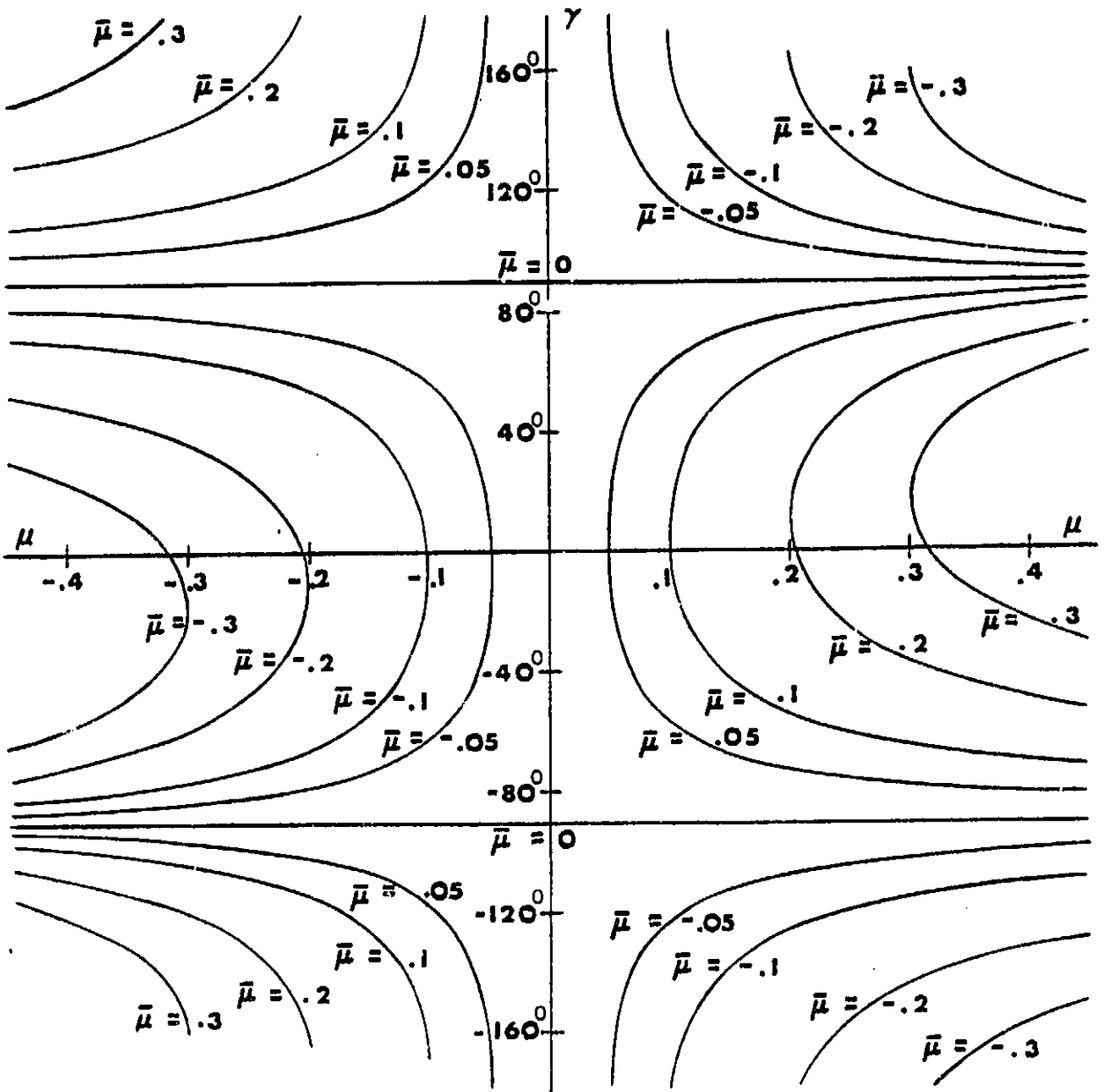
Fig. 1 . Flight-Path Angle vs. Acceleration variable for the
Range Problem

ORIGINAL PAGE IS
OF POOR QUALITY
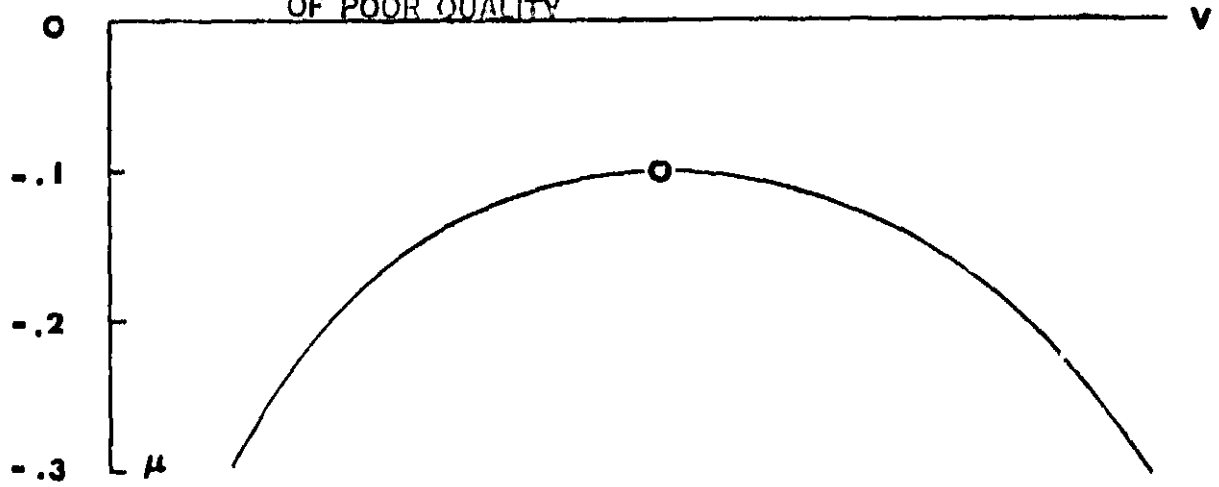
Acceleration variable vs Airspeed
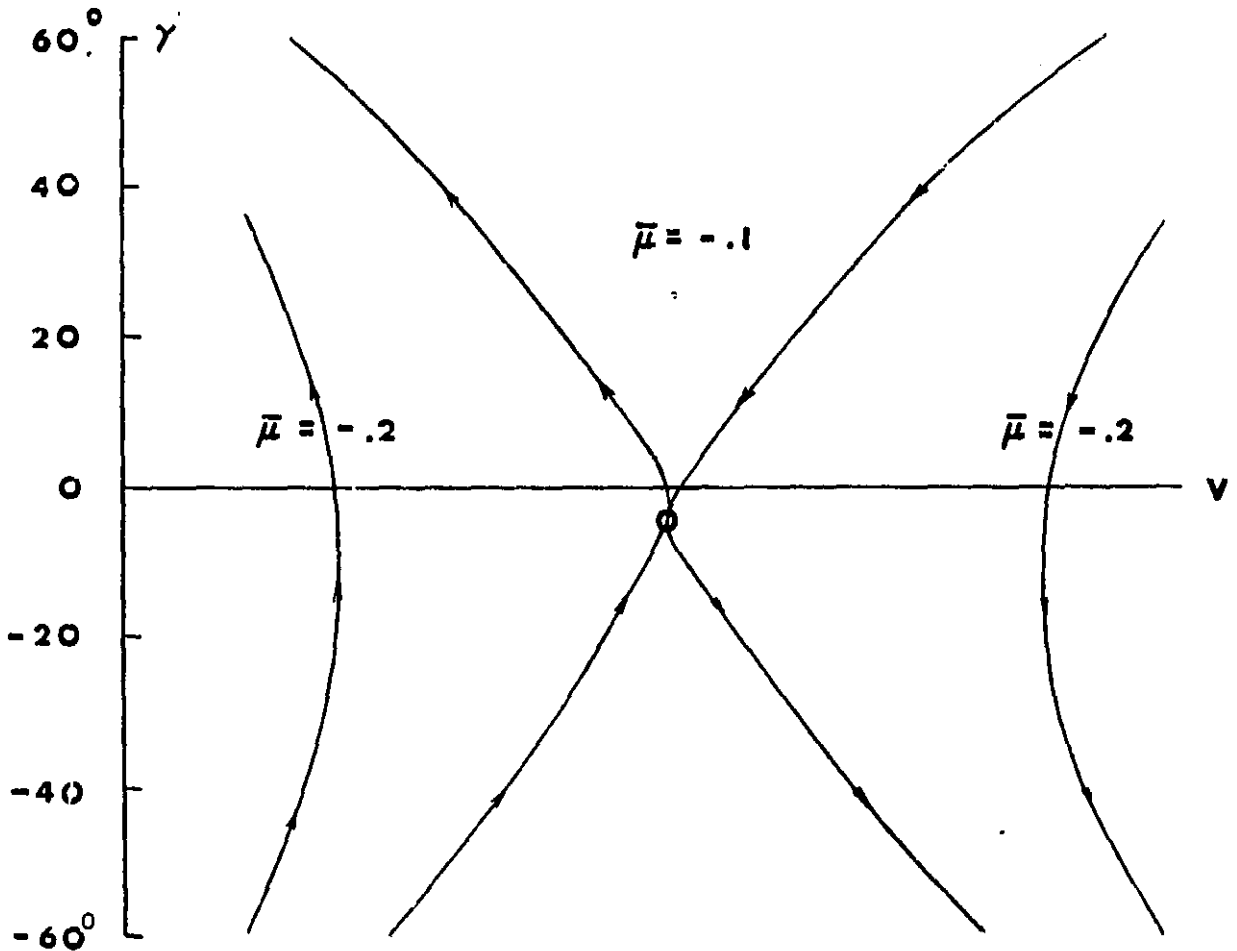
Fig. 2 . Flight-Path Angle vs. Airspeed in Gliding Flight

for the Range Problem
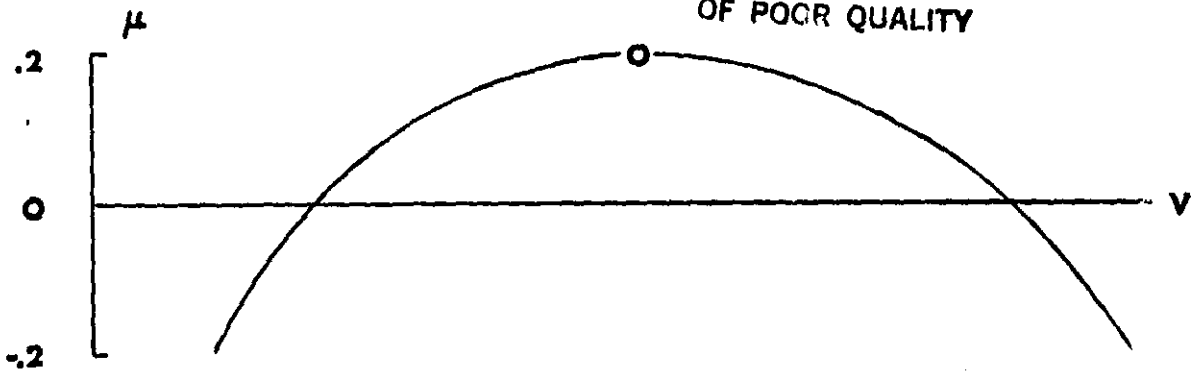
Acceleration variable vs Airspeed
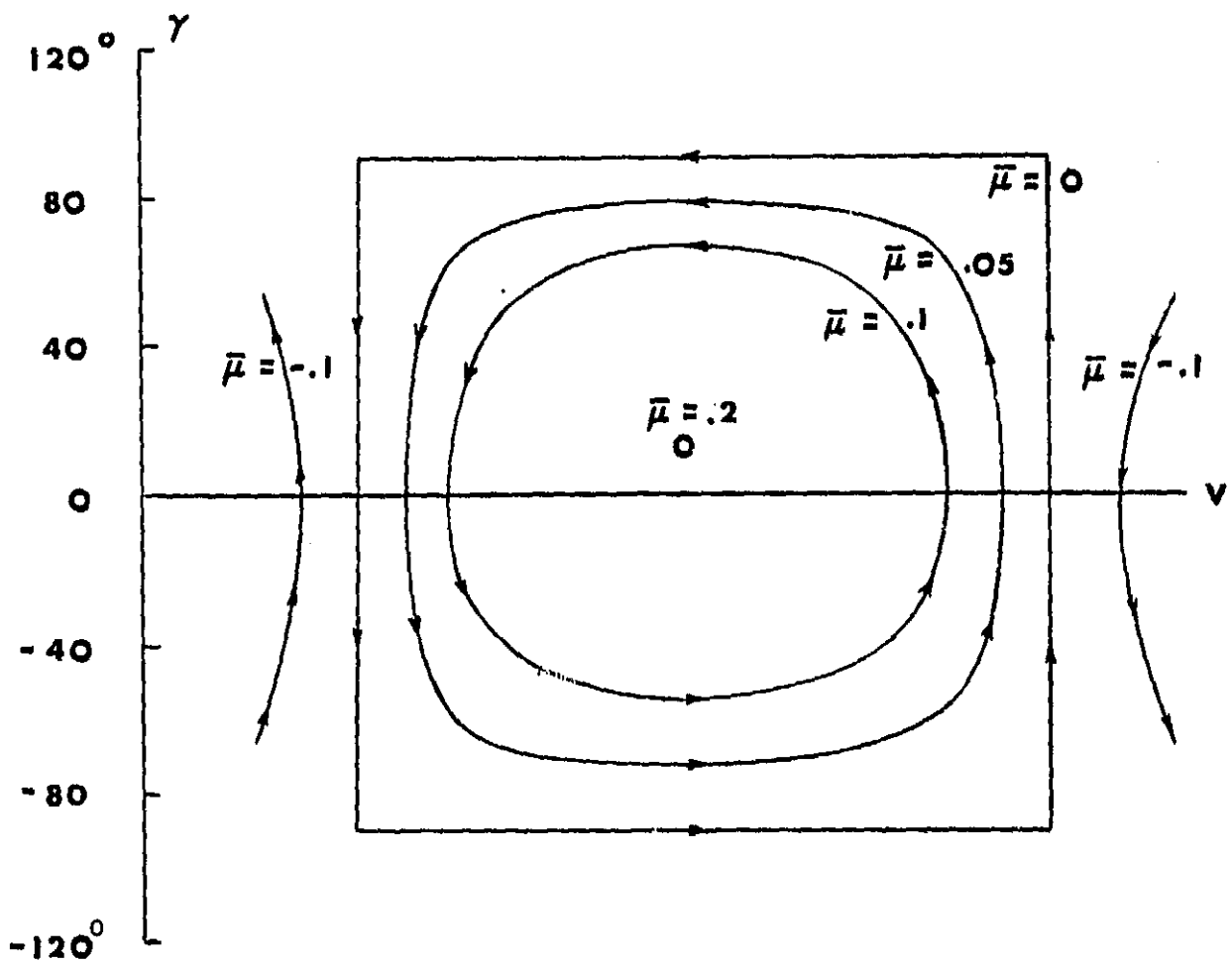
Fig. 3 . Flight-Path Angle vs. Airspeed in Powered Flight

for the Range Problem
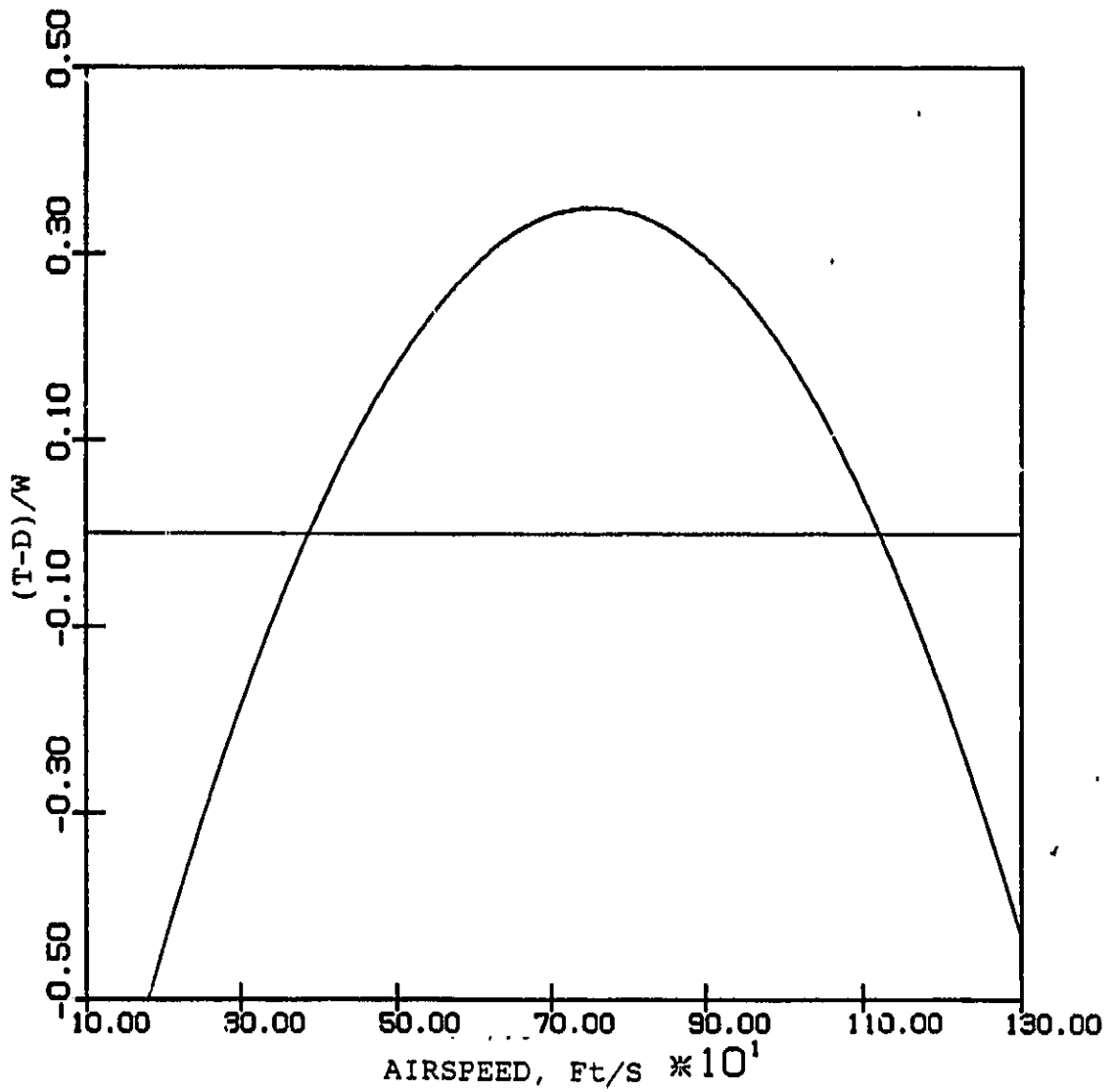
Fig. 4 . (T-D)/W vs. Airspeed - A Typical Parabolic
Distribution
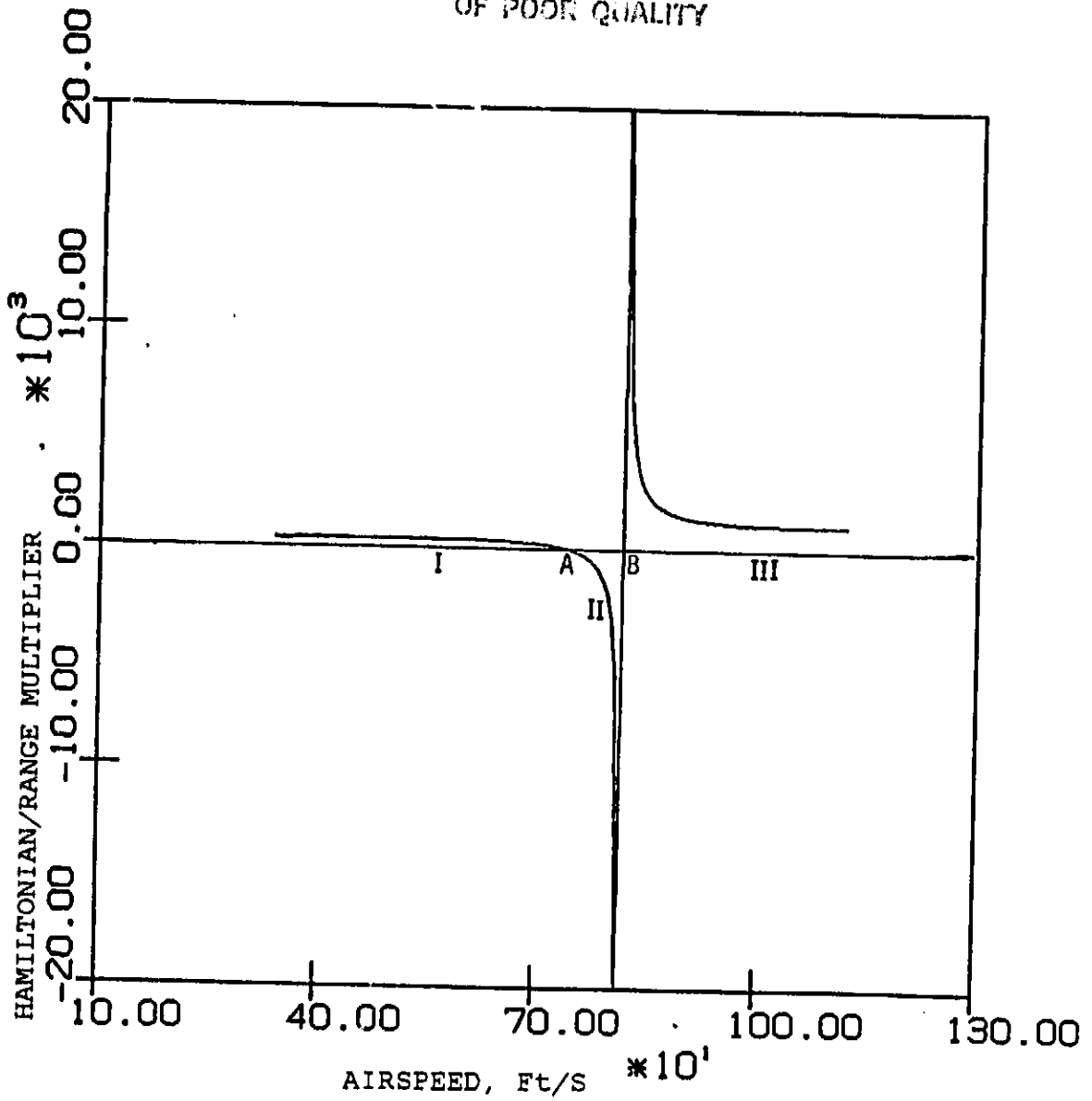
Fig. 5 . H/λ_x vs. Airspeed for Equilibrium Flight (Parabolic
(T-D)/W distribution)

A : $(T-D)_{max}$

B : $V(T-D)_{max}$
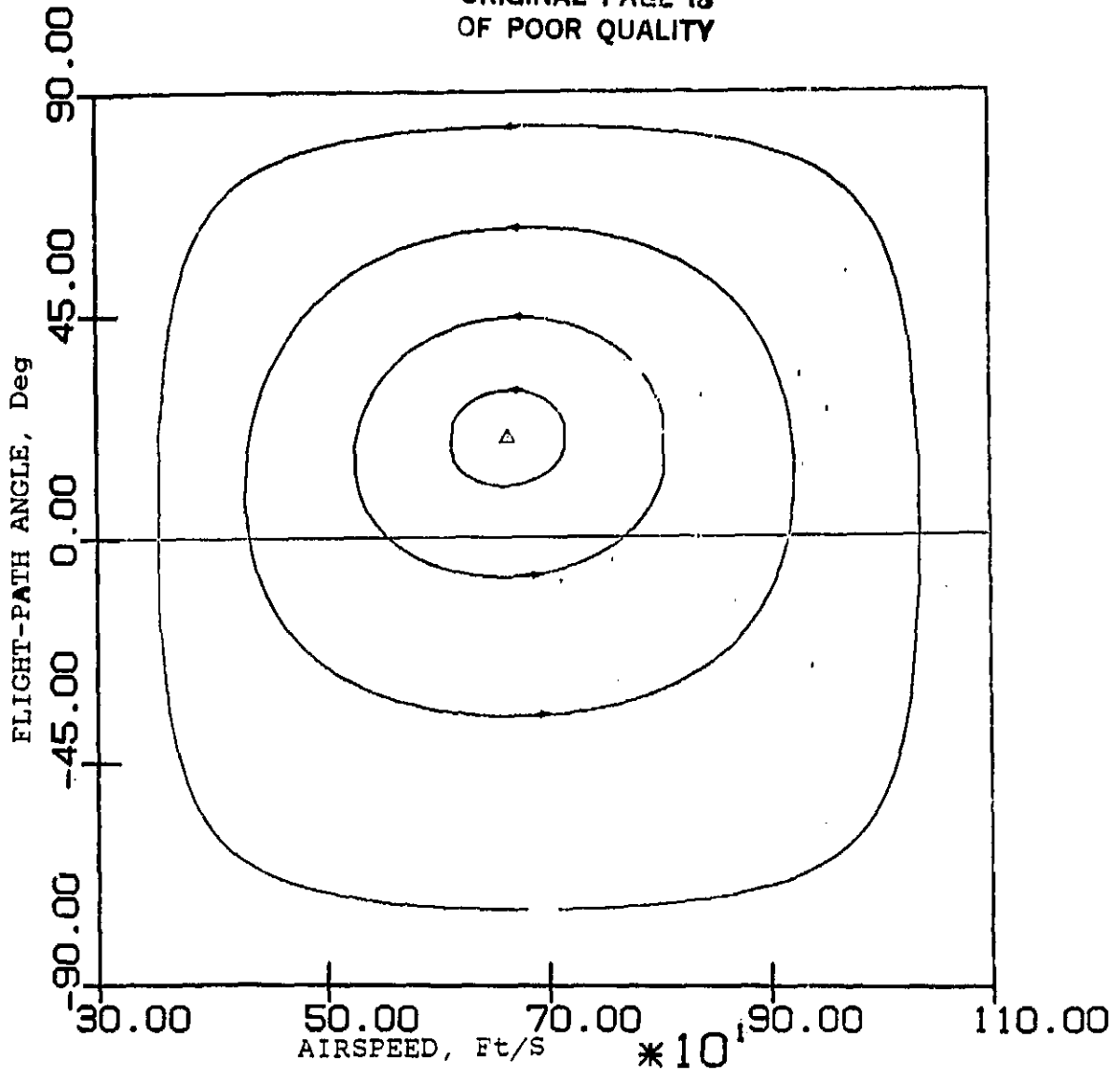
Fig. 6 . Representative Analytical Solution for H/λ_x in the

First Equilibrium Regime
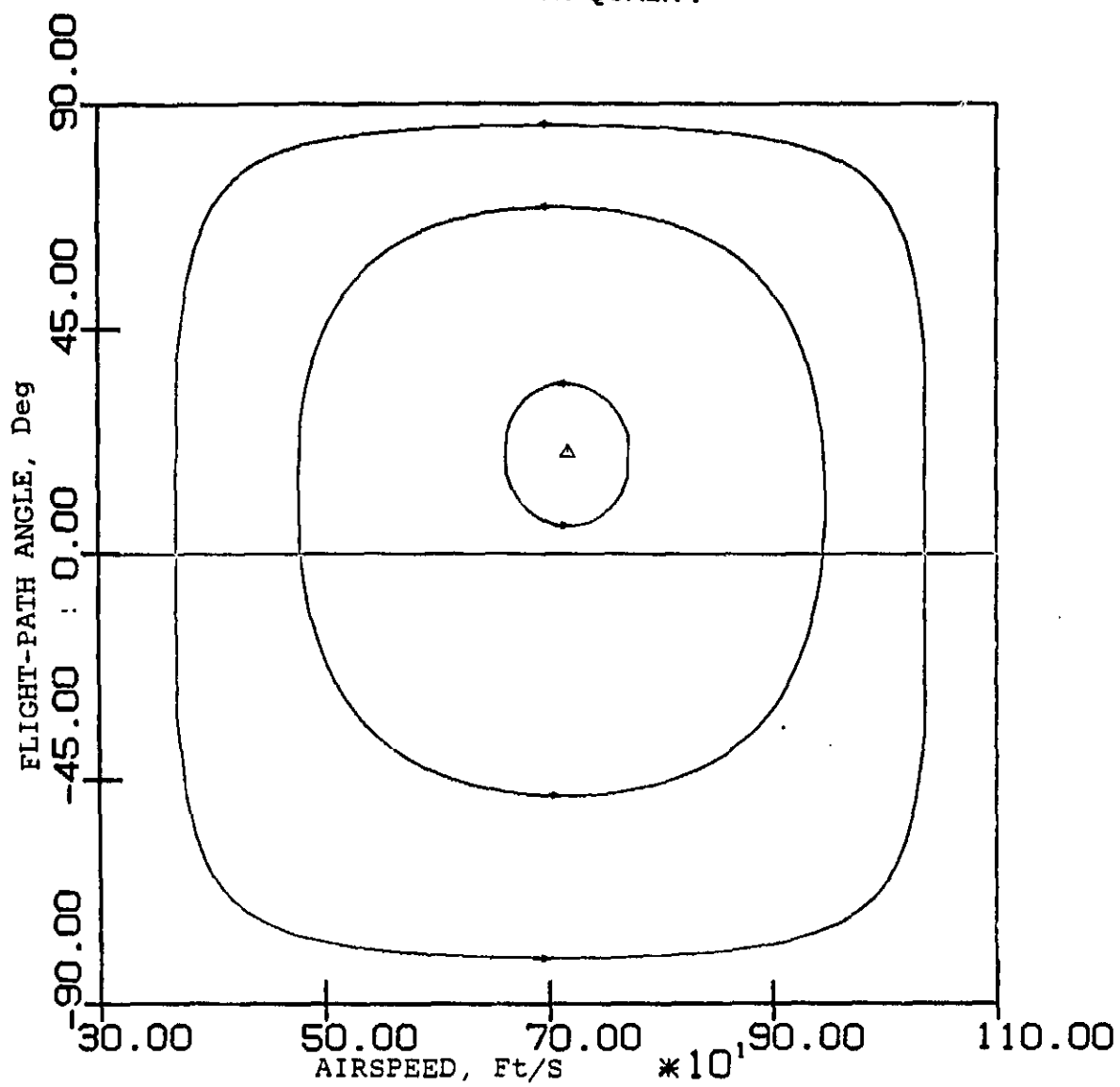
Fig. 7 . Representative Analytical Solution for H/λ_x in the
Second Equilibrium Regime
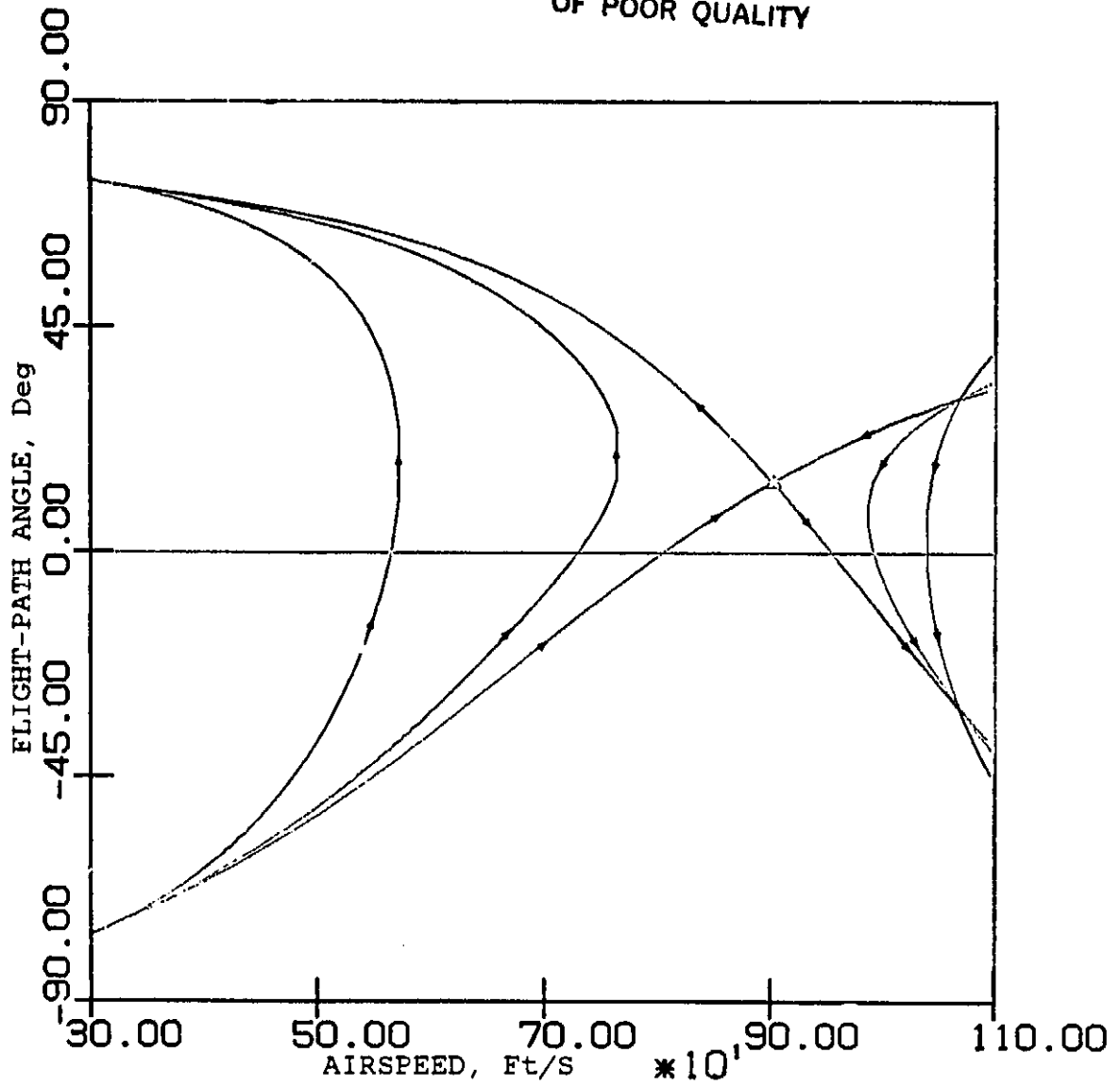
Fig. 8 . Representative Analytical Solution for H/λ_x in the Third Equilibrium Regime
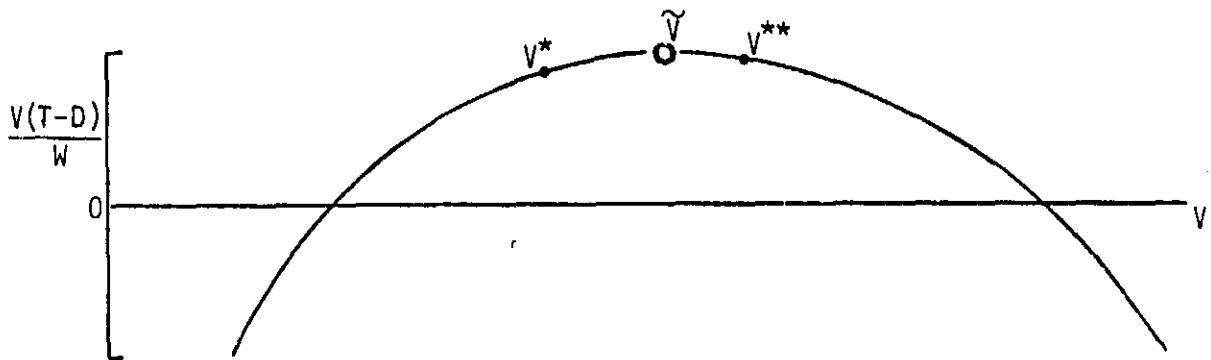
Fig. 9 . A Parabolic distribution of Specific Excess Power

vs. Airspeed
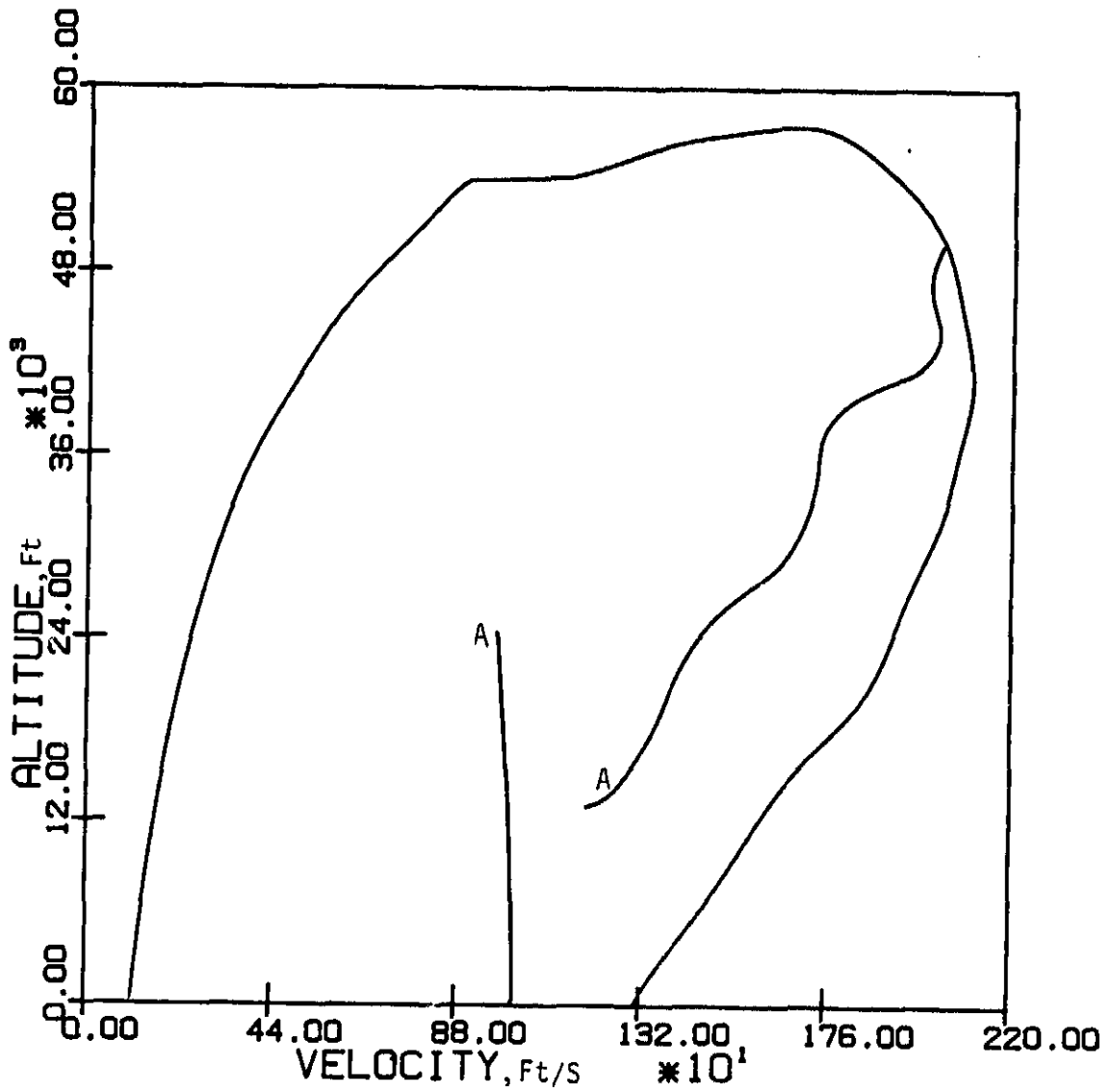
Fig. 10 . Level-Flight Envelope and the "Energy Climb" schedule for F-4 Aircraft

A : Energy Climb Path
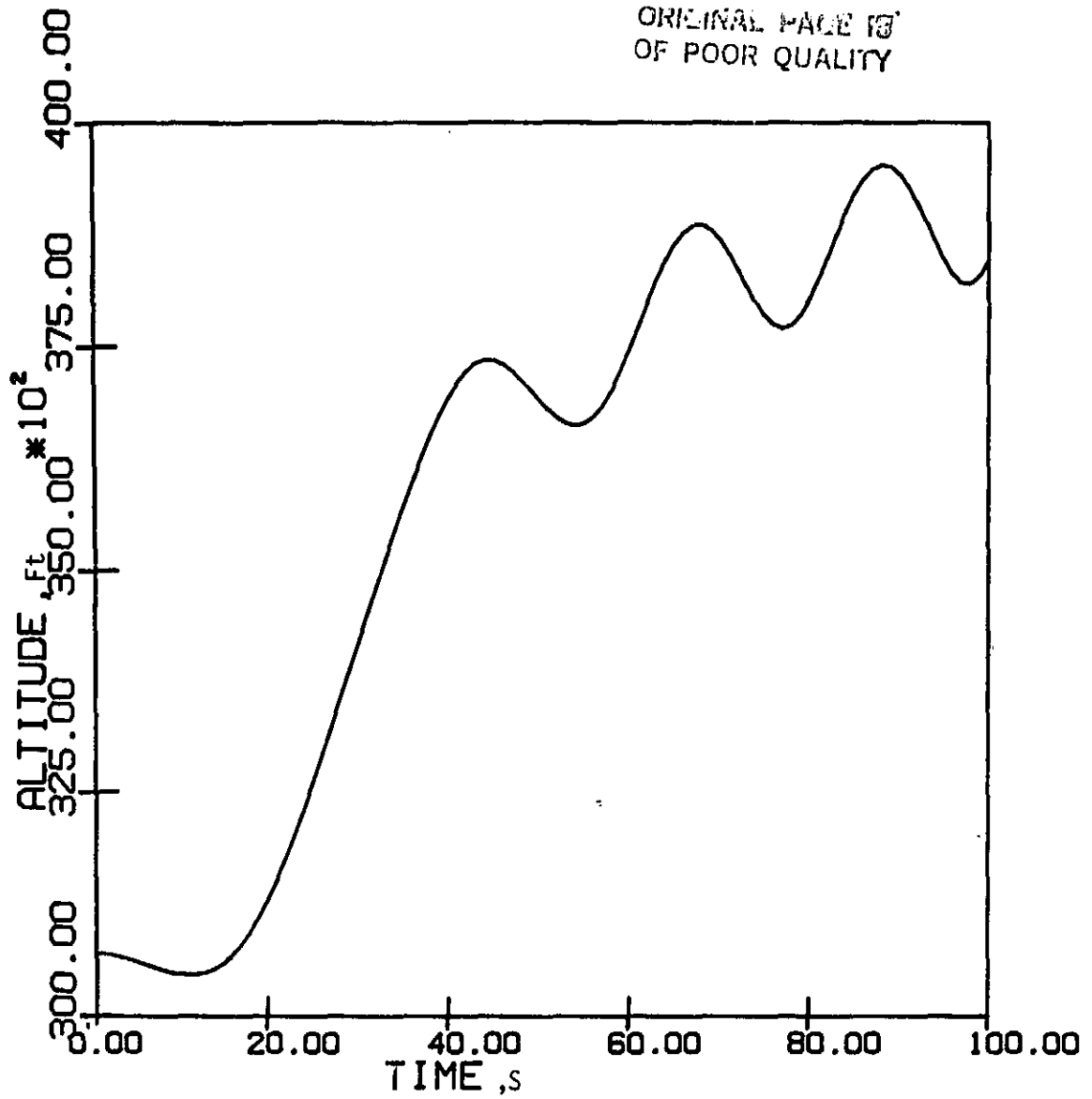
Fig. 11 . Sample Euler Solution for Minimum-Range Climb, Altitude vs. Time
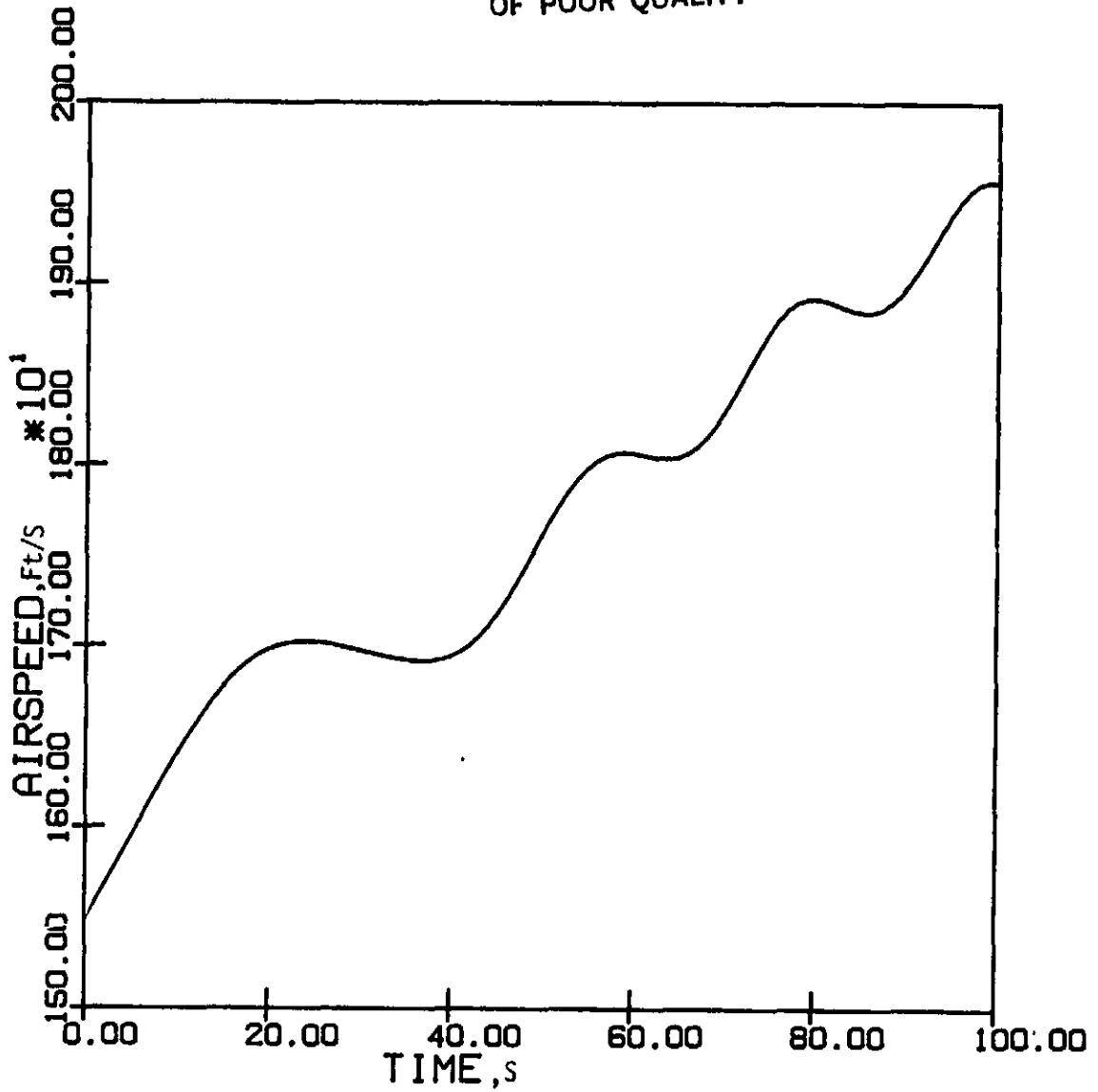
Fig. 12 . Sample Euler Solution for Minimum-Range Climb,
Airspeed vs Time
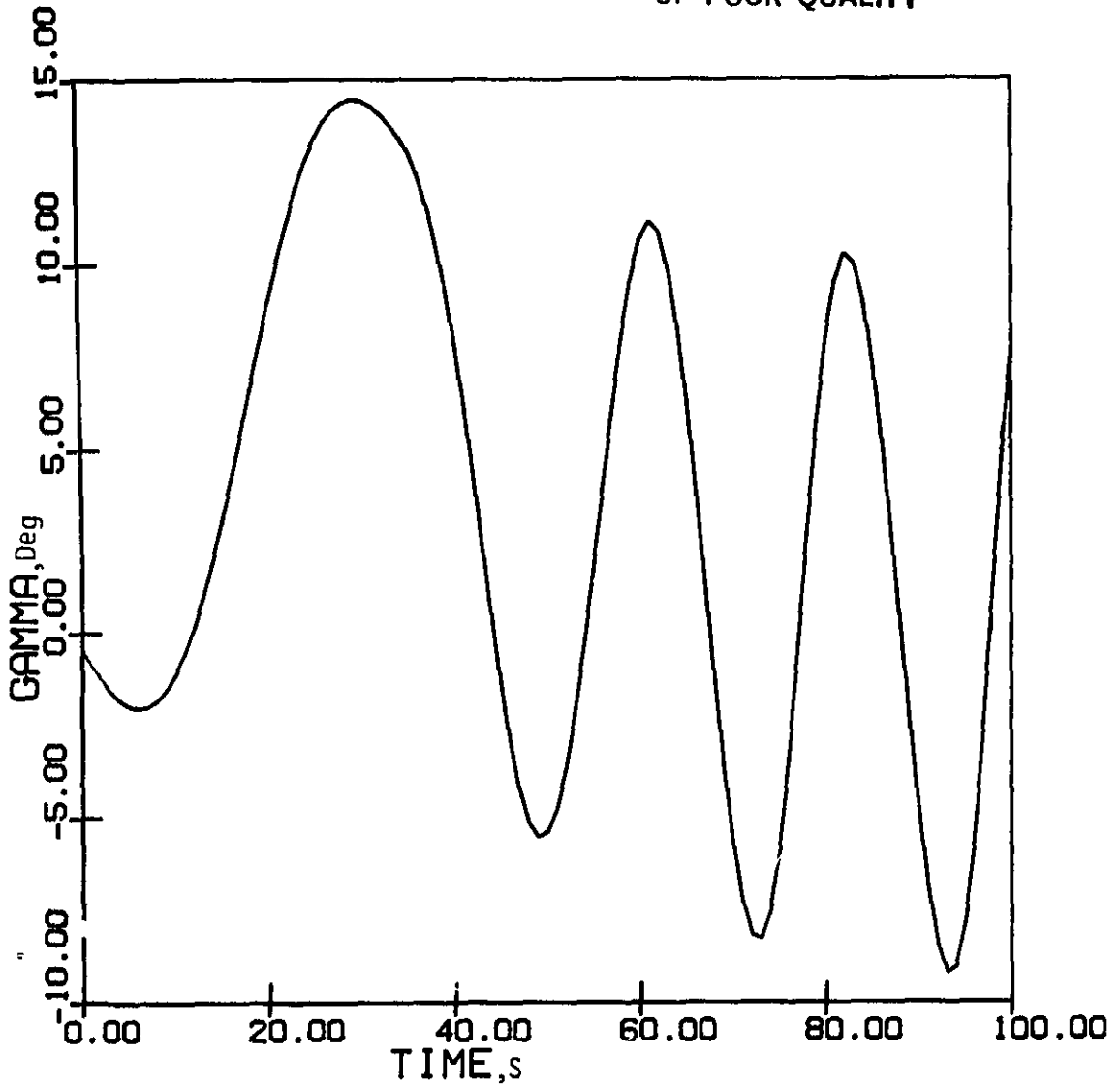
Fig. 13 . Sample Euler Solution for Minimum-Range Climb,
Flight-Path Angle vs. Time
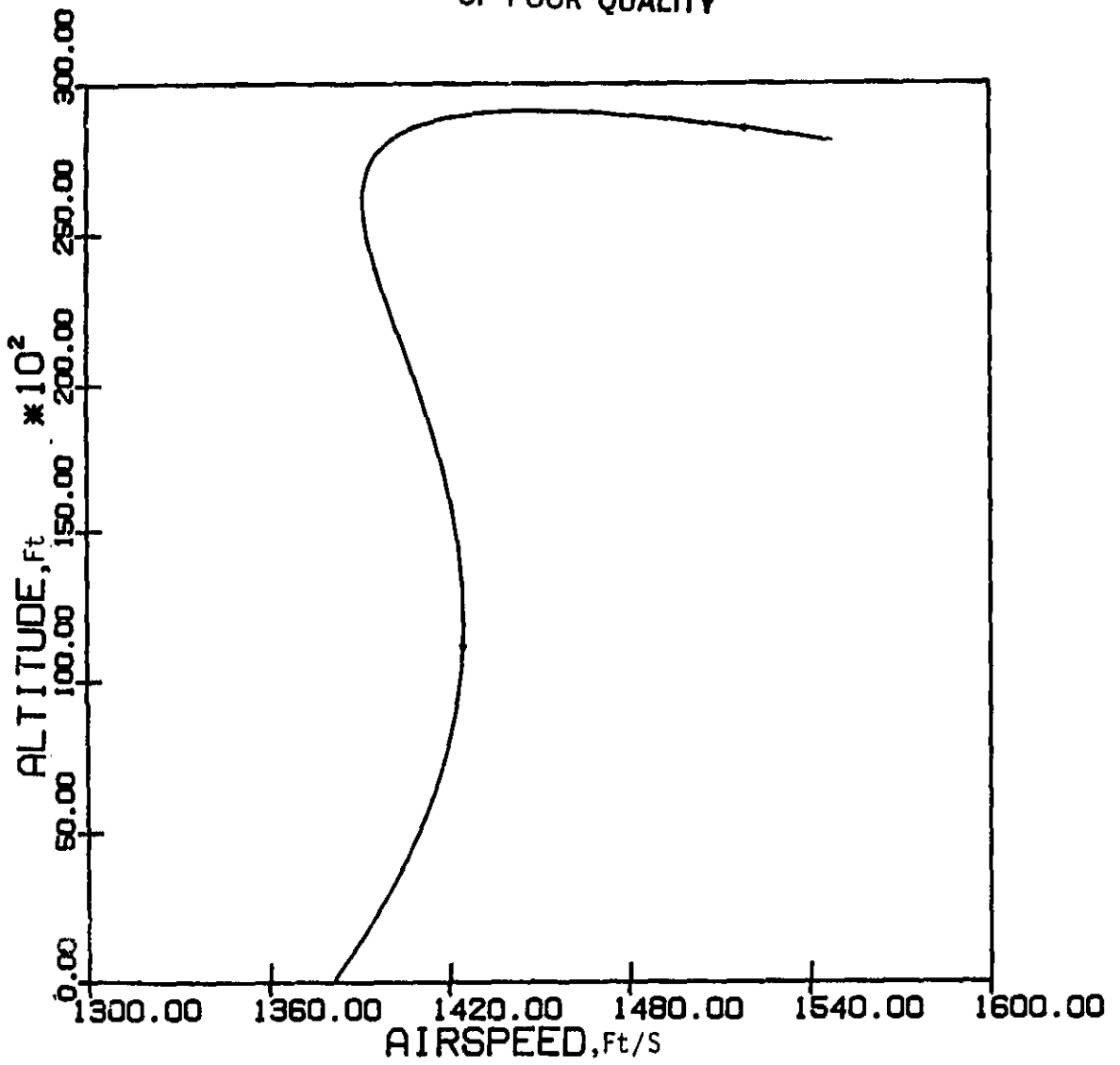
Fig. 14 . A Maximum-Range Glide Path in Airspeed-Altitude
Plane
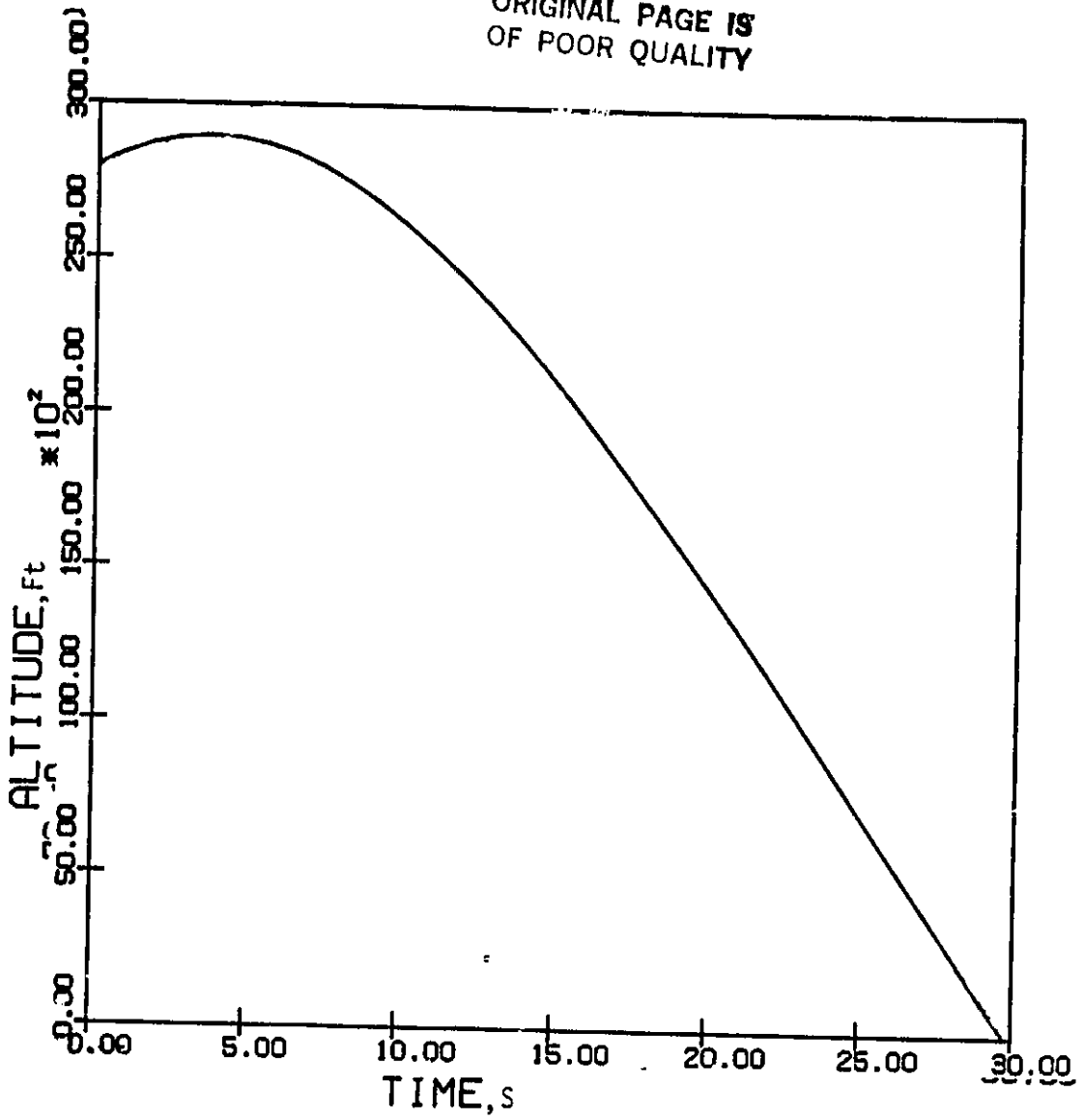
Fig. 15 . Sample Maximum-Range Glide Path, Altitude vs. Time
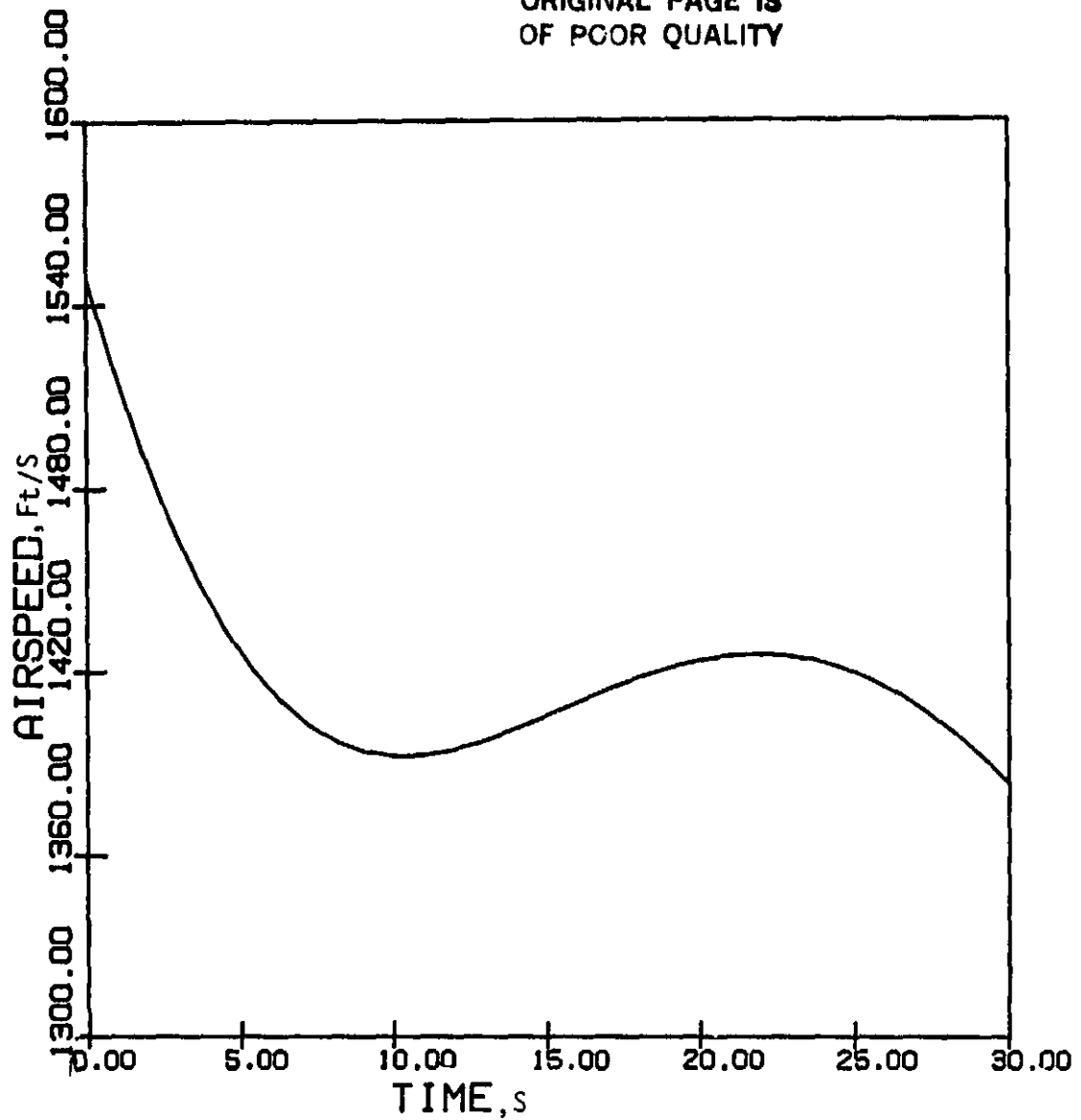
Fig. 16 . Sample Maximum-Range Glide Path, Airspeed vs. Time
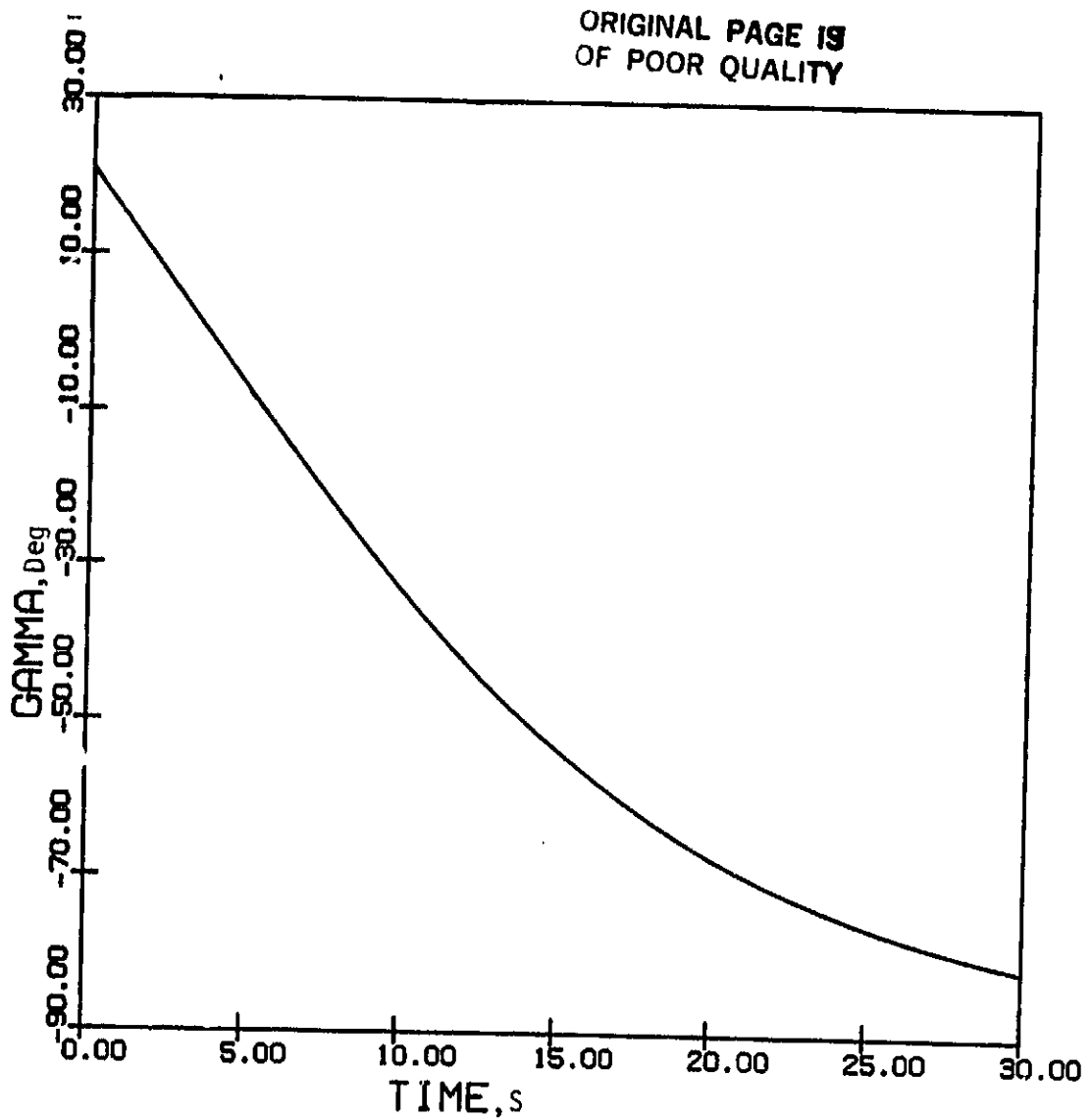
Fig. 17 . Sample Maximum-Range Glide Path, Flight-Path Angle
vs. Time

124

ORIGINAL PAGE IS
OF POOR QUALITY
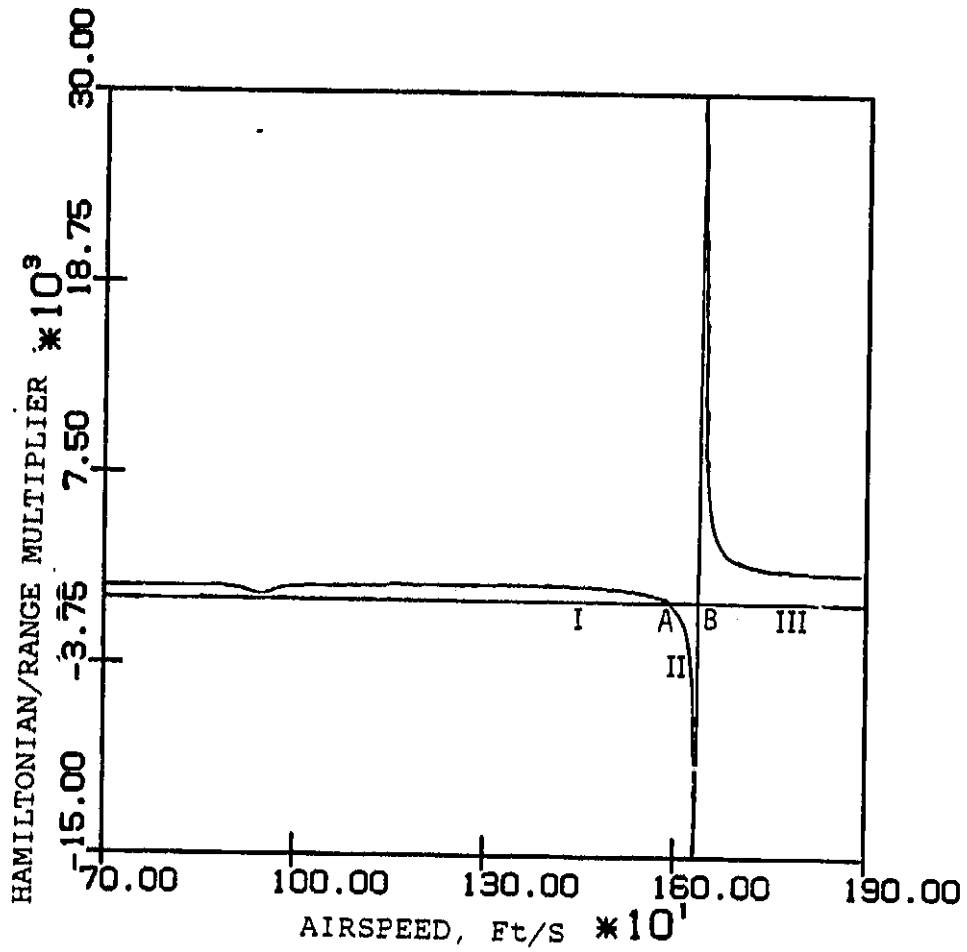
Fig. 18 . H/λ_x vs. Airspeed at Constant Specific Energy for
F-4 Aircraft for Unaccelerated Flight
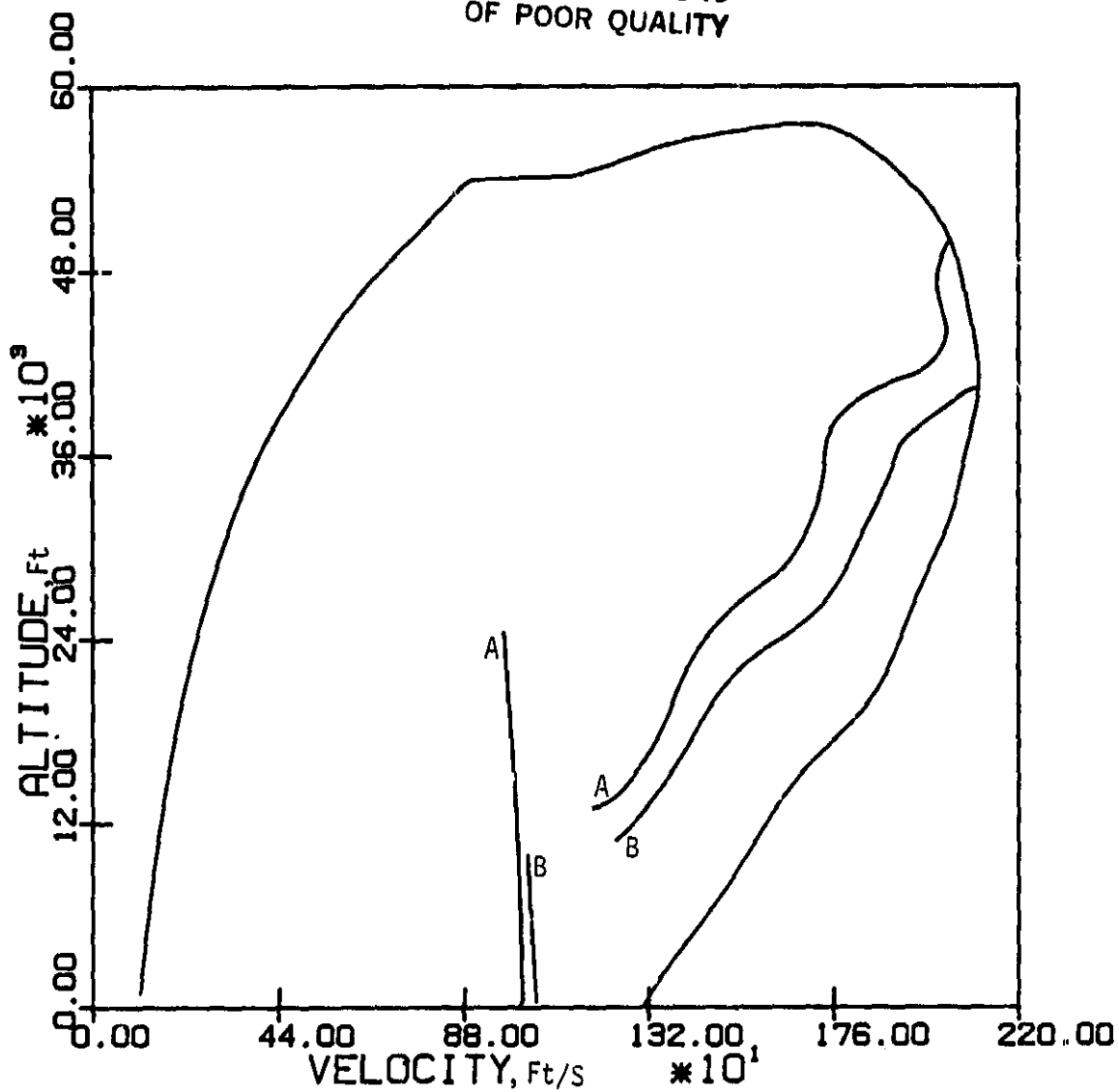
Fig. 19 . Level Flight Envelope, "Energy Climb" Schedule and
Climb-Dash Equilibrium Locus corresponding to
unaccelerated Flight for the F-4 Aircraft

A : Energy Climb Schedule

B : Equilibrium Locus
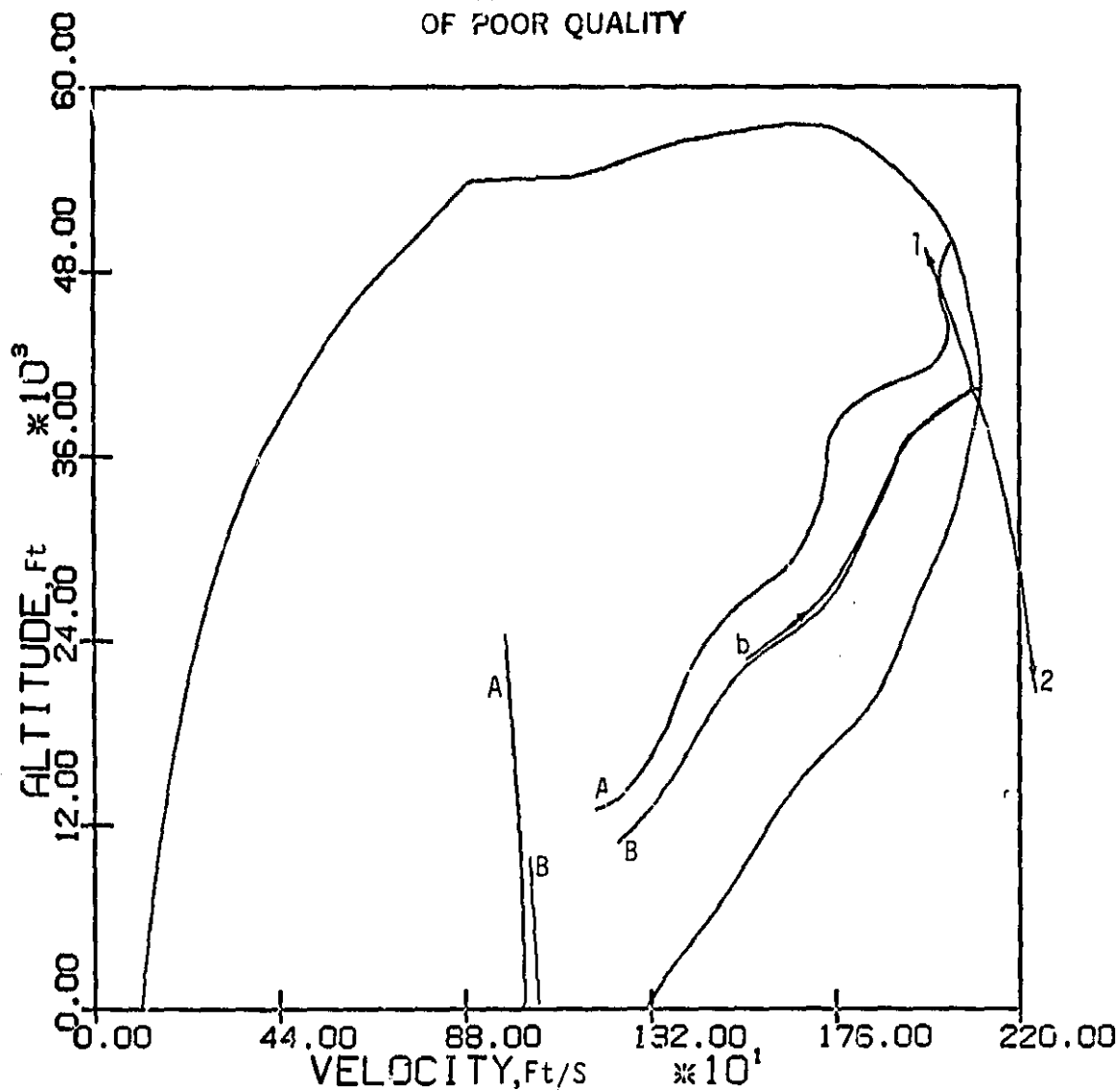
Fig. 20 . Flight Envelope, Energy Climb Schedule,
Equilibrium Locus and a Climb-Dash Euler Solution.

A : Energy Climb Schedule

B : Equilibrium Locus

b : Climb-Dash Euler Solution

1, 2 : See P. 69 for details
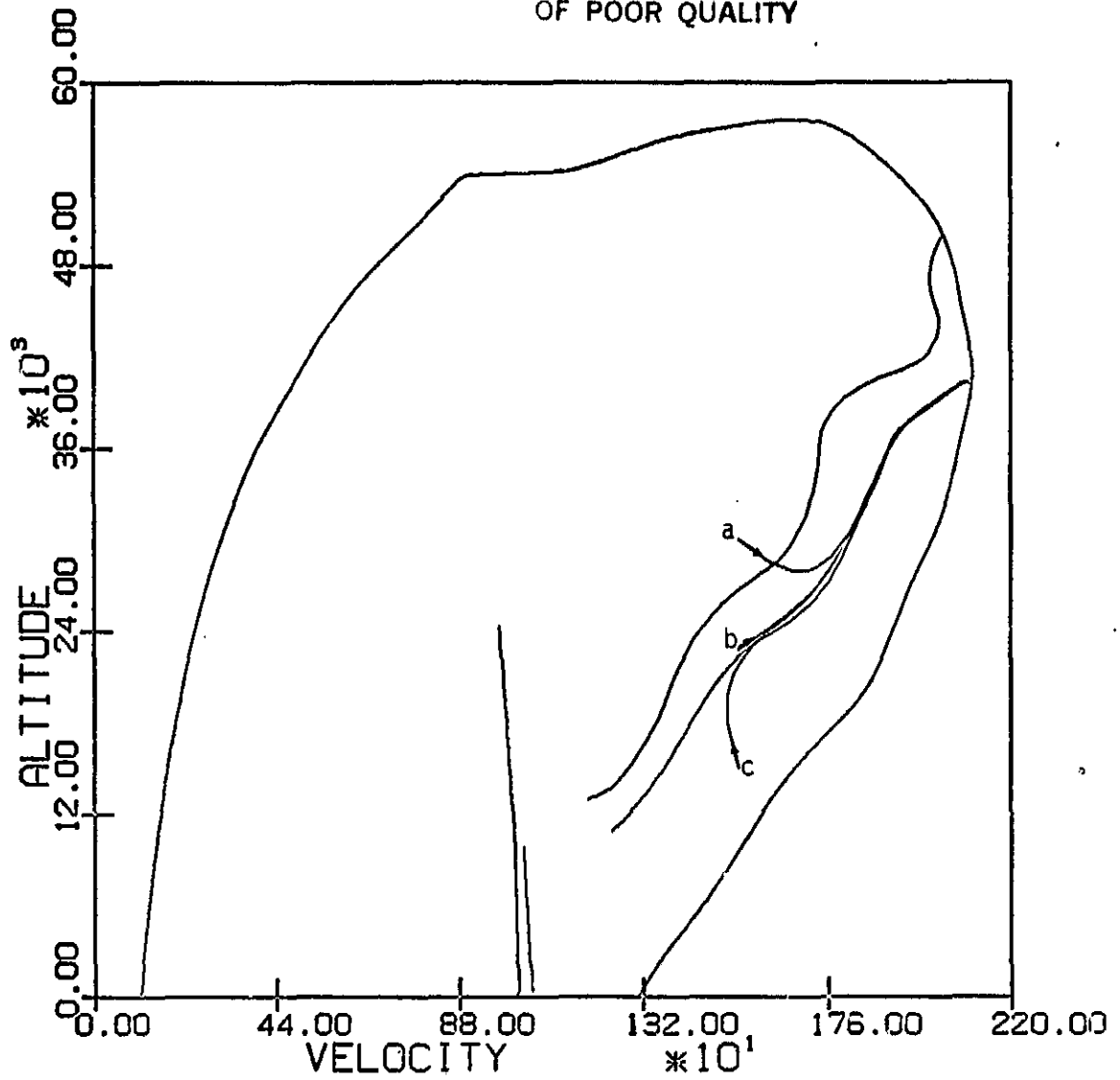
Fig. 21 . Euler Solutions for the Climb-Dash Problem
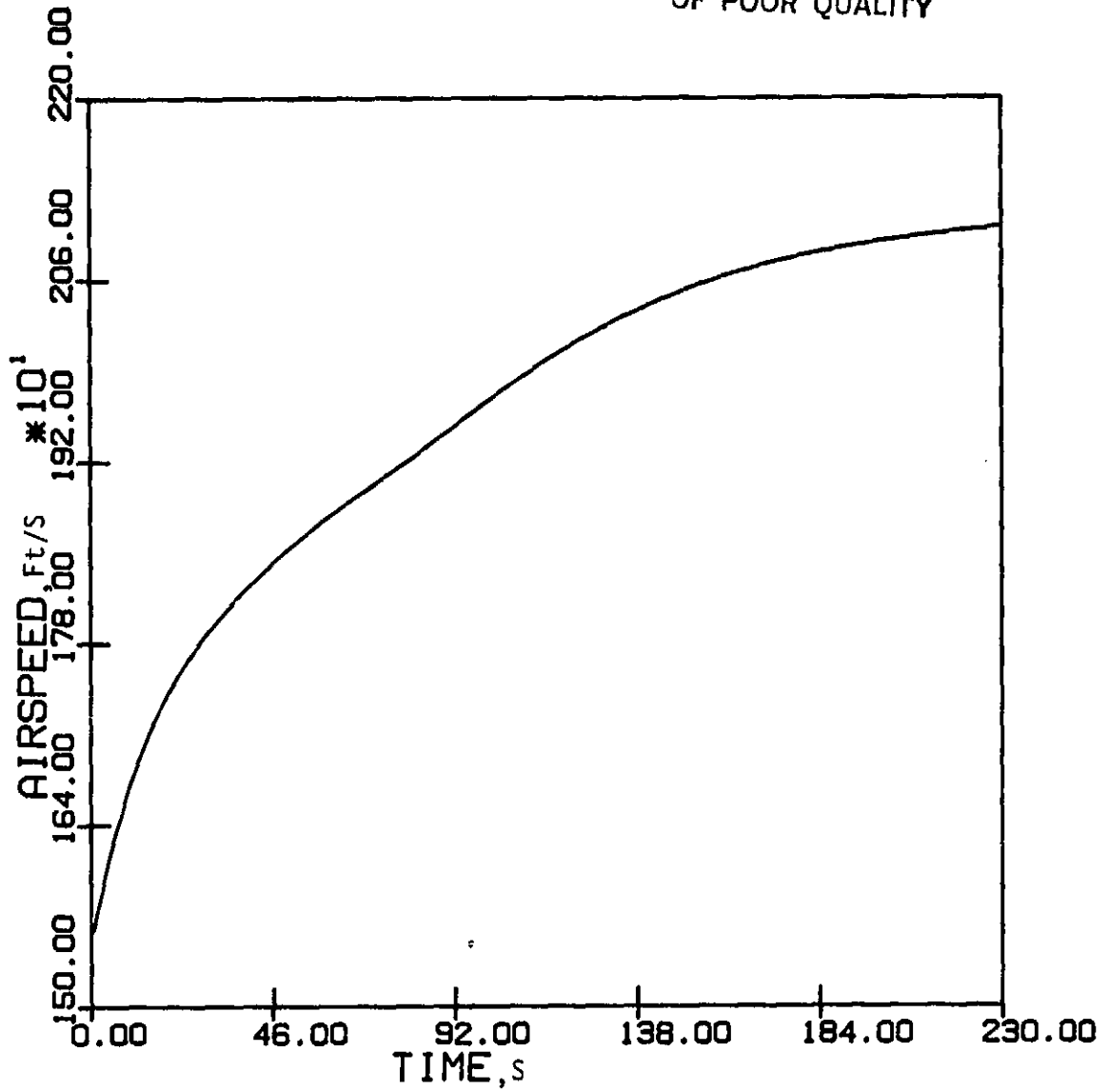
a,b,c : Euler Solutions
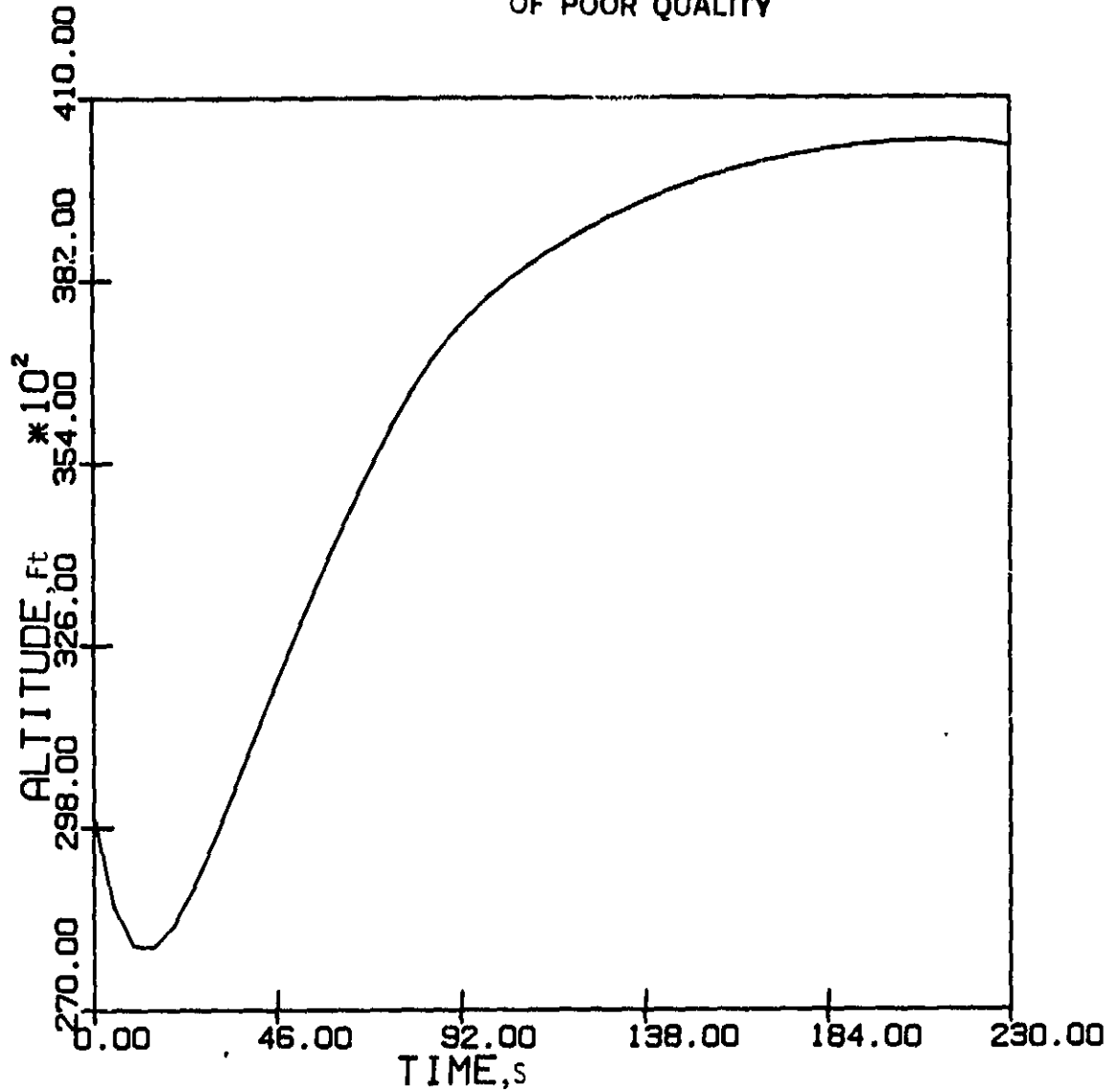
Fig. 22 . Altitude vs. Time for an Optimal Climb-Dash Path

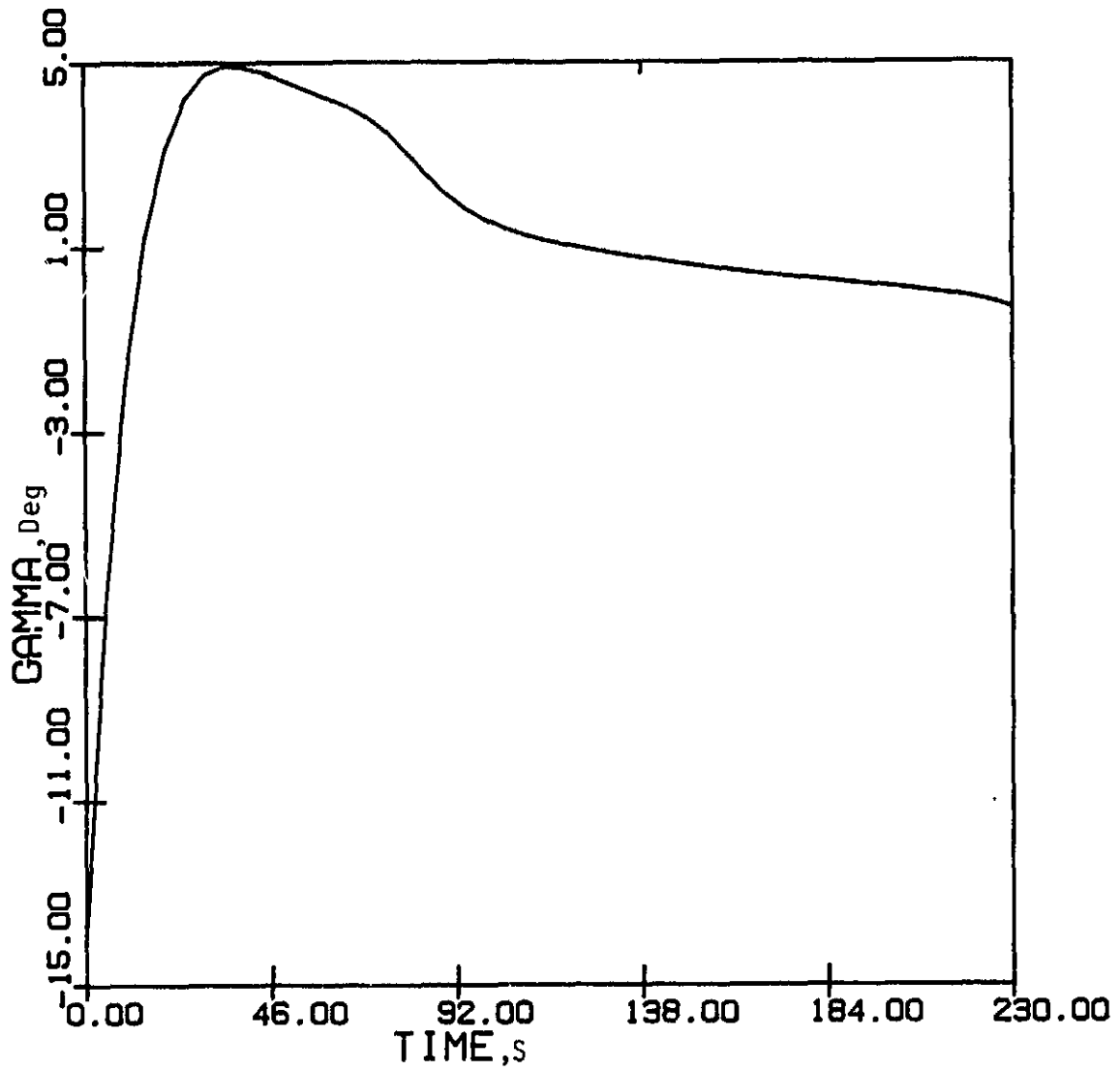Fig. 23 . Airspeed vs. Time for an Optimal Climb-Dash Path

Fig. 24 . Flight-Path Angle vs. Time for an Optimal Climb-
Dash Path